Strategies for Regio- and Enantiocontrol in Nickel-Catalyzed Reductive Couplings of Aldehydes and Alkynes

by

Hasnain A. Malik

A dissertation submitted in partial fulfillment
of the requirements for the degree of
Doctor of Philosophy
(Chemistry)
in the University of Michigan
2011

Doctoral Committee:

Professor John Montgomery, Chair
Professor David H. Sherman
Associate Professor Melanie S. Sanford
Associate Professor John P. Wolfe

Dedication

I dedicate this to my family and friends.

Acknowledgements

I would like to acknowledge and thank my advisor Professor John Montgomery for helping me develop as a scientist and for supporting me throughout during my doctoral studies. I would like to thank Professor Melanie S. Sanford for her assistance and guidance on numerous issues throughout my graduate career. I would also like to acknowledge my dissertation committee members for their feedback and support. I would like to thank Dr. Scott Bader for being a mentor during my early years in the Montgomery Group. I would also like to thank my collaborators throughout my time at the University of Michigan: Grant J. Sormunen, Ryan D. Baxter, Dr. Mani Raj Chaulagain, and Dr. Lopa V. Desai.

I would like to thank my undergraduate advisor Professor Ned D. Heindel for "opening the door." I would also like to acknowledge Dr. Julian Levell for having the patience to teach me the basics of laboratory technique during my first internship experience.

Finally, and most importantly, I would like to acknowledge my friends and family for putting up with me throughout these years.

Table of Contents

Dedication..……...ii

Acknowledgements……..……..……iii

List of Schemes……...……...……viii

List of Tables……...…..….xii

List of Figures……..xiii

List of Abbreviations..……...……...xiv

Abstract……xvi

Chapter

Chapter 1: Nickel-Catalyzed Reductive Couplings and Cyclizations

1. Introduction……..…….……1

1.1. Three-Component Couplings via Alkyl Group Transfer – Method Development...3

1.2. Reductive Couplings via Hydrogen Atom Transfer – Method Development……...5

1.3. Simple Aldehyde and Alkyne Reductive Couplings……5

1.4. Directed Processes……...…...9

1.5. Diastereoselective Variants: Transfer of Chirality……10

1.6. Asymmetric Variants……..12

1.7. Mechanistic Insights……...14

1.8. Cyclocondensations via hydrogen gas extrusion……..19

1.9. Use in Natural Product Synthesis……21

1.10. Conclusions and Outlook……..27

Chapter 2: Cooperativity of Regiochemistry Control Strategies in Reductive Couplings of Propargyl Alcohols and Aldehydes

2. Introduction……..29

2.1. Synthetic Methods for the Synthesis of Allylic Alcohols……...30

2.1.1. Early Methods for the Synthesis of Allylic Alcohols……..30

2.1.2. Modern Methods for the Synthesis of Allylic Alcohols……..33

2.2. Regioselective Nickel-Catalyzed Aldehyde–Alkyne Reductive Couplings……38

2.3. Results & Discussion……41

2.3.1. Strategies for Regiocontrol……41

2.3.2. Substrate Scope……44

2.3.3. Development of a Predictive Model for Reductive Couplings……45

2.3.4. Illustration of Regiocontrol Strategies Based on the Predictive Model……..46

2.3.5. Product Utility……..48

2.4. Conclusion……...50

Chapter 3: A General Strategy for Regiocontrol in Reductive Couplings of Aldehydes and Alkynes

3. Introduction……...51

3.1. Methods to Attain Regioselectivity in Alkyne Addition Reactions……...53

3.2. *N*-Heterocyclic Carbenes……..58

3.3. Results & Discussion……60

3.3.1 Development of Catalyst-Controlled Regioselectivity Studies……..……..60

3.3.2. Substrate Scope……..……...63

3.4. Development of a Simple Ligand Steric Control Model for Nickel-Catalyzed Reductive Coupling of Aldehydes and Alkynes……67

3.5 Conclusion……...70

Chapter 4: Regio- and Enantiocontrol Strategies in Reductive Couplings of Aldehydes and Alkynes

4. Introduction……..71

4.1. Methods for the Synthesis of Chiral Allylic Alcohols……72

4.2. Results & Discussion……77

4.2.1. Chiral Ligand Design……..77

4.2.2. Enantio- and Regiocontrol using Chiral NHCs……..81

4.3. Future Directions for Enantio- and Regiocontrol Studies……85

4.4. Conclusion……...87

Chapter 5: Experimental Supporting Information

5. Introduction……88

5.1. General Procedures……90

5.1.1. General Procedure A for the $Ni(COD)_2$/NHC-Promoted Reductive Coupling of Silyl(propargyl)ethers.....90

5.1.2. General Procedure B for Palladium-Catalyzed Allylic Reductions to Form External Olefins……90

5.1.3. General Procedure C for Palladium-Catalyzed Allylic Reductions to Form 1,3-Dienes……90

5.1.4. General Procedure D for Deoxygenation via $SO_3 \cdot Py$ S_N2 Displacement Protocol……..91

5.1.5. General Procedure E for the $Ni(COD)_2$/*i*-Pr-BAC-Promoted Reductive Coupling of Alkynes, Aldehydes, and Di-*tert*-butylsilane.....91

5.1.6. General Procedure F for the $Ni(COD)_2$/SIPr-Promoted Reductive Coupling of Alkynes, Aldehydes, and Triisopropylsilane.....92

5.1.7. General Procedure G for the $Ni(COD)_2$/IMes-Promoted Reductive Coupling of Alkynes, Aldehydes, and Triisopropylsilane.....92

5.1.8. General Procedure H for the $Ni(COD)_2$/Ph_2SIPr-Promoted Reductive Coupling of Alkynes, Aldehydes, and Triethylsilane.....92

5.2. Spectral Characterization……93

5.2.1. Chapter 2 Starting Propargyl Alcohol Derivatives……..93

5.2.2. Chapter 2 Nickel-Catalyzed Reductive Coupling Substrates……94

5.2.2.1. Scheme 52 Entries……..94

5.2.2.2. Table 1 Entries……99

5.2.2.3. Scheme 54 Entries……111

5.2.2.4. Scheme 57 Entries……120

5.2.2.5. Scheme 58 Entries……123

5.2.2.6. Scheme 59 Entries……126

5.2.2.7. Scheme 60 Entries……127

5.2.3. Chapter 3 Ligands for Nickel-Catalyzed Reductive Couplings……..131

5.2.4. Chapter 3 Nickel-Catalyzed Reductive Couplings Substrates……...133

5.2.4.1. Table 4 Entries……...133

5.2.5. Chapter 4 Ligands for Nickel-Catalyzed Reductive Couplings……..…147

5.2.6. General Procedure for Asymmetric Nickel-Catalyzed Reductive Couplings…149

Literature Cited……151

List of Schemes

1. Intramolecular Aldehyde–Alkyne Alkylative Coupling……..3
2. Intermolecular Aldehyde–Alkyne Alkylative Coupling……..4
3. Synthesis of 1,3-Dienes……4
4. Diastereoselective Synthesis of 1,3-Dienes……..5
5. Catalyst-Controlled Alkylative or Reductive Coupling Pathways……6
6. Silanes as Reducing Agents in Aldehyde–Alkyne Couplings……7
7. Nickel-Catalyzed Et_3B-Mediated Reductive Couplings……7
8. Nickel-Catalyzed Silane-Mediated Reductive Couplings……8
9. Regiocontrol in Nickel-Catalyzed Macrocyclizations……9
10. Aldehyde–1,3-Enyne Reductive Couplings……..10
11. Aldehyde–1,6-Enyne Reductive Couplings……..10
12. Diastereoselective Nickel-Catalyzed Aldehyde–Alkyne Couplings……11
13. Diastereoselective α-Siloxy Aldehyde–Alkyne Couplings……11
14. Chirality Transfer in Aldehyde–Alkyne Reductive Couplings……14
15. Asymmetric Nickel-Catalyzed Et_3B-Mediated Reductive Couplings……13
16. Asymmetric Nickel-Catalyzed Silane-Mediated Reductive Couplings……13
17. Postulated Mechanism for Aldehyde–Alkyne Couplings……...14
18. Role of Ligands in Alkylative and Reductive Pathways……15
19. Postulated Mechanism for Silane-Mediated Couplings……15
20. Crossover Studies……16

21. X-Ray of Metallacycle Intermediate……..17

22. Directed Aldehyde–1,3-Enyne Couplings……18

23. Postulated Origin of Regiocontrol in Aldehyde–1,6-Enyne Couplings……18

24. Empirical Evidence for Metallacycle Pathway……19

25. Use of Dialkylsilane Reducing Agents……..19

26. Substrate Scope for Silacycle Formation……20

27. Postulated Mechanism for Silacycle Formation……..20

28. Total Synthesis of (+)-Allopumiliotoxin-339A and -339B……...22

29. Total Synthesis of Testudinariol A……23

30. Total Synthesis of Amphidinolide T1……24

31. Total Synthesis of Amphidinolide T4……25

32. Total Synthesis of Aigialomycin D……26

33. Total Synthesis of (+)-Epi- and (+)-Terpestacin……..27

34. The Wharton Olefin Synthesis……...31

35. The Prins Reaction……..35

36. The Guillemonat Variant of the Reiley Oxidation……32

37. The Morita-Baylis-Hillman Reaction……32

38. The Mislow-Evans Rearrangement……..33

39. The Luche Reduction……..33

40. The Nozaki-Hiyama-Kishi Coupling……..34

41. Hydrometallation/Transmetallation Methods……...35

42. Titanium-Mediated Reductive Couplings……35

43. A Titanium-Catalyzed Silane-Mediated Reductive Coupling……36

44. Alkoxy-Directed Titanium-Mediated Reductive Couplings……37

45. Rhodium-Catalyzed Hydrogen-Mediated Reductive Couplings……...37

46. Ruthenium-Catalyzed Variants via Hydrogen-Transfer……38

47. Trends in Nickel-Catalyzed Aldehyde–Alkyne Reductive Couplings……..39

48. Regiocontrol via Olefin-Direction……...40

49. Regio- and Diastereocontrol via Olefin-Coordination……40

50. Ynamide-Directed Couplings……40

51. Research Goals for Removable Directing Group Strategy……...41

52. An Initial Test of Regiocontrol using R_3P and NHC Ligands……42

53. Other Propargyl Functional Groups for Direction……44

54. Substrate Scope of Propargyl Silyl Ether–Aldehyde Couplings……...44

55. Hypothesis for an Inductive Effect in Achieving Regiocontrol……..45

56. Predictive Model for Aldehyde–Alkyne Couplings……..46

57. Illustration #1 of Regiocontrol Strategies……47

58. Illustration #2 of Regiocontrol Strategies……47

59. Illustration #3 of Regiocontrol Strategies……48

60. Utility of Propargyl Alcohol Substrates……49

61. Postulated Mechanism of 1,3-Diene Formation……..50

62. Trends of Alkyne Regioselectivity in Reductive Couplings……...52

63. Research Goals of Achieving Regiocontrol in a Variety of Alkynes……53

64. Perfect Regiocontrol by the Use of Preformed Vinyl Halides……...54

65. The Nozaki-Hiyama-Kishi Coupling in Total Syntheses……55

66. Methods for the Synthesis of Vinyl Halides……56

67. Use of NHC Ligands in Reductive Couplings……..57

68. Major Classes of Alkynes that Undergo Coupling with Regiocontrol……..57

69. Lack of Regioselectivity using Monodentate Phosphine Ligands……61

70. Postulated Means of Regiocontrol……66

71. Synopsis of Optimal Alkyne–Ligand Combination for Regiocontrol……67

72. Refined Predictive Model……68

73. Previous Predictive Model……..68

74. Asymmetric Methods for Linear Allylic Alcohols……72

75. The Asymmetric NHK Coupling for 1,1-Disubstitued Allylic Alcohols……73

76. An Asymmetric Silane-Mediated 1,2-Reduction for Internal Allylic Alcohols…….73

77. An Asymmetric Rhodium-Catalyzed Aldehyde–Alkyne Coupling……74

78. An Asymmetric Aldehyde–Alkyne Alkylative Coupling……..75

79. Chiral Phosphines in Asymmetric Reductive Couplings……75

80. Chiral NHCs in Asymmetric Reductive Couplings……..76

81. Research Goals for an Enantio- and Regioselective Reductive Coupling……77

82. NHC Frameworks for Inducing Asymmetry and Regiocontrol……..78

83. An Example of a C_2 NHC Synthesis……79

84. The Synthesis of Another Type of C_2 Symmetric NHC Ligand ……...80

85. Postulated Dynamic Kinetic Resolution……80

86. An Example of a C_1 NHC Ligand Synthesis……81

87. Unpublished Optimization Studies……82

88. Results of Chiral NHC Screening Efforts……83

89. Experiments to Study Trends……84

90. Trends of Asymmetric Induction of the Product Based on Alkyne Sterics……84

91. An Illustration of the Importance of Extended Branching in Alkynes……...85

92. Future Directions……..87

List of Tables

1. Optimization of Reductive Couplings of Propargyl Alcohol Derivatives……..43

2. Ligand Effects in Couplings of 2-Hexyne…….62

3. Optimization Study for *i*-Pr-BAC Ligand……...63

4. Ligand-Controlled Regioselectivity Reversal……...65

5. Ligand Steric Effects Across a Range of NHCs……..66

6. Theoretical Basis for Catalyst-Controlled Regioselectivity……68

List of Figures

1. The Model Used for Calculating $\%V_{bur}$……59

2. $\%V_{bur}$ of Quadrants Around a Metal Center…..……60

3. Small Ligand System Transition-State Structures……..69

4. Large Ligand System Transition-State Structures……..70

List of Abbreviations

n-Bu	butyl
t-Bu	*tert*-butyl
COD	1,5-cyclooctadiene
ºC	temperature in degrees centigrade
Cy	cyclohexyl
d	day(s)
Et	ethyl
equiv	equivalent
GCMS	gas chromatography mass spectrometry
h	hour(s)
n-Hept	heptyl
c-Hex	cyclohexyl
n-Hex	hexyl
Hex	hexanes/hexyl
IMes	1, 3-bis-(1, 3, 5-trimethylphenyl)imidazol-2-ylidene
IPr	1, 3-bis-(2, 6-diisopropylphenyl)imidazol-2-ylidene
Me	methyl
min	minute(s)
NHC	*N*-heterocyclic carbene
PCC	pyridinium chlorochromate
n-Pent	pentyl

Ph	phenyl
i-Pr	isopropyl
n-Pr	propyl
rt	room temperature
TBAF	tetrabutylammonium fluoride
TBS	*tert*-butyldimethylsilyl
THF	tetrahydrofuran
TLC	thin layer chromatography
Tol	toluene

Abstract

A highly regioselective nickel-catalyzed reductive couplings of propargyl alcohol derivatives and aldehydes have been developed. Consideration of the interplay of sterics and electronics between reactive starting materials and the $Ni(COD)_2$/NHC/R_3SiH catalyst system allows for a strategy to predictably control regiochemistry in the coupling of propargyl alcohol derivates, aldehydes, and silanes. The derivatization of these products can lead to several otherwise largely inaccessible regioisomers in an indirect but efficient manner.

The ability to reverse alkyne regioselectivity via divergent chemical pathways is known, but to do so with high selectivity across a broad range of substrates is unprecedented. With internal alkynes that lack a strong steric or electronic bias, regioselective couplings to provide either regioisomer selectively are now possible, whereas previously reported protocols were uniformly unselective. With alkynes that possess a strong steric and/or electronic bias, such as aryl alkynes, 1,3-enynes, or terminal alkynes, only a single regioisomer was previously accessible, but our strategy now allows either regioisomer to be selectively obtained. Therefore, the ligand-based control reported herein can override even substantial substrate biases. This study thus provides the first general strategy for controlling regioselectivity in the reductive coupling of aldehydes and alkynes. Regioselectivity reversal for the range of alkynes studied herein rivals that documented for any class of alkyne 1,2-difunctionalization processes.

Studies are ongoing for a general regio- and enantioselective nickel-catalyzed aldehyde–alkyne reductive coupling using chiral *N*-heterocyclic carbenes.

Chapter 1[1]

Nickel-Catalyzed Reductive Couplings and Cyclizations

1. Introduction

Many classes of standard organic transformations involve the coupling or cycloaddition of two different π-components to assemble a more functionalized product. Many such processes are amenable to the union of two complex fragments, thus allowing convergent approaches to complex organic molecules. Diels Alder cycloadditions, Prins addition reactions, and ene reactions are examples of broadly useful processes that involve the union of two π-components in a selective manner. As a complement to these classical transformations, the *reductive* coupling of two π-components provides an alternative strategy for assembly of complex fragments from the same types of starting materials.[2-9] Whereas the starting components resemble those required for the types of standard organic transformations noted above, the products obtained structurally differ and are obtained in a reduced oxidation state based on the action of the reducing agent employed.

A number of transition metal catalyst/reducing agent combinations are known to promote various reductive coupling processes. In addition to the nickel-catalyzed variants that are the subject of this chapter, important advances have been made with titanium-,[10-14] iridium-,[15] and rhodium-catalyzed variants.[16] Many reducing agents have been employed, and the most widely used classes include silanes, organozincs,

organoboranes, molecular hydrogen, and alcohols. The specific focus of this chapter will be the development of nickel-catalyzed reductive couplings and cyclizations between a polar π-component and a non-polar π-component. This strategy allows the two π-components to be differentiated in catalytic reactions, and thus avoids homocoupling processes that are often problematic in transformations of this type. The use of either aldehydes or α,β-unsaturated carbonyls as the polar component, and alkynes as the non-polar component have been a primary focus of our laboratories; however, only aldehyde–alkyne couplings will be discussed. Extensive related developments involving dienes as the non-polar component have been reported by the laboratories of Mori,[17] Sato,[18] and Tamaru[19] have been reviewed elsewhere[4] and will not be extensively discussed in this chapter. In addition to advances from our laboratory, seminal contributions from the Jamison group are described in various sections of this chapter.

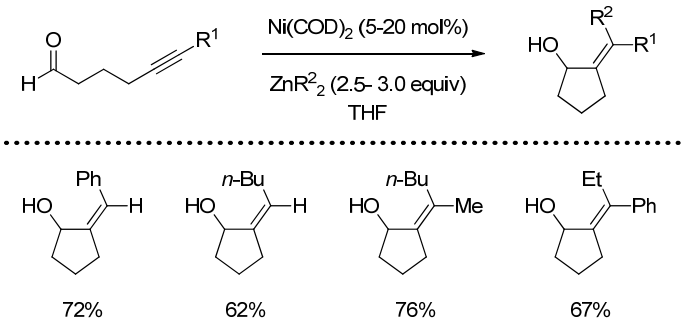
Since the first reported example of nickel-catalyzed cyclization of ynals in 1997, many variants now exist that undergo either alkylative (transferring a carbon substituent) or reductive (transferring a hydrogen atom substituent) coupling. The methodology has been applied to both inter- and intramolecular couplings, allowing access to acyclic products and small or macrocyclic ring systems. In this nickel-catalyzed process, COD-stabilized zero-valent nickel, monodentate phosphine or *N*-heterocyclic carbene (NHC) ligands, and a reducing agent such as a silane, organozinc, organoborane, or vinylzirconium reagent are typically used. There are several mechanistic insights that have emerged that shed light onto the subtle aspects that govern the reactivity and outcome of various nickel-catalyzed processes. These protocols have been applied in complex settings, illustrating their utility in the total synthesis of various natural products.

1.1. Three-Component Couplings via Alkyl Group Transfer – Method Development

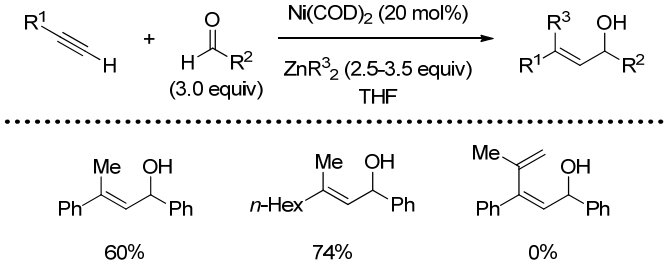
The nickel-catalyzed alkylative coupling of aldehydes and alkynes was first described using organozinc reducing agents.[20] Using methodology previously developed for the intramolecular coupling of alkynyl enones, derivatives of 5-hexynal were cyclized in the presence of $Ni(COD)_2$ and various organozinc reducing agents to afford cyclic allylic alcohols with stereodefined exocyclic tri- or tetrasubstituted olefins. The methodology was tolerant of a variety of alkyne substitutions as well as various organozinc reducing agents (Scheme 1).

Intermolecular couplings involving aldehydes, terminal alkynes, and organozincs also proceeded with high levels of chemo- and regioselectivity (Scheme 2). However, unlike intramolecular couplings, direct addition of more reactive organozincs to the aldehyde component competed with the desired three-component coupling. As a result, the scope of the intermolecular variant is limited to the use of sp^3 hybridized organozinc reagents, as sp^2 hybridized organozincs add to the aldehyde much faster than the three-component couplings occur.

Scheme 1. *Intramolecular Aldehyde–Alkyne Alkylative Coupling*

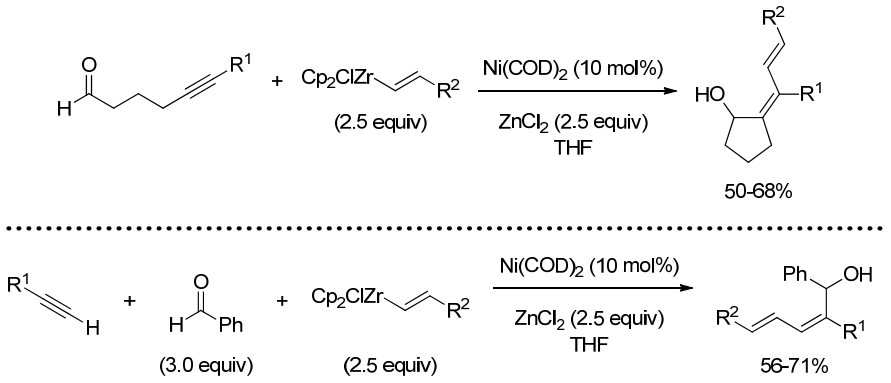


Scheme 2. *Intermolecular Aldehyde–Alkyne Alkylative Coupling*

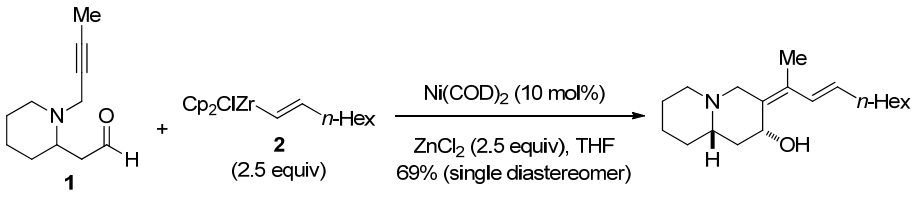


The studies above illustrate the limitations associated with organozinc reducing agents in the intermolecular alkylative coupling of aldehydes and alkynes. However, alkenylzirconium reducing agents, derived from hydrozirconation of alkynes, participated in both inter- and intramolecular coupling reactions without suffering competing addition to the carbonyl (Scheme 3).[21] This methodology provides a facile entry to functionalized cyclic or acyclic 1,3-dienes, and expands the generality of the multicomponent coupling to include the introduction of sp^2 hybridized centers from the reducing agent. While aromatic, aliphatic, and terminal alkynes were tolerated in the intramolecular coupling, more highly functionalized ynals were also good substrates, as evidenced by the efficient cyclization of substrate **1** with the vinylzirconium reagent **2** (Scheme 4).

Scheme 3. *Synthesis of 1,3-Dienes*



Scheme 4. *Diastereoselective Synthesis of 1,3-Dienes*



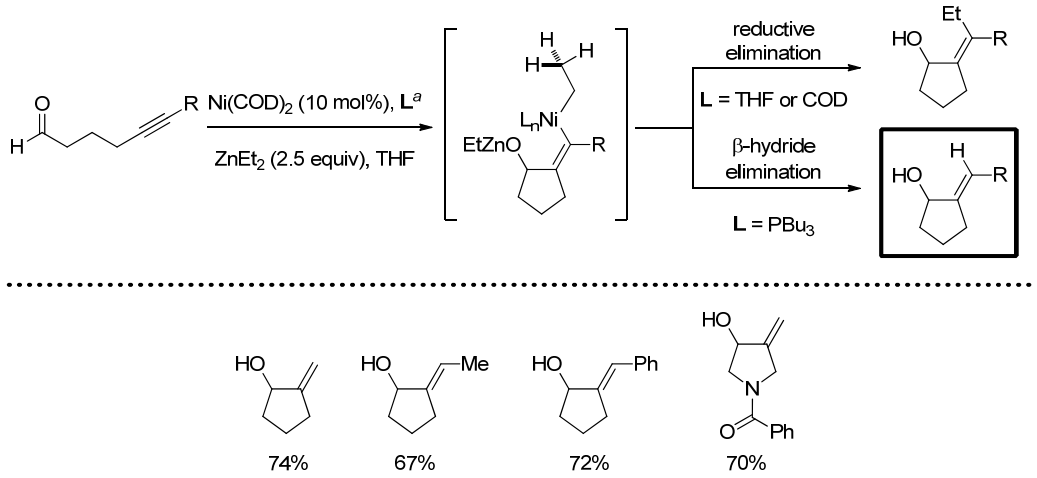
1.2. Reductive Couplings via Hydrogen Atom Transfer – Method Development

The field of nickel-catalyzed reductive couplings has seen substantial interest in the past decade and numerous advances have been made in the area. There now exist several protocols, including simple aldehyde/alkyne coupling, diastereoselective variants using transfer of chirality, asymmetric variants using either chiral monodentate phosphine or NHC ligands, and macrocyclization methodology for which there are both diastereoselective and asymmetric variants.

1.3. Simple Aldehyde and Alkyne Reductive Couplings

The nickel-catalyzed aldehyde-alkyne reductive coupling was first reported using a $Ni(COD)_2/PBu_3$ catalyst system with $ZnEt_2$ as the reducing agent.[20] Various ynals were cyclized to produce allylic alcohols in good yield with complete hydrogen atom transfer (Scheme 5). It is important to state that organozinc mediated reductive coupling can only be achieved when zero-valent nickel is pretreated with tributylphosphine and used with organozinc reducing agents bearing β-hydrogens. However, under these specific reaction conditions, the methodology is limited to intramolecular couplings only, and requires the use of highly reactive reducing agents such as $ZnEt_2$.

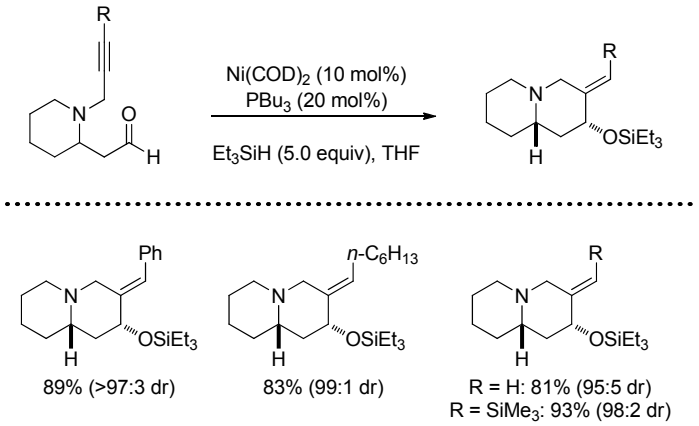
Scheme 5. *Catalyst-Controlled Alkylative or Reductive Coupling Pathways*



[a] 20 mol% of PBu_3 is used for reductive coupling.

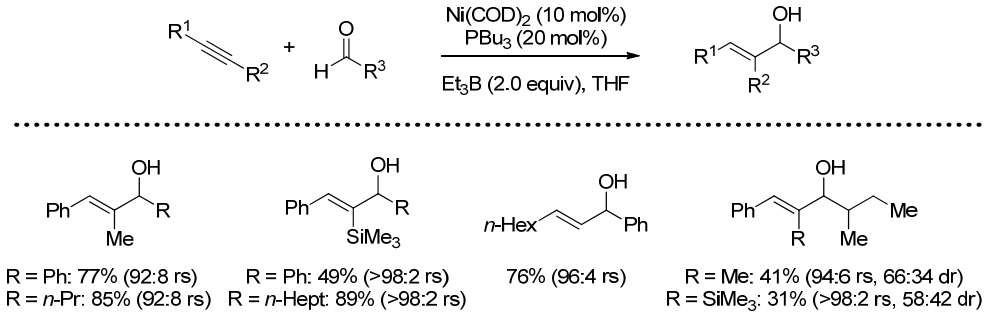
The combination of monodentate phosphine ligands and silane reducing agents proved to be a much more effective process in intramolecular couplings, and involves the use of a mild, bench-stable reducing agent.[22,23] This methodology was developed for the total synthesis of (+)-allopumiliotoxin 267A, (+)-allopumiliotoxin 339A, and (+)-allopumiliotoxin 339. High yields and excellent diastereoselectivities were observed in the synthesis of bicyclic substrates (Scheme 6). However, the PBu_3/Et_3SiH combination was not amenable for intermolecular reductive couplings, for which there are generally two reaction systems conducive for coupling, namely either $Ni(COD)_2/PR_3/BEt_3$ or $Ni(COD)_2$/NHC/Et_3SiH reagent combinations.

Scheme 6. *Silanes as Reducing Agents in Aldehyde–Alkyne Couplings*



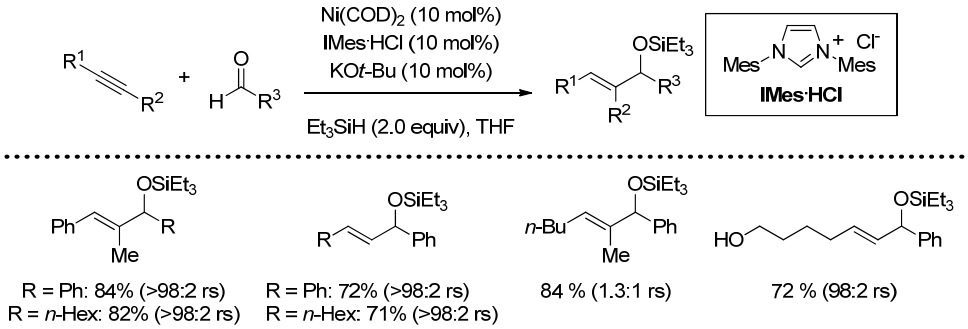
The first nickel-catalyzed intermolecular reductive coupling utilized the combination of COD-stabilized zero-valent nickel, monodentate phosphine ligands, and a borane reducing agent (Scheme 7).[24] The process works best for aromatic alkynes but is quite tolerant of various aldehydes.

Scheme 7. *Nickel-Catalyzed Et_3B-Mediated Reductive Couplings*



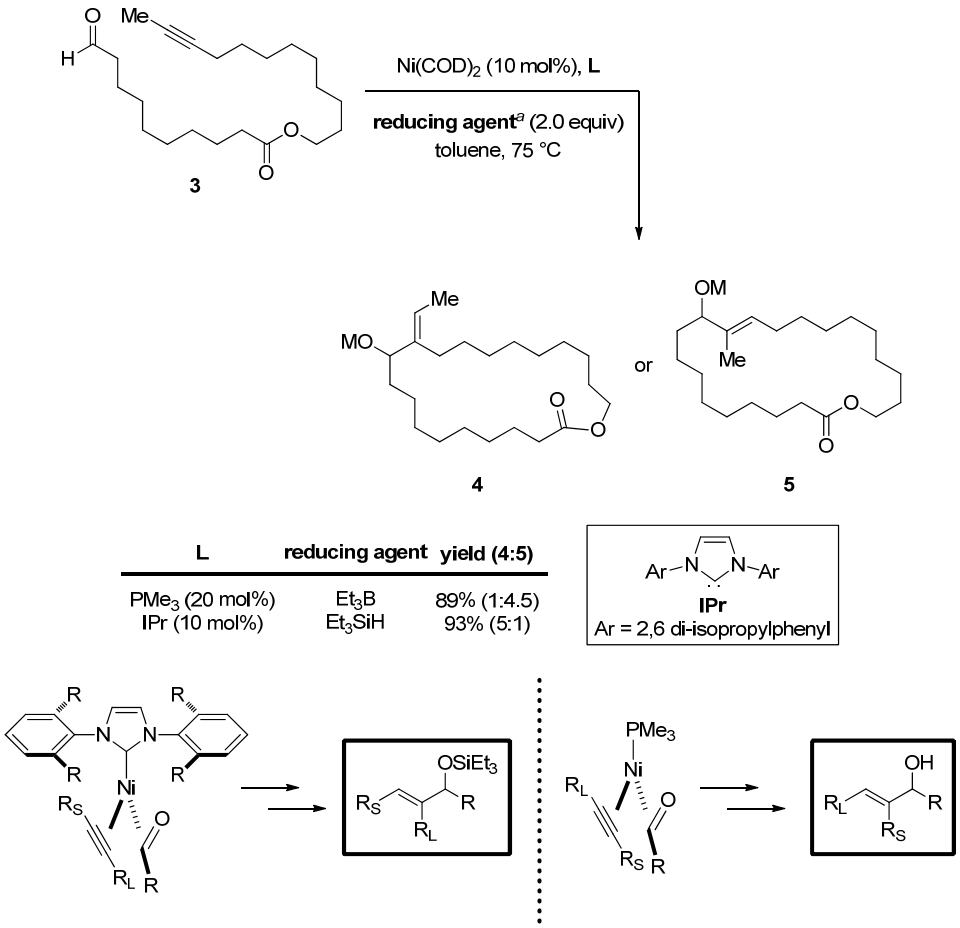
Another effective catalyst system for intermolecular reductive coupling is the combination of $Ni(COD)_2$/NHC with Et_3SiH as a stoichiometric reducing agent (Scheme 8).[25] The NHC catalyst is more reactive than analogous phosphine-based catalysts and a broad range of alkynes and aldehydes undergo reductive coupling under these conditions.

Scheme 8. *Nickel-Catalyzed Silane-Mediated Reductive Couplings*



Macrocyclization via nickel-catalyzed reductive coupling has been shown to be a powerful tool in the synthesis of several natural products, including amphidinolide T1,[26] amphidinolide T4,[26] (–)-terpestacin,[27] and aigialomycin D.[28] A general protocol for nickel-catalyzed macrocyclizations was published using ligand-based control of regioselectivity (Scheme 9).[29] $Ni(COD)_2/PBu_3/BEt_3$ and $Ni(COD)_2$/NHC/Et_3SiH combinations are both effective and complementary in reductive macrocyclizations. Ynal **3** was cyclized to afford the endocyclic product **5** in 89% yield with a 4.5:1 regioselectivity using a $Ni(COD)_2/PBu_3$ catalyst system and Et_3B reducing agent. However, with the $Ni(COD)_2$/NHC catalyst system and Et_3SiH reducing agent, the regioselectivity is reversed to favor the exocyclic product **4** which was formed in 93% yield and a 5:1 regioselectivity.

Scheme 9. *Regiocontrol in Nickel-Catalyzed Macrocyclizations*



R_S = Small Substituent. R_L = Large Substituent.

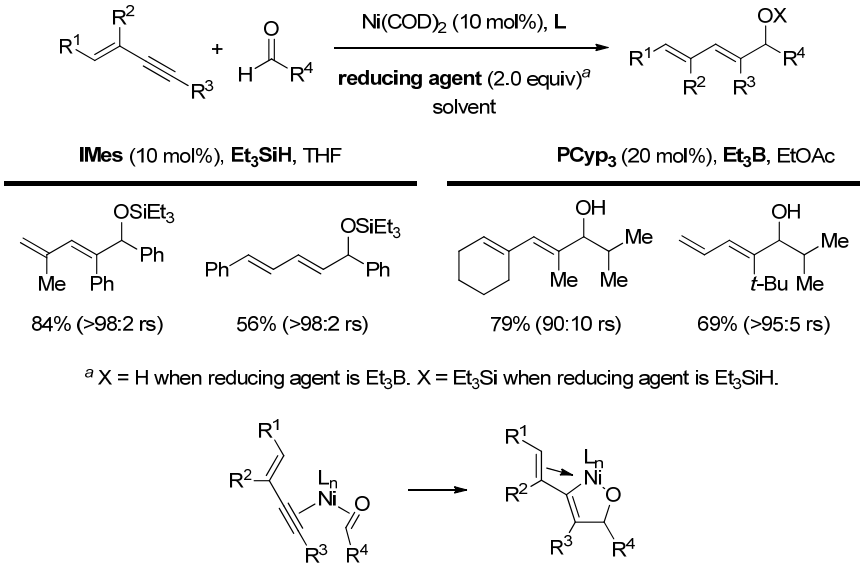
[a] X = H when reducing agent is Et_3B. X = Et_3Si when reducing agent is Et_3SiH.

1.4. Directed Processes

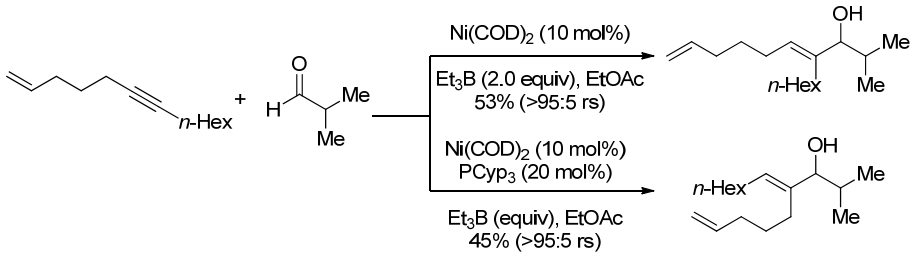
The reductive coupling of 1,3-enynes and aldehydes has been shown to be an extremely regioselective reaction, yielding high levels of regiocontrol for both the NHC/Et_3SiH and PBu_3/Et_3B combinations (Scheme 10).[25,30] The conjugated olefin of the 1,3-diene directs coupling to take place at the alkyne terminus distal to the alkene moiety. Olefin-directed couplings are also shown to be exceptionally effective in 1,6-enyne–aldehyde couplings, providing a high level of regiocontrol dependent on ligand structure and stoichiometry (Scheme 11).[31-33] Mechanistic considerations for such

control of regioselectivity for both 1,3- and 1,6- enynes will be discussed in a later section.

Scheme 10. *Aldehyde–1,3-Enyne Reductive Couplings*



Scheme 11. *Aldehyde–1,6-Enyne Reductive Couplings*



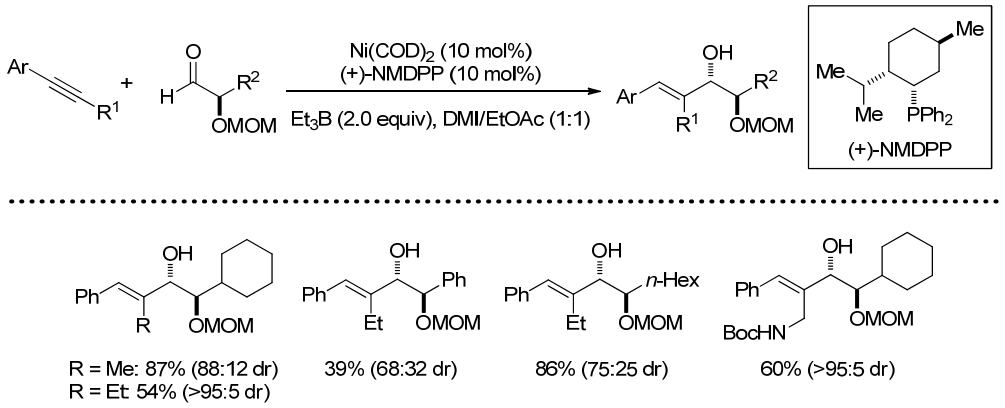
1.5. Diastereoselective Variants: Transfer of Chirality

Reductive cyclizations have been shown to be diastereoselective in the synthesis of bicyclic products as well as various macrocycles. There are also instances of chirality transfer in intermolecular reductive couplings. The synthesis of *anti* 1,2-diols has been demonstrated using α-alkoxyaldehydes with a methoxymethyl ether (MOM) protecting

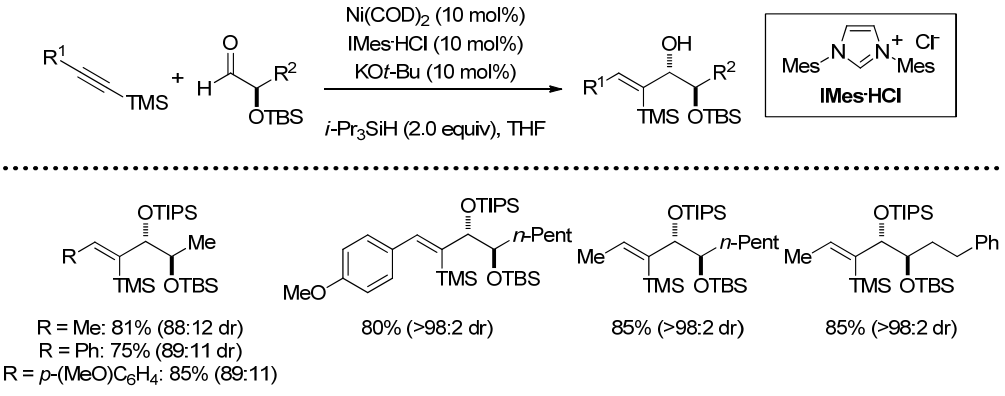
group and mono-aryl internal alkynes (Scheme 12).[34] Diastereoselectivities are high for the formation of *anti* 1,2-diols in cases where the aldehyde has a branched sp^3 β-carbon.

A similar protocol employs α-silyloxyaldehydes with a *t*-butyldimethylsilyl (TBDMS) protecting group and TMS-protected alkynes.[35] In this protocol, β-unbranched aldehydes afforded the highest level of diastereoselectivity (Scheme 13). The method is general for both aromatic and non-aromatic alkynes and complements the prior report in terms of scope.

Scheme 12. *Diastereoselective Nickel-Catalyzed Aldehyde–Alkyne Couplings*

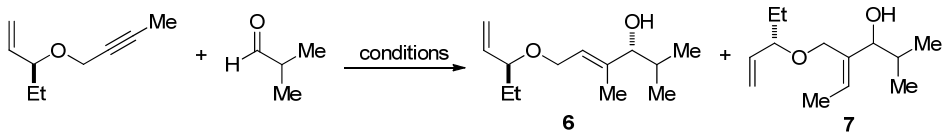


Scheme 13. *Diastereoselective α-Siloxy Aldehyde–Alkyne Couplings*



The transfer of chirality is not limited to chiral aldehydes. It has been shown that in 1,6-enyne–aldehyde couplings, a chiral moiety on the 1,6-enyne could make the process diastereoselective (Scheme 14).[32,33] If no phosphine ligands are employed, **6** was formed in >95:5 regioselectivity and 95:5 diastereoselectivity. However, the use of tricyclopentylphosphine as a ligand led to reversal of regioselectivity with no chiral induction in the resulting allylic alcohol subunit of **7**. The mechanistic implications of this process will be discussed in a later section.

Scheme 14. *Chirality Transfer in Aldehyde–Alkyne Reductive Couplings*

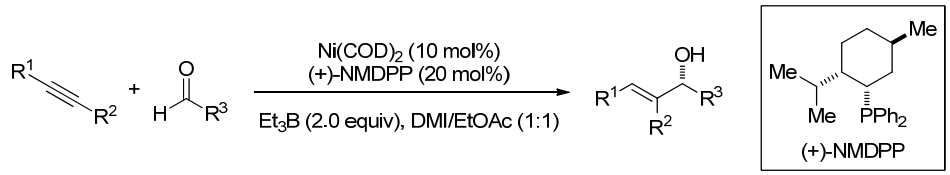


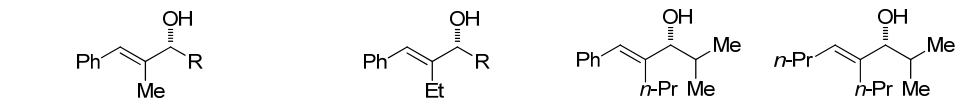
Reaction Conditions	**6**:**7**	dr **6**	dr **7**
$Ni(COD)_2$ (10 mol%) Et_3B (2 equiv)	> 95:5	95:5	—
$Ni(COD)_2$ (10 mol%) $PCyp_3$ (20 mol%) Et_3B (2 equiv)	< 5:95	—	45:55

1.6. Asymmetric Variants

Two general protocols exist for nickel-catalyzed reductive couplings of aldehydes and alkynes. The first employs (+)-NMDPP as a chiral monodentate phosphine ligand. Internal aromatic alkynes were shown to undergo reductive coupling in good yields with enantioselectivities ranging from 42%–96% *ee* (Scheme 15).[36] The scope of this asymmetric reaction is limited to aryl-substituted alkynes, and α-branched aldehydes provide the highest levels of asymmetric induction.

Scheme 15. *Asymmetric Nickel-Catalyzed Et_3B-Mediated Reductive Couplings*





R = *i*-Pr: 95% (90% ee)
R = *n*-Pr: 82% (65% ee)
R = *c*-Hex: 97% (90% ee)
R = Ph: 79% (91:9 rs, 73% ee)

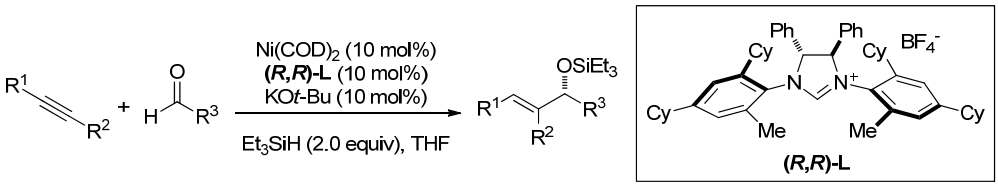
R = *c*-Hex: 78% (89% ee)
R = *i*-Pr: 95% (90% ee)

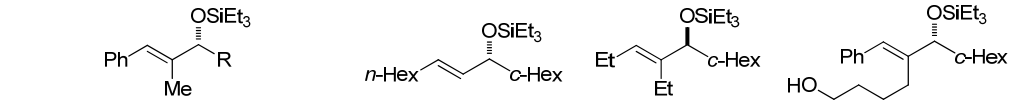
74% (92% ee)

35% (42% ee)

The second protocol for asymmetric nickel-catalyzed reductive coupling utilizes chiral NHC ligands (Scheme 16).[37] The scope was general for alkynes and aldehydes, and enantioselectivities ranged from 65%–85% *ee*. Both internal and terminal aromatic or non-aromatic alkynes were effective participants, as were aromatic and aliphatic aldehydes.

Scheme 16. *Asymmetric Nickel-Catalyzed Silane-Mediated Reductive Couplings*





R = Ph: 98% (10:1 rs, 78% ee)
R = *i*-Pr: 86% (>19:1, 70% ee)
R = c-Hex: 78% (>19:1 rs, 81% ee)
R = *n*-Hex: 70% (10:1 rs, 73% ee)

64% (>19:1 rs, 65% ee)

84% (85% ee)[a]

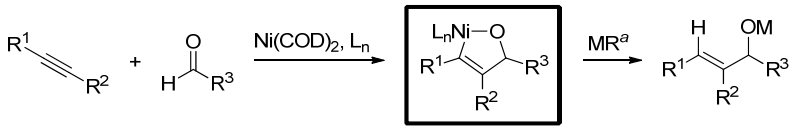
99% (9:1 rs, 79% ee)

[a] **(*S*,*S*)-L** was used to obtain this stereoisomer.

1.7. Mechanistic Insights

Several mechanistic pathways have been proposed for nickel-catalyzed aldehyde–alkyne reductive couplings, and an overview of the possible mechanisms has been provided elsewhere.[4] Therefore, this description will focus on what is generally believed to be the operative mechanism. The key features of this mechanism are the oxidative cyclization of a zero-valent nickel aldehyde–alkyne complex to form a five-membered oxametallacycle, followed by reductive cleavage of the nickel-carbon bond, and carbon–hydrogen bond formation via reductive elimination (Scheme 17).

Scheme 17. *Postulated Mechanism for Aldehyde–Alkyne Couplings*



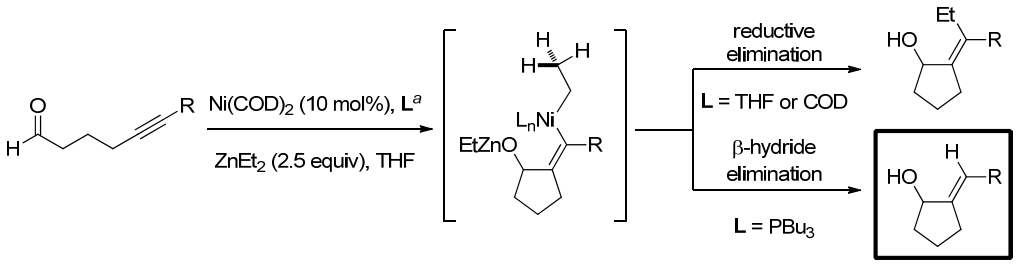
nickel(II)-oxametallacycle

[a] MR = Reducing Agent.

Being able to tune nickel-catalyzed couplings from an alkylative to a reductive pathway has been demonstrated not only in couplings of alkynes and α,β-unsaturated carbonyls but alkynes and aldehydes as well. Using a $Ni(COD)_2$ catalyst system and organozinc reagents, ynals were efficiently cyclized to produce exocyclic allylic alcohols with alkyl transfer at the terminus of the exocyclic olefin (Scheme 18).[20] However, in a $Ni(COD)_2/PBu_3$ catalyst system with β-hydrogen-bearing organozincs, a reductive coupling pathway could be achieved with transfer of a hydrogen atom substituent at the distal carbon of the newly formed olefin. This change in reaction mechanism is unique to the intramolecular variant, as identical reaction conditions in the intermolecular variant did not allow crossover from alkylative to reductive coupling. However, the ability to change mechanism in the intramolecular system from an alkylative to a reductive

pathway suggests that the electronic environment on the nickel-center plays an important role in chemical reactivity and reaction outcome. The σ-donation to the metal-center that results from the addition of phosphine ligands can enable the nickel catalyst to undergo β-hydride elimination.

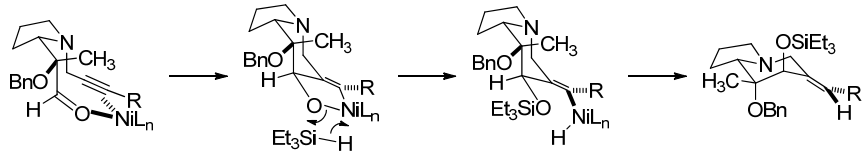
Scheme 18. *Role of Ligands in Alkylative and Reductive Pathways*



[a] 20 mol% of PBu_3 is used for reductive coupling.

Stereo- and regiocontrol via nickel-catalyzed reductive coupling is illustrated in the construction of the indolidizine skeleton of (+)-allopumiliotoxin 267A via nickel-catalyzed ynal cyclization (Scheme 19).[22,23] The prerequisite of forming two adjoining rings likely allows for a single, highly ordered nickel-metallacycle **8** to be preferentially formed. σ-Bond metathesis, followed by reductive elimination, leads to a single observable diastereomer in 93% yield.

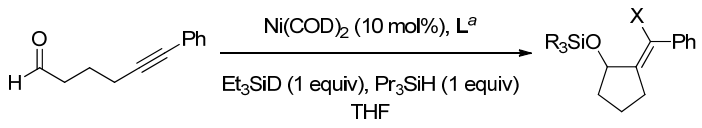
Scheme 19. *Postulated Mechanism for Silane-Mediated Couplings*



8

A mechanistic probe was developed involving crossover experiments with Et_3SiD and Pr_3SiH that would allow for a comparison of reaction mechanisms in different ligand classes (Scheme 20).[25] For the $Ni(COD)_2$/IMes catalyst system, results were similar in both inter- and intramolecular reductive couplings, with little or no crossover observed. Products **10** and **11** were produced in 55% and 41% yield, respectively, and crossover products **9** and **12** were observed in <2% yield each, consistent with a metallacycle-based mechanism. However, in the $Ni(COD)_2/PBu_3$ catalyst system, significant crossover was observed, with **9**, **10**, **11**, and **12** produced in a 25:34:23:18 ratio. This result implies a change of mechanism, and the origin of this outcome is currently being studied.

Scheme 20. *Crossover Studies*

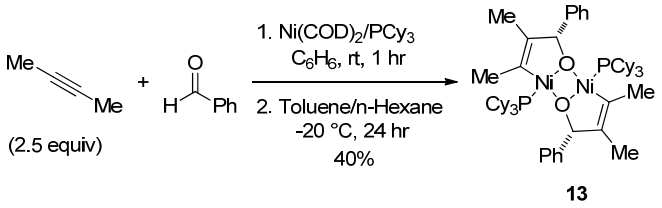


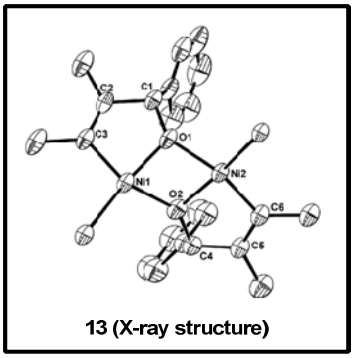
[a] 10 mol% IMes·HCl with 10 mol% *n*-BuLi was used. 20 mol% PBu_3 was used.

			relative %	
R	**X**	**product**	**IMes**	**PBu_3**
Et	H	**9**	<2	25
Et	D	**10**	55	34
Pr	H	**11**	41	23
Pr	D	**12**	<2	18

Evidence for the existence of a nickel-metallacycle intermediate has been demonstrated by the Ogoshi group.[38] Ogoshi and coworkers were able to obtain a crystal structure of oxametallacycle complex **13** generated from an aldehyde, alkyne, $Ni(COD)_2$, and PCy_3, which exists as an oxygen-bound dimer (Scheme 21).

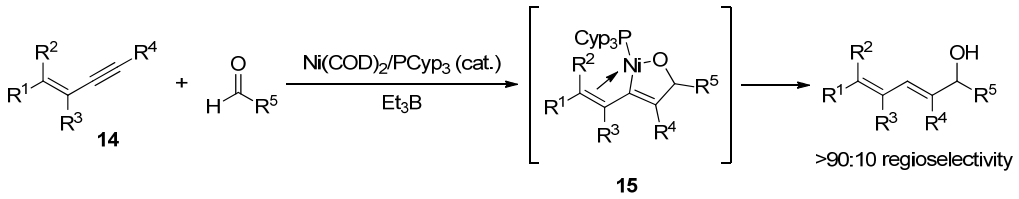
Scheme 21. *X-Ray of Metallacycle Intermediate*





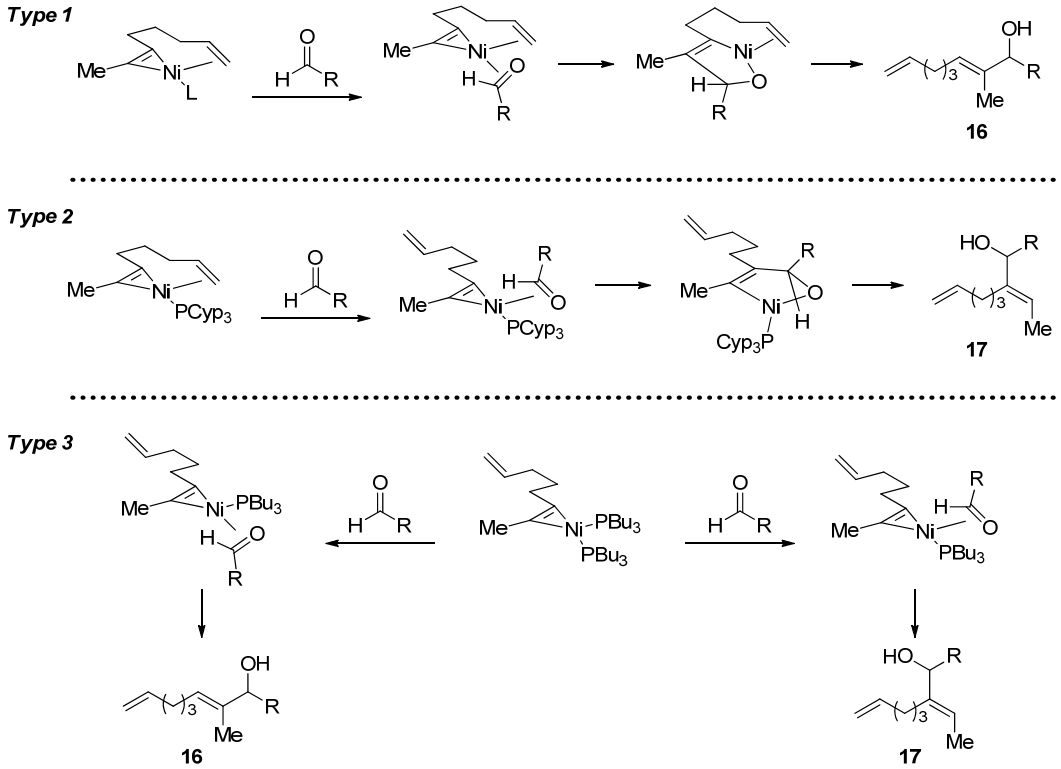
The formation of an oxametallacycle intermediate has also been proposed in couplings of 1,3- or 1,6-enynes with aldehydes.[30-33] In the use of conjugated enynes, this directed process works for both $Ni(COD)_2/NHC/R_3SiH$ and $Ni(COD)_2/PR_3/BEt_3$ reaction systems. Precoordination of the enyne **14** to form metallacycle **15** can explain the excellent regioselectivities in this process (Scheme 22). 1,6-Enynes have also proven to be interesting both synthetically and mechanistically. Three reaction pathways were proposed in which regioselectivities are rationalized (Scheme 23). In type 1 conditions (no phosphine, **L** = weakly bound ligand), regioselective metallacycle formation is dictated by olefin coordination, leading to regioisomer **16**. In type 2 conditions with a bulky tricyclopentylphosphine ($PCyp_3$) ligand, substitution of the alkyne by the aldehyde occurs, leading to the selective formation of the opposite regioisomer, **17**. However, when tributylphosphine is used in type 3 conditions, the reaction is made unselective, leading to formation of both possible regioisomers since either phosphine in the bis-phosphine adduct can be substituted by the aldehyde.

Scheme 22. *Directed Aldehyde–1,3-Enyne Couplings*



14 15

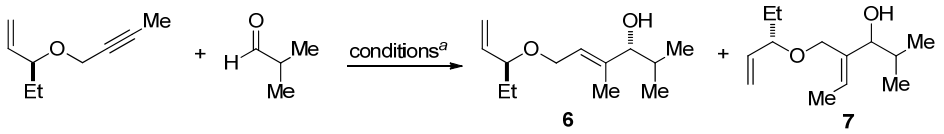
Scheme 23. *Postulated Origin of Regiocontrol in Aldehyde–1,6-Enyne Couplings*



16 17

This mechanistic rationale is further supported by transfer of chirality from the 1,6-enyne to product **6**, which was produced in >95:5 regioselectivity and 95:5 diastereoselectivity (Scheme 24). When coordination of the olefin was disrupted by addition of $PCyp_3$, regioselectivity was reversed to <5:95 and diastereoselectivity was reduced to 45:55 of **7**. Therefore, it is implicit that olefin coordination leads to metallacycle formation in a regio- and diastereoselective manner.

Scheme 24. *Empirical Evidence for Metallacycle Pathway*

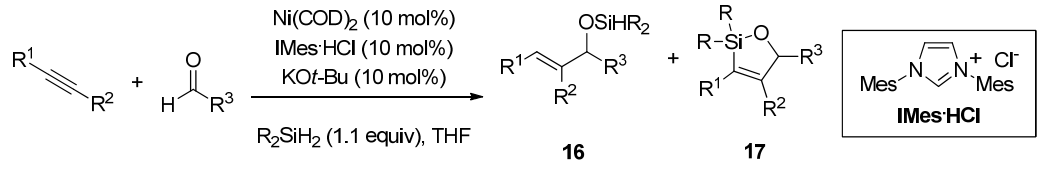


[a] $Ni(COD)_2$, Et_3B: **6**:**7** >95:5 rs (95:5 dr). $Ni(COD)_2$, $PCyp_3$, Et_3B: **6**:**7** <5:95 (45:55 dr **6**)

1.8. Cyclocondensations via hydrogen gas extrusion.

Based on the previously described crossover studies, it was proposed that the identity of the silane reducing agent would have little effect on the heterocoupling of aldehyde and alkyne π-components using the $Ni(COD)_2$/NHC catalyst system. In an effort to expand the scope and utility of nickel-catalyzed aldehyde alkyne couplings, dialkylsilane reducing agents were explored. It was shown that, in some instances, the expected silylated allylic alcohol **16** was accompanied by the concurrent formation of silacycle **17** (Scheme 25).[39]

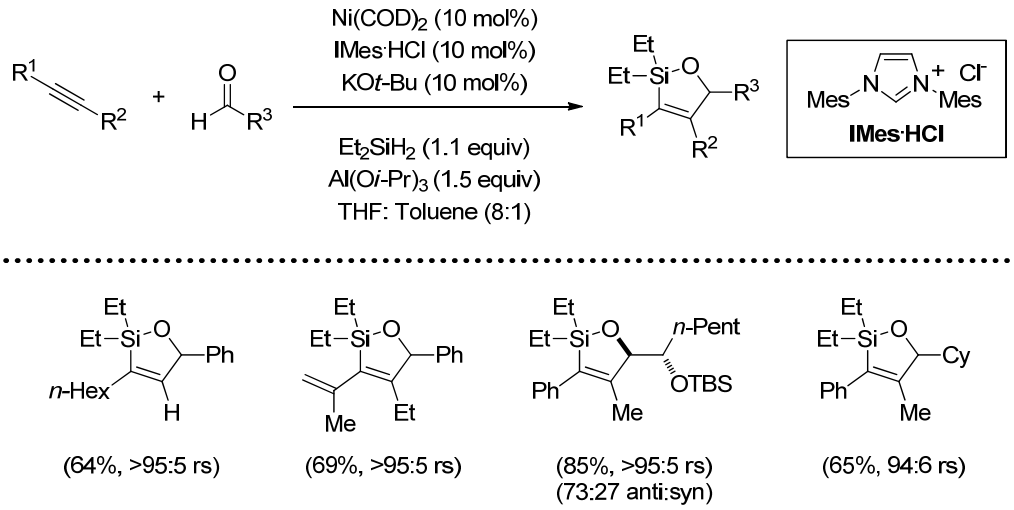
Scheme 25. *Use of Dialkylsilane Reducing Agents*



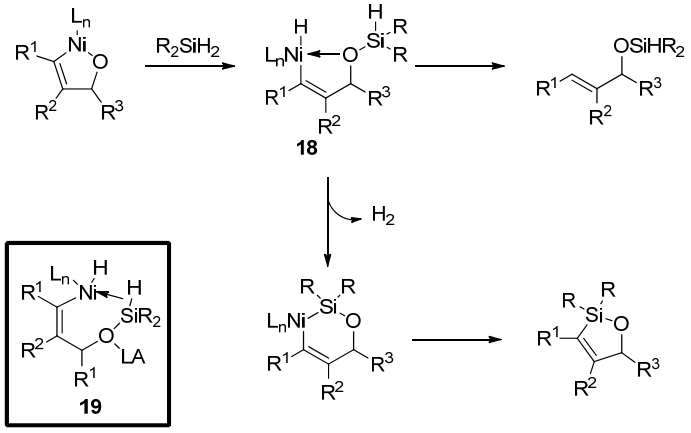
The formation of silacycle **17** was further promoted by alkoxy Lewis acids and represents a formal silylene transfer across the two π-components via the extrusion of an equivalent of H_2. The scope and generality of the dehydrogenative cyclocondensation of aldehydes, alkynes, and Et_2SiH_2 is similar to that of the reductive coupling of aldehydes, alkynes, and Et_3SiH (Scheme 26).[40]

Such similarity can be explained by the presence of vinyl nickel species **18** as a common intermediate in both processes (Scheme 27). The direct role of the Lewis acid is unclear, although disruption of a nickel-oxygen interaction in intermediate **18** via Lewis acid coordination to oxygen, as depicted in **19**, may facilitate H_2 extrusion.

Scheme 26. *Substrate Scope for Silacycle Formation*



Scheme 27. *Postulated Mechanism for Silacycle Formation*

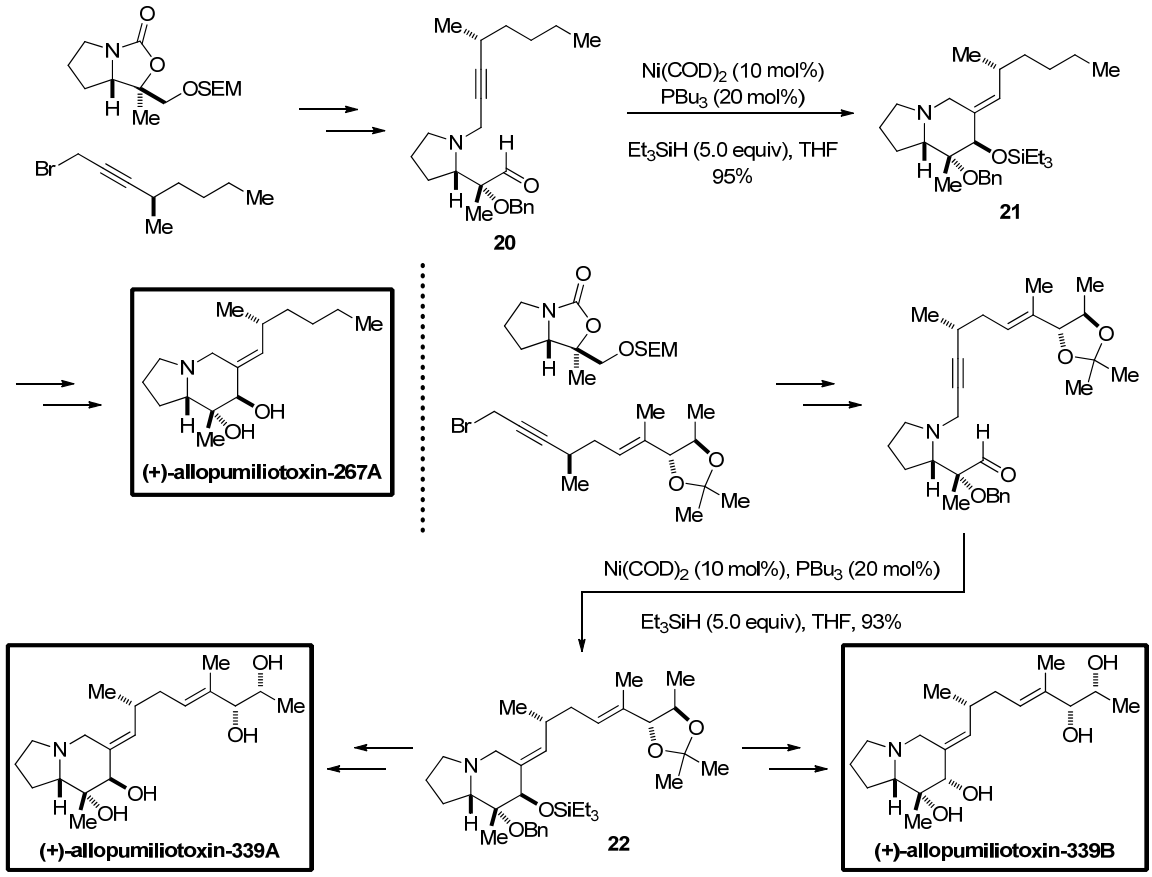


1.9. Use in Natural Product Synthesis

A defining feature of any synthetic methodology is its applicability in a complex environment. In this regard, nickel-catalyzed alkylative and reductive couplings of alkynes and aldehydes are especially robust as this methodology has been applied in the total synthesis of several natural products. For each of the following examples the general synthetic plan is briefly described, followed by the key nickel-catalyzed coupling step that is critical for the construction of the overall structural motif of the natural product in question.

The allopumiliotoxin alkaloids are some of most complex members of the pumiliotoxin class of indolizidine alkaloids. Their scarcity, difficulty of isolation, potent cardiotonic and myotonic activity have made them targets of several synthetic efforts, including total syntheses involving nickel-catalyzed reductive coupling as the key step. The first use of silane reducing agents in nickel-catalyzed reductive couplings of aldehydes and alkynes was highlighted in the total synthesis of (+)-allopumiliotoxin 267A, (+)-allopumiliotoxin 339A, and (+)-allopumiliotoxin 339B (Scheme 28).[22,23] Late-stage nickel-catalyzed cyclization using a $Ni(COD)_2/PBu_3$ catalyst system with Et_3SiH as a reducing agent proved to be instrumental in arriving at the bicyclic core of the pumiliotoxin class of indolizidine alkaloids in a highly diastereoselective fashion. Ynal **20** was cyclized to **21** in 95% yield as a single observable diastereomer, and subsequent deprotection steps led to the synthesis of (+)-allopumiliotoxin 267A. (+)-Allopumiliotoxin 339A and 339B were synthesized from a common intermediate **21**, which was produced as a single observable diastereomer in 93% yield.

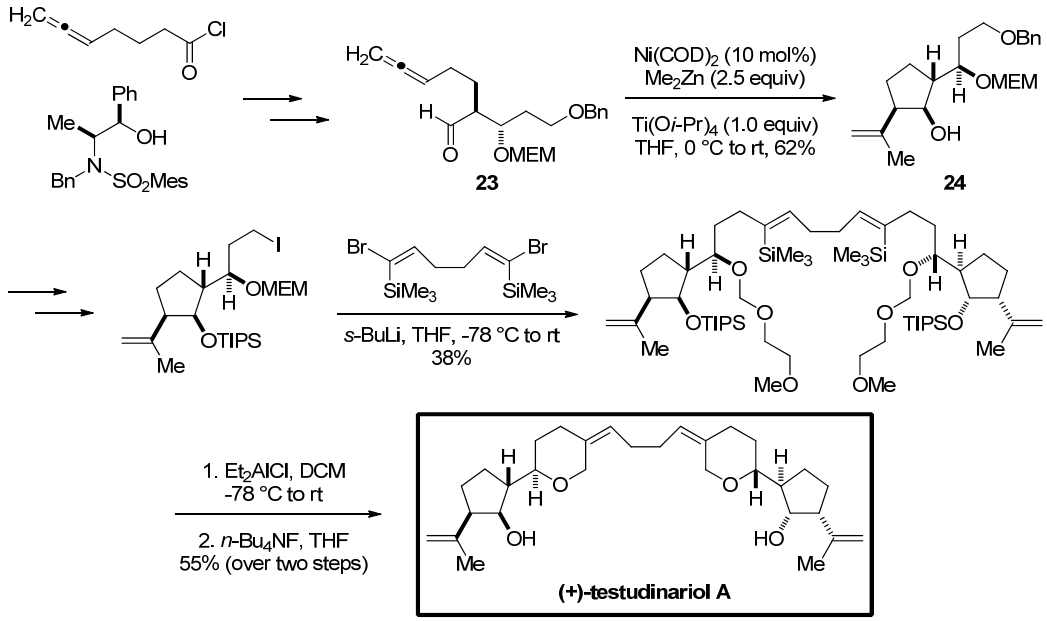
Scheme 28. *Total Synthesis of (+)-Allopumiliotoxin-339A and -339B*



Testudinariol A and B are epimeric triterpene marine natural products possessing a highly functionalized cyclopentanol framework with four contiguous stereocenters appended to a central 3-alkylidene tetrahydrofuran ring. A number of total syntheses of these natural products have been reported, including one that used the C_2-symmetric nature of (+)-testudinariol A to construct the framework in a two-directional synthesis (Scheme 29).[41] Nickel-catalyzed allene/aldehyde alkylative coupling is a closely related reaction to alkyne/aldehyde alkylative coupling and an application of this methodology is illustrated in the total synthesis of (+)-testudinariol A. This strategy proved successful, as **23** underwent alkylative coupling in the presence of a Lewis acid additive to afford **24** in 62% yield as a single observable diastereomer. This was followed by dianion

alkylation, a two-directional oxocarbenium ion/vinyl silane cyclization, and silyl deprotection to afford (+)-testudinariol A.

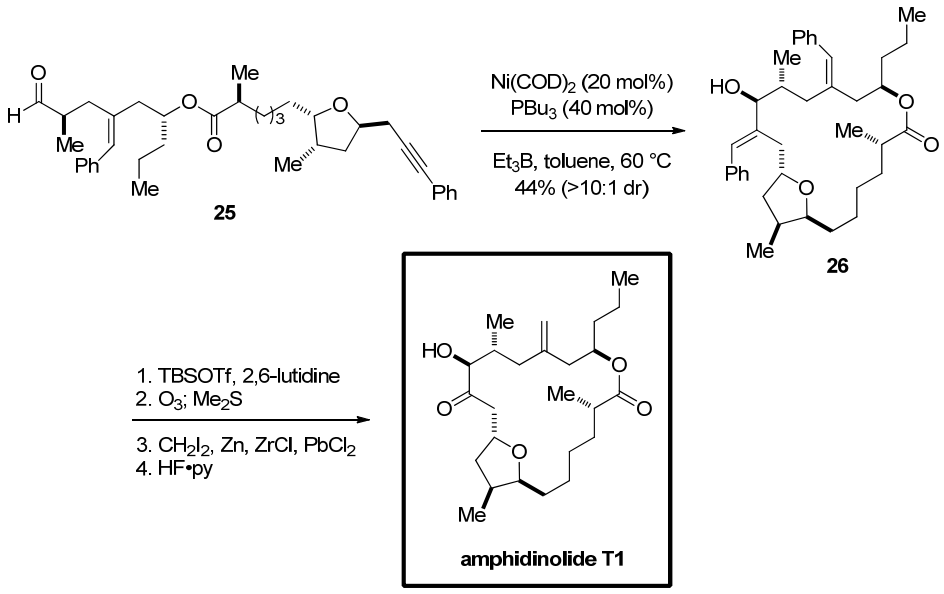
Scheme 29. *Total Synthesis of Testudinariol A*



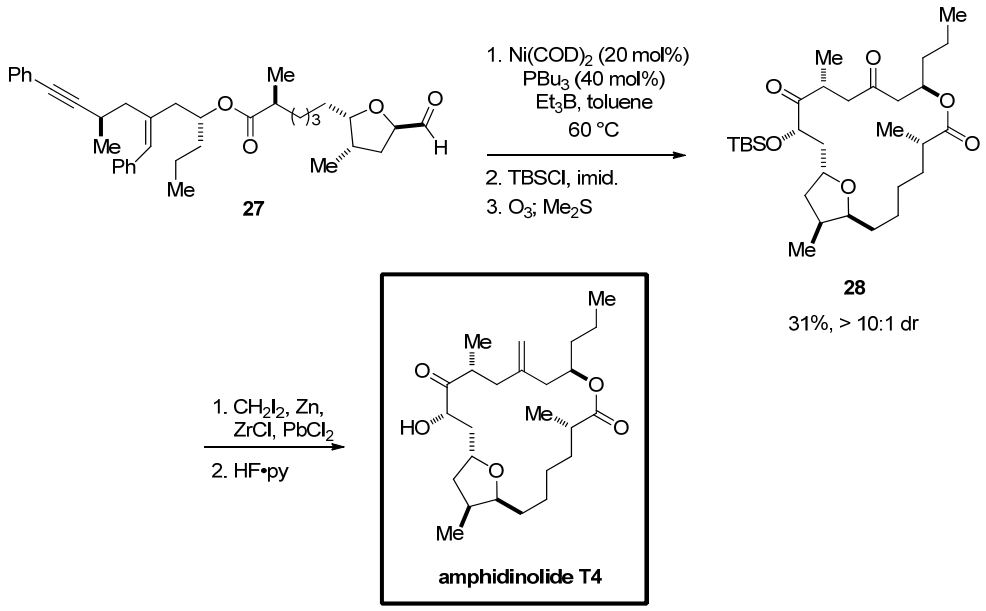
The amphidinolide family of marine natural products has attracted a great deal of interest from the synthetic community due to their structural diversity as well as their potent biological activity. In the synthesis of amphidinolide T1 (Scheme 30) and amphidinolide T4 (Scheme 31), late-stage nickel-catalyzed macrocyclization was employed to afford the core natural product structures.[26] Nickel-catalyzed macrocyclization offers a powerful and complementary method to macrolactonization to afford large macrocyclic rings of varying sizes. Several variants exist as the exact reaction conditions are predicated by the molecular scaffold in question.[29] As such, this strategy has been applied in the total synthesis of several complex natural products and this section will briefly highlight the synthesis of both amphidinolide T1 and amphidinolide T4. Macrocycle precursor **25** was cyclized to **26** in 44% yield with >10:1

diastereoselectivity. This was followed by protection, ozonolysis, Tebbe methylenation, and deprotection to afford amphidinolide T1. Cyclization product **28** was produced in 31% yield and >10:1 diastereoselectivity over three steps from **27**, followed by a similar endgame sequence to afford amphidinolide T4.

Scheme 30. *Total Synthesis of Amphidinolide T1*

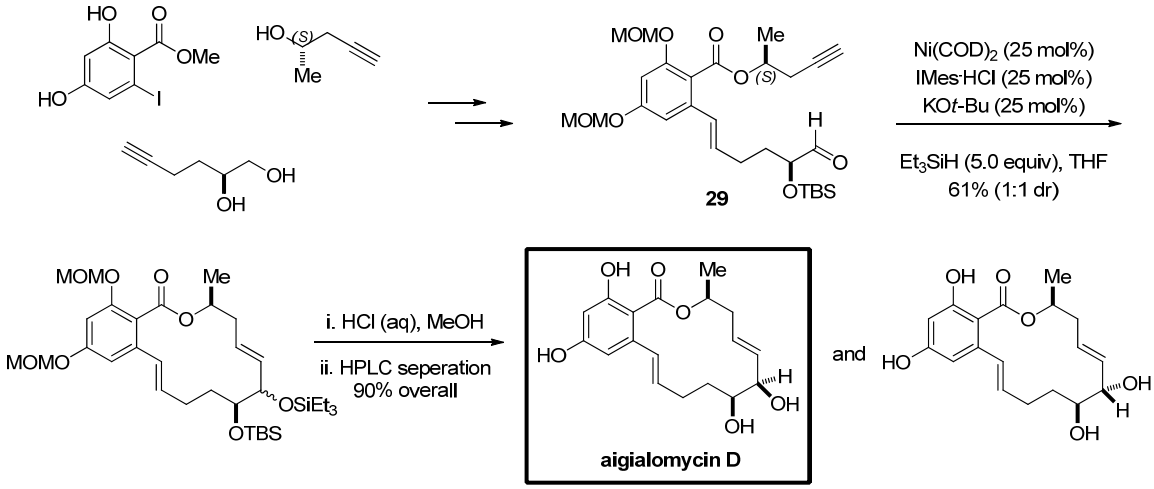


Scheme 31. *Total Synthesis of Amphidinolide T4*



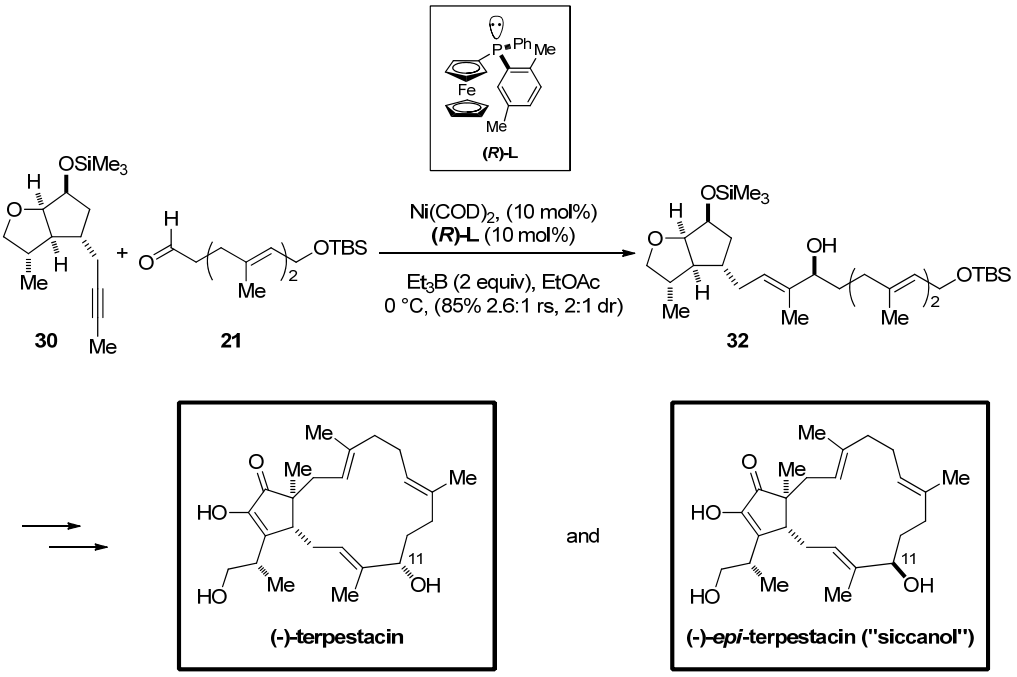
Resorcinylic macrolides are a family of natural products that possess a 14-membered macrolide core with a fused benzenoid subunit. A member of this family that has drawn significant scientific attention due to its antimalarial and cytotoxic activity is aigialomycin D. In one total synthesis of aigialomycin D, late-stage nickel-catalyzed macrocyclization was employed to afford the macrocyclic core (Scheme 32).[28] Macrolide precursor **29** was cyclized in 61% yield in a 1:1 diastereoselectivity. Subsequent global deprotection and HPLC purification afforded aigialomycin D and the allylic alcohol epimer in 90% overall yield.

Scheme 32. *Total Synthesis of Aigialomycin D*



The scientific community has given considerable attention towards the sesterterpene natural product (–)-terpestacin and several related scaffolds. (–)-Terpestacin has attracted synthetic interest due to its unique and challenging structural features along with its ability to inhibit angiogenesis. An enantiospecific total synthesis of both (–)-terpestacin and (+)-11-*epi*-terpestacin was conducted in the context of catalyst-controlled nickel-catalyzed reductive coupling of alkyne **30** and aldehyde **31** (Scheme 33).[27] The product **32** was formed in a 2.6:1 mixture of regioisomers, and a 2:1 diastereoselectivity in a combined 85% yield. A series of synthetic steps followed to afford both (–)-terpestacin and (+)-11-*epi*-terpestacin, which were differentiated only by their epimeric stereochemistry of the allylic alcohol subunit formed via nickel-catalyzed reductive coupling.

Scheme 33. *Total Synthesis of (+)-Epi- and (+)-Terpestacin*



1.10. Conclusions and Outlook

Multi-component coupling of differentiated π-systems in the presence of a zero-valent nickel catalyst can lead to many varied and unique structural motifs. The coupling of alkynes and α,β-unsaturated carbonyls results in the formation of functionalized γ,δ-unsaturated carbonyls containing stereodefined tri- or tetrasubstituted alkenes in a highly stereoselective manner. Allylic alcohols can be accessed by the coupling of alkynes and aldehydes, often with excellent levels of regio-, diastereo-, and enantioselectivity. Mechanistic investigation supports the presence of a metallacyclic intermediate being common to many of the nickel-promoted processes and mechanistic insight has led to the discovery and development of novel nickel-catalyzed processes.

Several issues regarding current methodology still exist such as control of regioselectivity of internal alkynes, asymmetric induction across a broad range of substrates, and complex mechanistic questions. These concerns are currently being

addressed by many research groups and new modifications of these processes as well as the development of new methodology will continue for some time. There should be a continued drive towards further increasing the simplicity and cost-effectiveness of the nickel pre-catalyst and reducing agents that participate in the types of coupling processes described in this chapter. This trend is evident in the shift from synthetically unfriendly pyrophoric reagents towards bench- and air-stable reagents that are widely commercially available. As these and other issues are addressed, these processes will be utilized with increasing frequency to afford solutions to intricate and interesting chemical challenges.

Chapter 2

Cooperativity of Regiochemistry Control Strategies in Reductive Couplings of Propargyl Alcohols and Aldehydes

2. Introduction

Regioselective coupling of π-components can be accomplished by many classical transformations such as Diels-Alder cycloadditions, Prins additions, and ene reactions to allow the convergent synthesis of complex organic molecules. A complement to these transformations that permits access to stereodefined allylic alcohols is the reductive coupling of aldehydes and alkynes.[5] Many important and synthetically divergent transformations utilize the reactivity of allylic alcohol derivatives, including π-allyl chemistry, directed epoxidation and cyclopropanation reactions, cationic cyclizations, S_N2' displacements, Claisen rearrangements, and other sigmatropic rearrangements. Numerous strategies have been reported that either involve stoichiometric (usually involving alkyne-derived vinyl organometallic reagents) or catalytic methods for the construction of allylic alcohols. The common challenge that plagues such intermolecular strategies is regiocontrol of alkyne insertion. Control of alkyne insertion is arguably the most challenging aspect of 1,2-difunctionalization methods development. The vast majority of regioselective additions to alkynes involve alkynes with a major size or electronic bias in the acetylenic substituents.[42] Internal alkynes with only subtle biases between the two acetylenic termini are notoriously difficult substrates for the

development of regioselective processes and are the focus of the research described in this chapter.

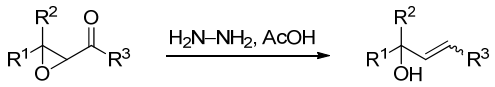
2.1. Synthetic Methods for the Synthesis of Allylic Alcohols

Allylic alcohols are a common structural motif found in natural products, synthetic intermediates, and drug molecules. The importance of this functional group has spawned many synthetic methods development efforts across the world. These protocols span the scope of classical to more modern transition metal-catalyzed multicomponent couplings. In this section, many of the most important and fundamentally useful methods will be highlighted. An effort will be made to show the progress and evolution of allylic alcohol synthesis strategies in literature. Furthermore, an effort will be made to highlight the major challenges faced in the field of reductive couplings and how the work described throughout this dissertation has helped lay the groundwork to solve these longstanding issues.

2.1.1. Early Methods for the Synthesis of Allylic Alcohols

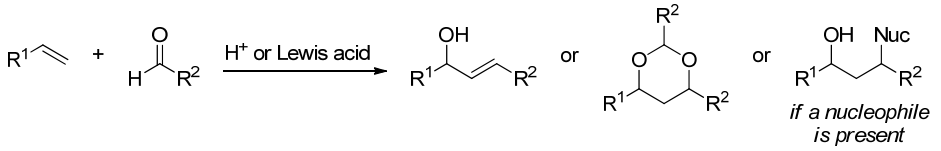
One of the earliest methods for the synthesis of allylic alcohols was the Wharton olefin synthesis (discovered in 1913, Scheme 34).[43] The conditions for the transformation are essentially identical to those of a standard Wolff-Kishner reduction, only that the Wharton olefin synthesis utilizes α,β-epoxy ketone starting materials. Although improvements and modifications have been made to this procedure, the scope remains limited due to the sensitivity of the starting materials and reagents. However, this reaction has been employed in many natural product syntheses despite its limitations.

Scheme 34. *The Wharton Olefin Synthesis*



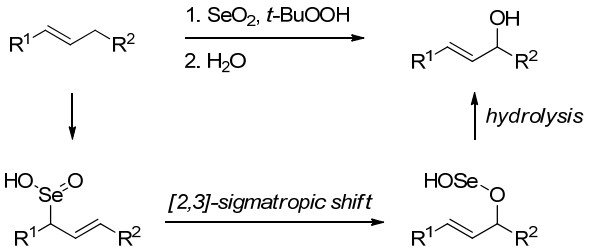
The development of the Prins reaction has given the chemical community an incredibly powerful and versatile transformation (discovered in 1919, Scheme 35).[44] The most impressive aspect of the Prins reaction is the diverse reactivity that can be developed through careful optimization of reaction conditions. A potentially large number of products can be formed by this method. The Prins reaction is extremely amenable to domino transformations and many research groups have exploited this aspect in elegant total synthesis studies.

Scheme 35. *The Prins Reaction*



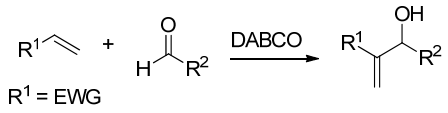
The Guillemonat variant of the Riley oxidation proceeds by reaction of an olefin with selenium dioxide in a manner similar to the ene reaction to form an allyl selenic acid, which then undergoes a sigmatropic shift to afford an allylic alcohol product (variant discovered in 1939, Scheme 36).[45] This variant has been well studied, and many classes of olefins can be utilized to afford a stereodefined allylic alcohol. However, problematic synthesis of multiple products may occur if numerous olefins exist. This reaction has been used in complex settings, but the examples were limited to systems where only one alkene was present.

Scheme 36. *The Guillemonat Variant of the Riley Oxidation*



The Morita-Baylis-Hillman reaction is an extensively studied and widely used reaction for the synthesis of allylic alcohols (discovered in 1968, Scheme 37).[46] This reaction has asymmetric variants that provide enantioselectivities up to 99% *ee*. Diastereoselectivities can also be quite high, depending on reaction conditions and substrate selection. The biggest shortcoming of this methodology is the limited substrate scope and long reaction times (which can be shortened for some cases by the use of organometallic Lewis acids). Despite its limitations, this reaction has seen much use in complex settings.

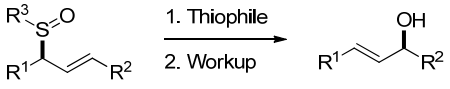
Scheme 37. *The Morita-Baylis-Hillman Reaction*



The Mislow-Evans rearrangement is another class of thermal rearrangements that results in the formation of an allylic alcohol (discovered in 1968, Scheme 38).[47] Mislow and coworkers disclosed the racemization of allylic sulfoxides under thermal conditions. Evans and coworkers recognized the potential of this protocol and exploited this reactivity by showcasing the synthesis of allylic alcohols using allylic sulfoxides. This reaction is highly stereoselective and the chirality of the sulfoxide can be transferred in

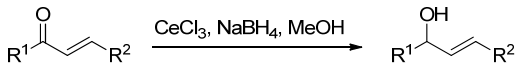
high levels. Almost exclusive formation of *E*-allylic alcohols are seen with the use of phosphite and amine thiophiles. Due to the high levels of chirality transfer and the ease of access to chiral sulfoxides starting materials, this method has seen much use in the synthesis of chiral allylic alcohol intermediates of natural products or in the penultimate step.

Scheme 38. *The Mislow-Evans Rearrangement*



One of the most classical methods for the synthesis of allylic alcohols is the 1,2-reduction of enones, known as the Luche reduction (discovered in 1978, Scheme 39).[48] This method has been widely used due to the exceptional chemoselectivity seen for 1,2-reduction of the carbonyl over 1,4-reduction pathways. Steric hindrance has little to no deleterious effect on chemoselectivity. Furthermore, this reaction can be highly diastereoselective if the appropriate reaction conditions are found (usually based on lowering of reaction temperature). For all these reasons, this reaction is a tried and true method and has been used in many total syntheses of complex natural products.

Scheme 39. *The Luche Reduction*

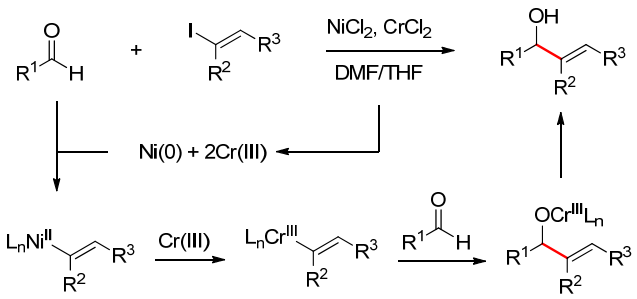


2.1.2. Modern Methods for the Synthesis of Allylic Alcohols

The gold standard reaction for the synthesis of allylic alcohols is the Nozaki-Hiyama-Kishi (NHK) reaction (discovered in 1977, Scheme 40).[49] The reaction involves the

addition of vinyl chromium(III) reagents, formed *in situ* from vinyl halides, to aldehydes or ketones to form allylic alcohols. Kishi and coworkers reported in 1986 that trace nickel salts help catalyze the formation of a C–Cr(III) species and make the reaction more reproducible and reliable.[48] Since then, this reaction has become the benchmark for multicomponent protocols involving the synthesis of allylic alcohols. It is noteworthy that the regiochemical outcome is decided based on the identity of the vinyl halide (these regioselectivity issues will be covered in Chapter 3 in further detail). The functional group tolerance of this procedure is exceptional and it has been employed in several total syntheses. The major drawbacks of this approach are that the chromium salts are highly toxic, super stoichiometric quantities of these toxic Cr(II) salts are required (unless the Fürstner modification is followed by using Mn reducing agents),[48] and enantioselective variants of the reaction are still very difficult to undertake as they require esoteric ligand synthesis (asymmetric variants discussed in Chapter 4).

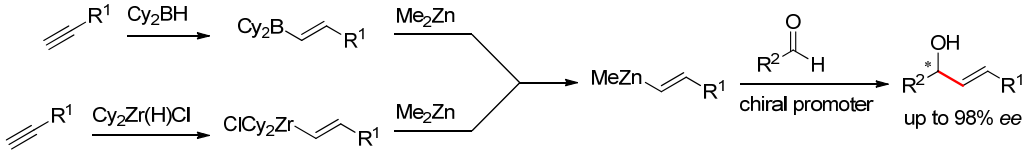
Scheme 40. *The Nozaki-Hiyama-Kishi Coupling*



Undoubtedly, the most powerful hydrometallation/transmetallation procedures for the synthesis of linear allylic alcohols were reported by the Oppolzer (hydroboration) and Wipf (hydrozirconation) groups (discovered in 1992 and 1994 respectively, Scheme 41).[50,51] Initial hydrometallation is followed by transmetallation by an organozinc, and the resulting vinyl zinc species can undergo asymmetric reductive coupling by way of a

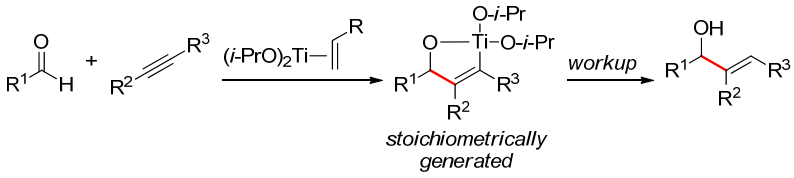
chiral promoter (chiral amino alcohols or amino thiols) to afford a *trans* olefin product. However, this method is limited to terminal alkynes and that renders this reaction considerably less attractive for a broad range of alkynes.

Scheme 41. *Hydrometallation/Transmetallation Methods*



Titanium alkoxide-mediated reductive couplings are a powerful strategy for aldehyde–alkyne reductive couplings (Scheme 42).[52] The low cost of titanium(IV) alkoxides and their ease of handling makes this method extremely attractive. Despite the lack of catalytic turnover, these reactions are noteworthy and practically useful. It is important to remember that the synthetic usefulness of this method is quite high as titanium is a relatively benign metal, and that silane or borane reducing agents are in fact more expensive than stoichiometric amounts of titanium.

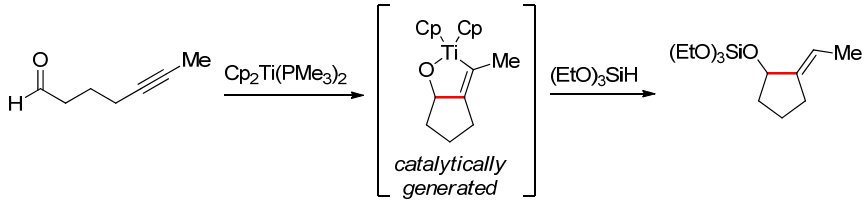
Scheme 42. *Titanium-Mediated Reductive Couplings*



Although most titanium-mediated reductive couplings are stoichiometric in titanium, there has been one catalytic example using a triethoxysilane reducing agent to form a silyl protected allylic alcohol (Scheme 43).[13] In fact, this was the first example of a silane-mediated metal-catalyzed aldehyde–alkyne reductive coupling reaction and has served

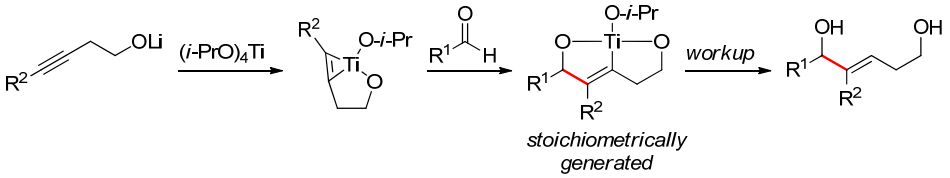
as the impetus for our own nickel-catalyzed reductive couplings using silane reducing agents (see Chapter 1 for a brief history of the development of nickel-catalyzed reductive couplings of aldehydes and alkynes).

Scheme 43. *A Titanium-Catalyzed Silane-Mediated Reductive Coupling*



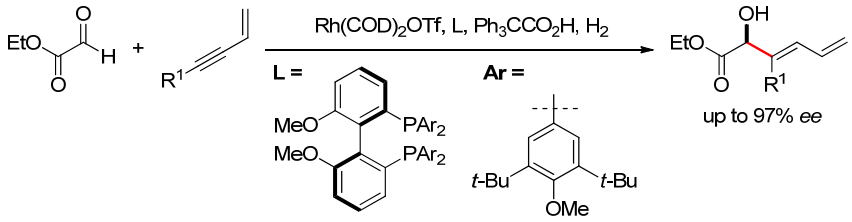
In recent years, Micalizio and coworkers have extensively studied titanium alkoxide-mediated aldehyde–alkyne reductive couplings (Scheme 44).[53] Although these methods have built and expanded upon past efforts of the Crowe, Sato, and Utimoto groups, Micalizio and coworkers have rendered these methods truly useful and have applied them in complex settings with great success. However, to date there are no asymmetric variants and diastereoselectivities are still quite low to moderate in range (based entirely on the steric factors that exist in the starting materials). Another limitation of this reaction is the necessity of an alkoxide-directing group for regiochemical control, thereby lowering the overall substrate scope and utility of the methodology. Despite these limitations, there is vast potential for this protocol if ligand-control can be achieved. Indeed, the future may hold important advances in aldehyde–alkyne reductive couplings based on titanium-based methods.

Scheme 44. *Alkoxy-Directed Titanium-Mediated Reductive Couplings*



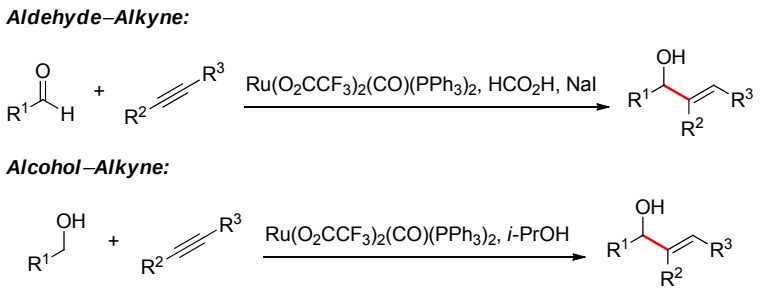
The rhodium-catalyzed hydrogen-mediated reductive coupling of aldehydes and alkynes developed by Krische and coworkers is an extremely important novel method for the construction of allylic alcohols (Scheme 45).[8,9] Enantioselectivities in these reactions are the highest in the field of transition-metal catalyzed reductive couplings but the substrate scope is limited at present. Although the use of hydrogen as the terminal reductant is attractive in this asymmetric protocol, the use of highly electronically biased coupling partners reduce the utility of this method.

Scheme 45. *Rhodium-Catalyzed Hydrogen-Mediated Reductive Couplings*



Krische and coworkers have developed a novel ruthenium-catalyzed aldehyde or alcohol–alkyne reductive coupling via transfer hydrogenation (Scheme 46).[54] This work is still quite preliminary in scope and is limited in its versatility. However, this method has potential for improvement as substrate scope is widened and the potential for regio- and enantiocontrol is studied.

Scheme 46. *Ruthenium-Catalyzed Variants via Hydrogen-Transfer*

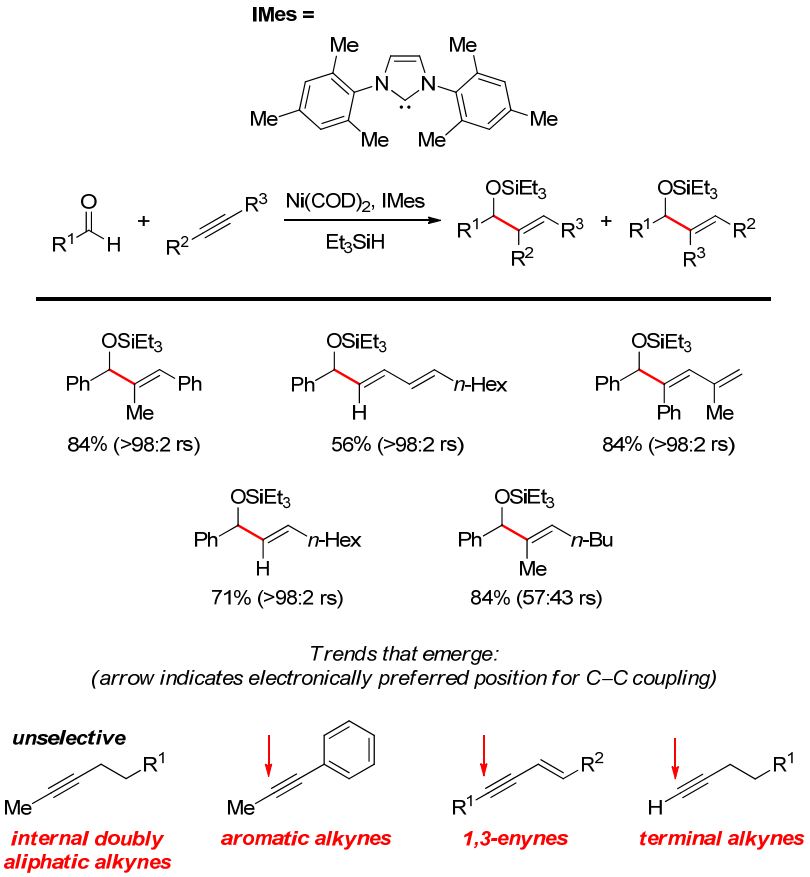


2.2. Regioselective Nickel-Catalyzed Aldehyde–Alkyne Reductive Couplings

In the nickel-catalyzed reductive couplings of aldehydes with electronically biased alkynes, regioselectivities are often excellent and are predicated on substrate structure. Exceptional regiocontrol is typically seen with terminal, silyl, and aryl alkynes, 1,3-enynes,[55] 1,6-enynes,[33] and ynamides.[56] Conversely, the use of internal alkynes lacking a strong electronic bias often leads to regioisomeric mixtures of products. In this section, an effort will be made to catalog and illustrate the various factors that are involved in many of the highly regioselective nickel-catalyzed aldehyde–alkyne reductive coupling processes.

Many trends for regioselectivity due to electronic biases have been shown in our disclosure of the intermolecular nickel-catalyzed silane-mediated aldehyde–alkyne reductive coupling (Scheme 47).[25] Terminal alkynes, internal aromatic alkynes, and 1,3-enynes all proceed with excellent regiocontrol to produce a single regioisomer. Internal doubly aliphatic-substituted alkynes were shown to be completely unselective at the time. This contribution from our group has generated numerous follow-up research studies that have either have been published or being studied currently.

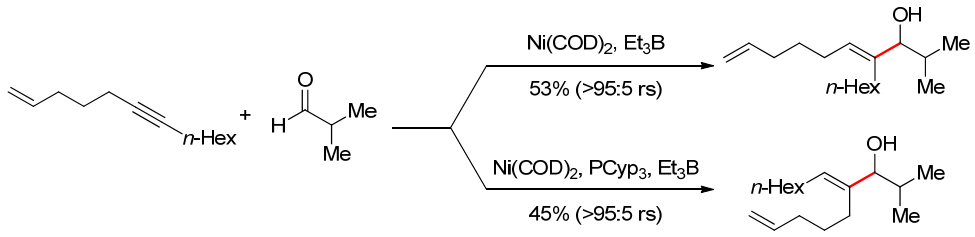
Scheme 47. *Trends in Nickel-Catalyzed Aldehyde–Alkyne Reductive Couplings*



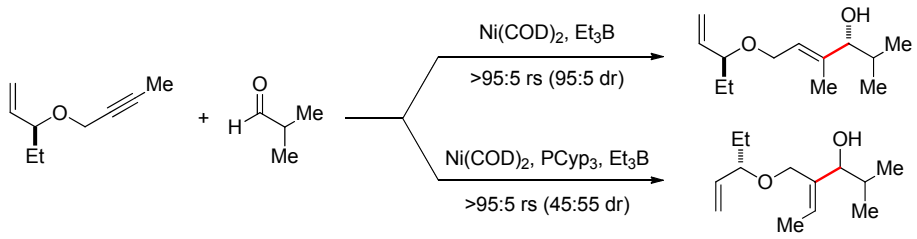
Many elegant studies by Jamison and coworkers highlight the directing capability of 1,3- and 1,6-enynes (Scheme 48, see Chapter 1 for in-depth analysis). It has been shown that distal olefins have a strong directing effect in the absence of monodentate phosphine ligands. In the presence of these phosphine ligands, regioselectivity can be reversed in good levels of control. These reactions have also been shown to be diastereoselective when a chiral center is strategically placed near the olefin directing group (Scheme 49). This also provides some empirical information about the mechanism of this transformation (discussed in detail in Chapter 1), specifically that the diastereoselectivity is high in the absence of phosphine ligands and probably results from olefin coordination during metallacycle formation. However, if olefin binding is

disrupted by addition of monodentate phosphine ligands, the reaction no longer displays diastereoselectivity by means of chirality transfer.

Scheme 48. *Regiocontrol via Olefin-Direction*

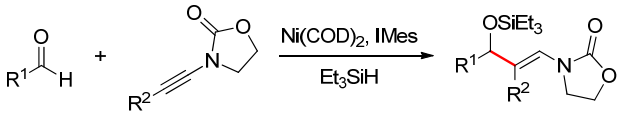


Scheme 49. *Regio- and Diastereocontrol via Olefin-Coordination*



Another highly regioselective, but albeit highly specialized process is the reductive coupling of aldehydes and ynamides (Scheme 50).[56] Sato and coworkers argue the high levels of regioselectivities may arise from favorable charge density buildup at the alkyne carbon distal to the directing group in the transition-state, but the authors concede that ynamides are electronically biased systems and regiocontrol may be due to a variety of factors. The main criticism of this work would be the lack of generality of this system and highly specialized nature of the final products.

Scheme 50. *Ynamide-Directed Couplings*

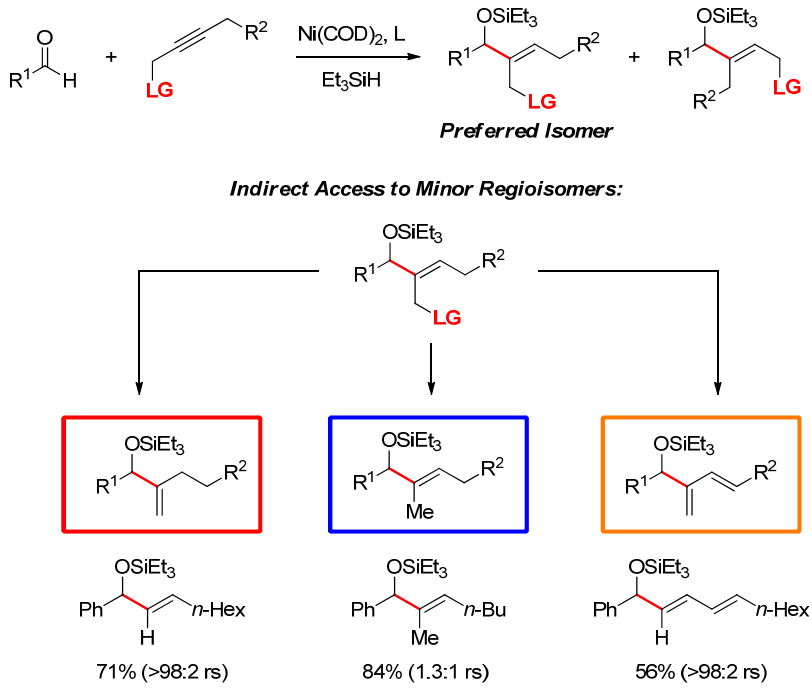


2.3. Results & Discussion

2.3.1. Strategies for Regiocontrol

Our research goal was to utilize a pendant directing group to achieve a highly regioselective reductive coupling and then to remove the directing functionality in order to access olefin regioisomers in an indirect but synthetically useful fashion (Scheme 51). In particular, we wished to access the minor (electronically disfavored but potentially desirable) regioisomers resulting from the reductive couplings of aldehydes with terminal alkynes and enynes. Since internal alkynes with aliphatic substituents produce a regioisomeric mixture of products, we needed to access one regioisomer selectively.

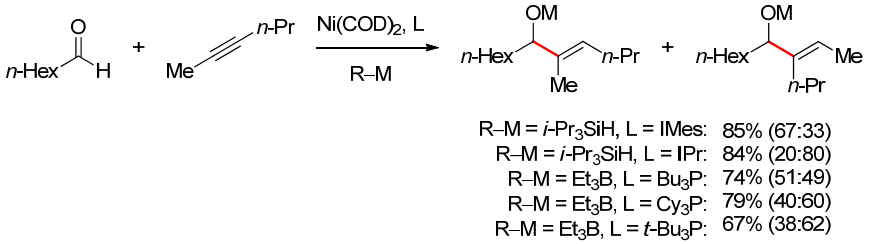
Scheme 51. *Research Goals for Removable Directing Group Strategy*



The level of regioselectivity obtained from the nickel-catalyzed reductive coupling of electronically unbiased unsymmetrical internal alkynes and aldehydes from the use of both $Ni(COD)_2$/NHC/silane and $Ni(COD)_2/R_3P/Et_3B$ reagent combinations is illustrated by

the coupling of 2-hexyne and heptanal (Scheme 52). Monodentate phosphines offered the lowest levels of regiocontrol, ranging from 51:49 to 38:62. The two NHC ligands screened showed a wider range, from 67:33 to 20:80. With these experiments, an initial benchmark for ligand size influence on the regiochemical outcome of nickel-catalyzed reductive couplings of unsymmetrical internal alkynes with aliphatic substituents, aldehydes, and silanes was established.

Scheme 52. *An Initial Test of Regiocontrol using R_3P and NHC Ligands*

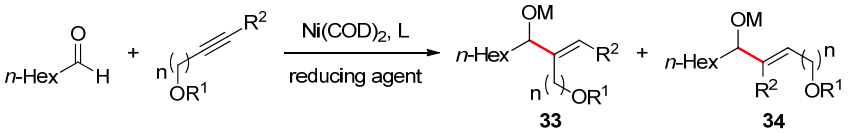


R–M = *i*-Pr_3SiH, L = IMes: 85% (67:33)
R–M = *i*-Pr_3SiH, L = IPr: 84% (20:80)
R–M = Et_3B, L = Bu_3P: 74% (51:49)
R–M = Et_3B, L = Cy_3P: 79% (40:60)
R–M = Et_3B, L = *t*-Bu_3P: 67% (38:62)

Due to the broad availability of propargyl alcohol-derived substrates and the utility of the resulting allylic alcohols, regioselectivity studies of propargyl alcohols with aldehydes were undertaken (Table 1). The simple, free propargyl alcohol (2-hexyn-1-ol) underwent coupling using IMes as a ligand affording an 80:20 mixture of regioisomers (entry 1). Under the same conditions, using IPr and Cy_3P ligands results in a lowering of regioselectivity to 67:33 (entries 2 and 3). Free homopropargylic alcohols, using IMes, undergo coupling with 50:50 regioselectivity, which indicates a lack of hydroxyl chelation to the nickel metal center and that regioselectivity for 2-hexyn-1-ol is resulting from subtle inductive influences (entry 4). To further study regioselectivity attained by using IMes and to further dispel any remaining doubts in regards to chelation control pathways, we studied propargyl ethers (Me vs *t*-Bu) which underwent coupling with an identical loss of regioselectivity (75:25 rs, entries 5 and 6). However, protection of 2-hexyn-1-ol with a TBS group improved regioselectivity to 87:13 (entry 7). Use of IPr

resulted in a loss of regiocontrol with the same substrate (entry 8). Comparison of regioselectivity with the $Ni(COD)_2/R_3P/Et_3B$ reagent combination shows minimal ligand control of regiochemistry with such monodentate phosphines (entries 9–11). From the examples studied, the $Ni(COD)_2$/IMes/*i*-Pr_3SiH reagent combination using a TBS-protected silyl ether proved to be the optimal conditions for regiocontrol of **33**.

Table 1. *Optimization of Reductive Couplings of Propargyl Alcohol Derivatives*

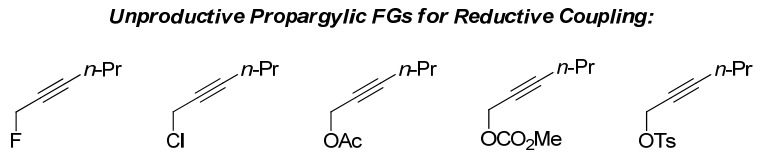


entry	R^1	R^2	n	L	reducing agent	yield (**33**:**34** rs)
1	H	*n*-Pr	1	IMes	*i*-Pr_3SiH	92% (80:20)
2	H	*n*-Pr	1	IPr	*i*-Pr_3SiH	78% (67:33)
3	H	*n*-Pr	1	PCy_3	*i*-Pr_3SiH	80% (67:33)
4	H	*n*-Pr	2	IMes	*i*-Pr_3SiH	82% (50:50)
5	Me	*n*-Hept	1	Imes	*i*-Pr_3SiH	57% (75:25)
6	*t*-Bu	*n*-Hept	1	IMes	*i*-Pr_3SiH	75% (75:25)
7	TBS	*n*-Pr	1	IMes	*i*-Pr_3SiH	75% (87:13)
8	TBS	*n*-Pr	1	IPr	*i*-Pr_3SiH	86% (71:29)
9	TBS	*n*-Pr	1	Bu_3P	Et_3B	65% (67:33)
10	TBS	*n*-Pr	1	Cy_3P	Et_3B	73% (58:42)
11	TBS	*n*-Pr	1	*t*-Bu_3P	Et_3B	71% (53:47)

Other propargyl functional groups were tested for productive coupling and regioselectivity (Scheme 53). However, halides, acetates, carbonates, and other propargyl functional groups did not provide productive coupling. The lack of reductive

coupling product may be due to oxidative addition pathways that result in allene formation and deactivation of the catalyst.

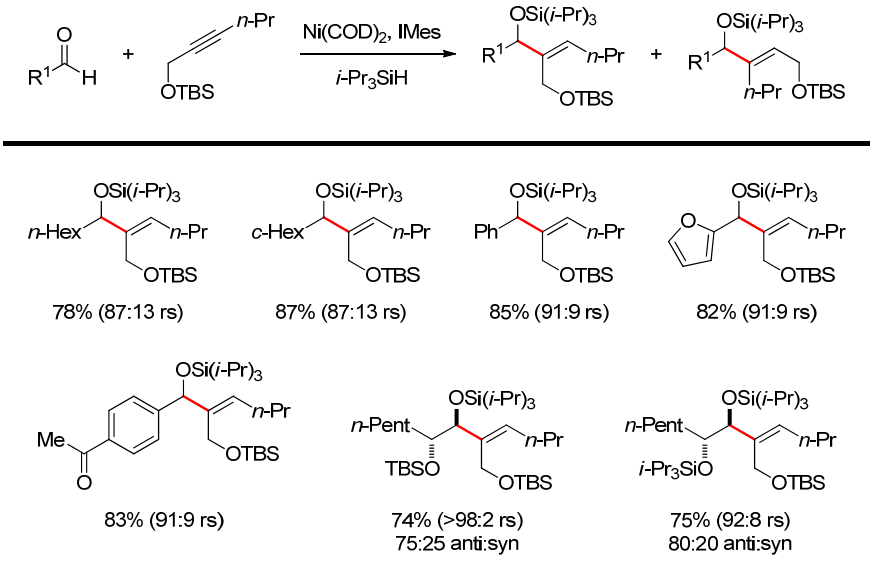
Scheme 53. *Other Propargyl Functional Groups for Direction*



2.3.2. Substrate Scope

We next examined substrate scope for the optimized reaction conditions (Scheme 54). Linear and branched aliphatic aldehydes proceed with 87:13 regioselectivity. Regioselectivities were further enhanced to 91:9 when aromatic and heteroaromatic aldehydes were employed. α-Silyloxyaldehydes were also excellent coupling partners, providing regioselectivities up to >98:2 and 80:20 diastereoselectivity.

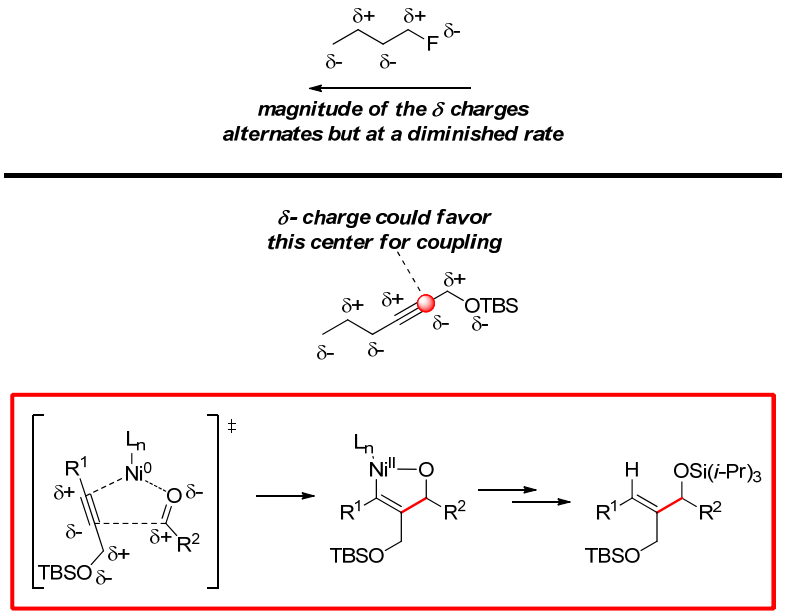
Scheme 54. *Substrate Scope of Propargyl Silyl Ether–Aldehyde Couplings*



2.3.3. Development of a Predictive Model for Reductive Couplings

We believe inductive influences may be involved in achieving the regioselectivity outcome observed in our particular reagent combination (Scheme 55). There is precedent for alternating charge distribution in inductively biased systems such as 1-fluoro-butane. We believe that a similar charge distribution may predispose a specific alkyne orientation in the transition-state of the metallacycle formation step. However, we have not performed transition-state computational calculations to verify this hypothesis.

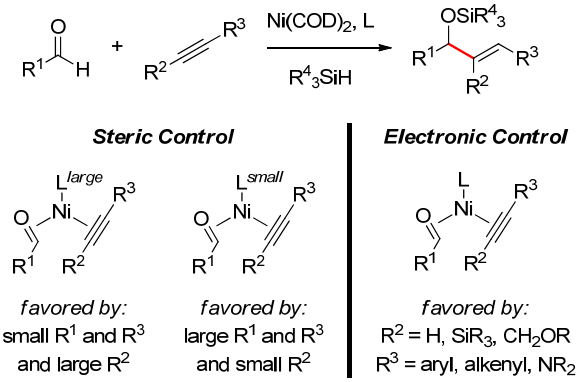
Scheme 55. *Hypothesis for an Inductive Effect in Achieving Regiocontrol*



When considered independently, the regiocontrol provided by NHC ligand size is subtle, and the electronic bias provided by propargyl derivatives is modest. However, these properties can act in a cooperative manner to provide preparatively useful levels of regioselectivity in relatively unbiased cases. We have proposed a simple predictive model that accounts for both ligand sterics and substrate steric and electronic biases based on results from this study and previous work (Scheme 56). As seen from the data

we had gathered through the course of our studies and as shown in predictive model, the optimal ligand for a particular regiochemical outcome is based on several factors. The characteristics of the alkyne, aldehydes, and ligand choice all interplay to provide a cooperative or destructive regiochemical outcome. We set out to study these factors in a series of reactions using a variety of propargyl alcohol derivatives.

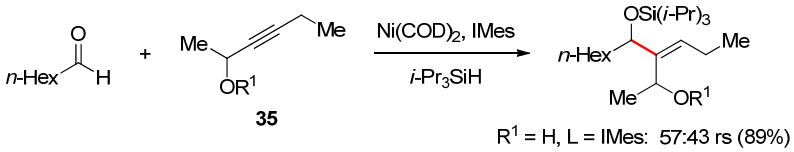
Scheme 56. *Predictive Model for Aldehyde–Alkyne Couplings*



2.3.4. Illustration of Regiocontrol Strategies Based on the Predictive Model

We decided to study the cooperativity of steric and electronic influences of ligand and substrate combinations. We began our studies by using substituted propargyl alcohol **35** (Scheme 57). Using the free alcohol, with IMes as a ligand, the reaction was unselective with a regioselectivity of 57:43. When the alcohol was protected as the TBS-silyl ether, using IMes as a ligand, the regioselectivity was increased to 77:23 due to inductive influences. However, when steric influences are maximized by use of the bulkier IPr ligand, regioselectivity is increased to >98:2.

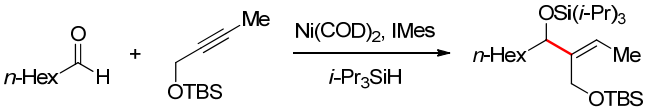
Scheme 57. *Illustration #1 of Regiocontrol Strategies*



R^1 = H, L = IMes: 57:43 rs (89%)
R^1 = TBS, L = IMes: 77:23 rs (85%)
R^1 = TBS, L = IPr: >98:2 rs (77%)

Propargyl alcohol derivative **36** undergoes coming with IMes as a ligand in modest regioselectivity of 69:31 with optimal inductive conditions (Scheme 58). Regioselectivity is increased to 90:10 using the bulkier IPr ligand, as predicted by our predictive model, showcasing the synergistic capabilities of judicious ligand selection.

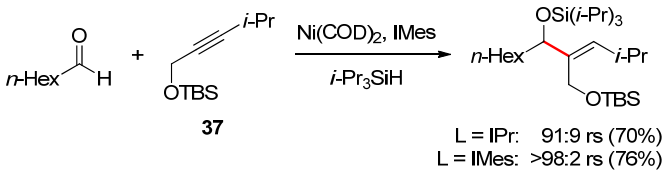
Scheme 58. *Illustration #2 of Regiocontrol Strategies*



L = IMes: 69:31 rs (89%)
L = IPr: 90:10 rs (88%)

As a final example, we studied substituted propargyl alcohol derivative **37** (a reversal of substrate sterics in the example using **35**, Scheme 59). By our predictive model, a small ligand would result in higher regioselectivity due to synergistic effects. Experimentally, both IMes and IPr result in good regiochemical outcomes but IMes does show the higher regioselectivity of >98:2.

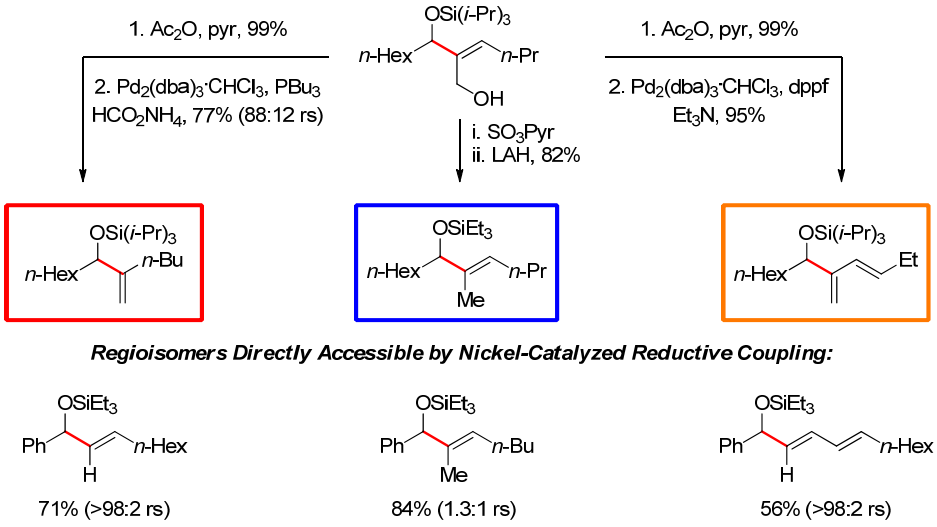
Scheme 59. *Illustration #3 of Regiocontrol Strategies*



2.3.5. Product Utility

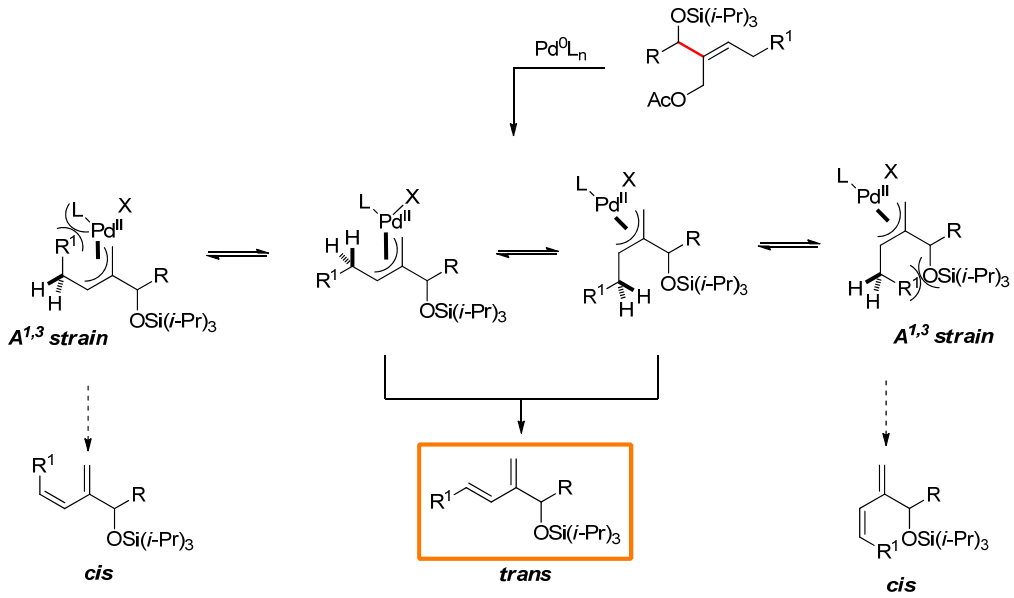
As described earlier, the goal of this project was to develop an indirect route to difficult-to-attain regioisomers of aldehyde–alkyne reductive couplings. As an illustration of this goal, we devised a protecting group swap of TBS to acetate, followed by palladium(0)-catalyzed base-assisted 1,3-diene formation.[57] Change of reaction conditions can change the pathway to an allylic reduction mechanism which results in an olefin transposition to afford a 1,1-disubstituted olefin.[58] Both 1,3-diene and 1,1-disubstituted olefin products represent minor regioisomers not accessible by reductive couplings at the time (see Chapter 3 for direct approaches). Finally, using a simple hydroxyl reduction produces a regioisomer not accessible in high regioselectivity by the ligands used in this study.[59]

Scheme 60. *Utility of Propargyl Alcohol Substrates*



Mechanistically, we were interested in the nuances of the palladium(0)-catalyzed 1,3-diene formation. In the course of developing this transformation, we wished to know whether allylic reduction or base-assisted elimination was occurring. We saw no change in yield or selectivity with the addition or removal of a reducing agent (HCO_2NH_4). However, the presence of Et_3N was essential to clean product formation. This result, in conjunction with a report on base-assisted 1,3-diene formation led us to realize that these transformations are base-assisted elimination reactions.[57] The postulated reaction pathway is shown (Scheme 61).

Scheme 61. *Postulated Mechanism of 1,3-Diene Formation*



2.4. Conclusion

In summary, highly regioselective nickel-catalyzed reductive couplings of propargyl alcohol derivatives and aldehydes have been developed. Consideration of the interplay of sterics and electronics between reactive starting materials and the $Ni(COD)_2$/NHC/R_3SiH catalyst system allows for a strategy to predictably control regiochemistry in the coupling of propargyl alcohol derivates, aldehydes, and silanes. The derivatization of these products can lead to several otherwise largely inaccessible regioisomers in an indirect but efficient manner.

Chapter 3

A General Strategy for Regiocontrol in Reductive Couplings of Aldehydes and Alkynes

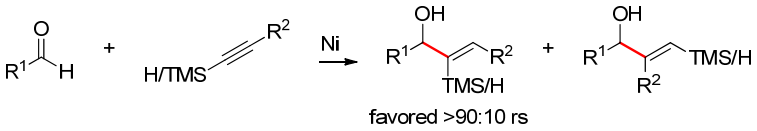
3. Introduction

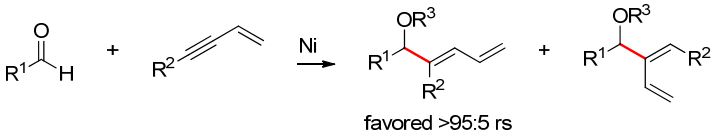
The ability to attain regiocontrol in alkyne addition reactions is something that has a broad general interest to the chemical community. New methods development programs focusing on the regiocontrol of alkyne additions have implications in many other related fields. The two preferred means of attaining regioselectivity are: (1) A change in mechanism to attain the desired regiochemical outcome; or (2) Ligand-derived regiocontrol using transition metal protocols. However, there has been minimal development of the second method. Generally, certain trends are seen for regioselectivity and most reactions are optimized for the preferred regioisomer.

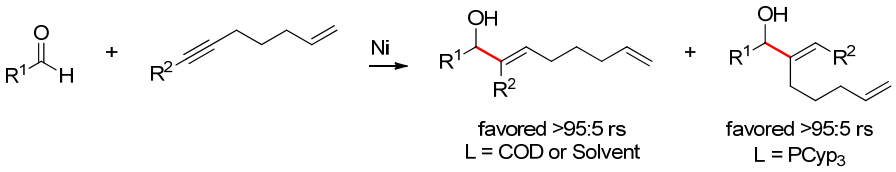
In the field of aldehyde–alkyne reductive couplings, there are clear regioselectivity trends that emerge for various classes of alkynes (Scheme 62, also discussed in detail in Chapter 2).[53] Alkynes that possess strong electronic or steric biases often proceed with excellent regioselectivity in addition reactions, generally with only one regioisomer being observed. However, alkynes that lack a strong electronic or steric bias tend to perform with poor regiocontrol. These distinctions in regioselectivity hold true for aldehyde–alkyne reductive couplings. Aromatic alkynes, terminal alkynes, silyl alkynes,

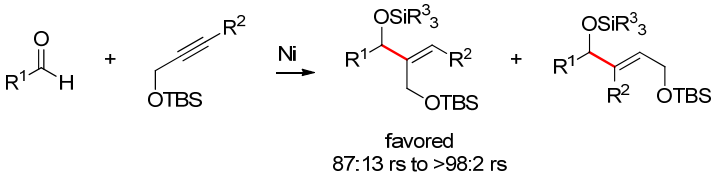
Scheme 62. *Trends of Alkyne Regioselectivity in Reductive Couplings*

Nickel-Catalyzed Reductive Couplings:

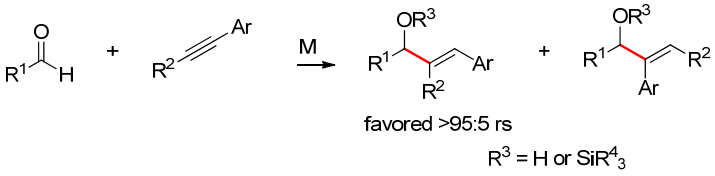




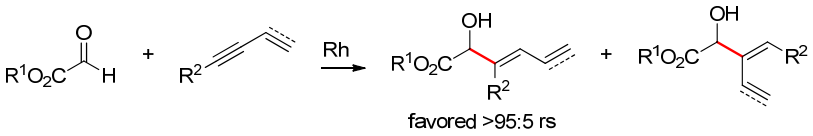




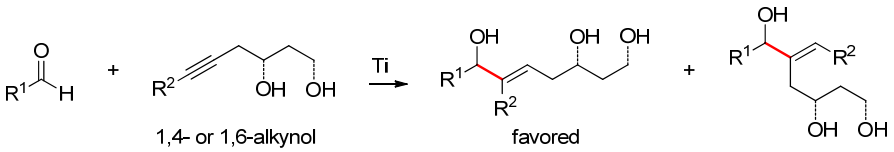
Nickel or Iridium or Rhodium or Ruthenium-Catalyzed Reductive Couplings:

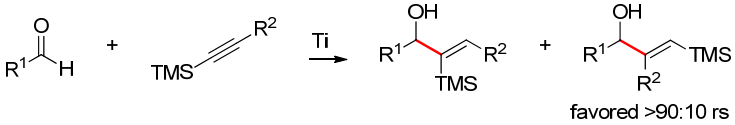


Rhodium-Catalyzed Reductive Couplings:



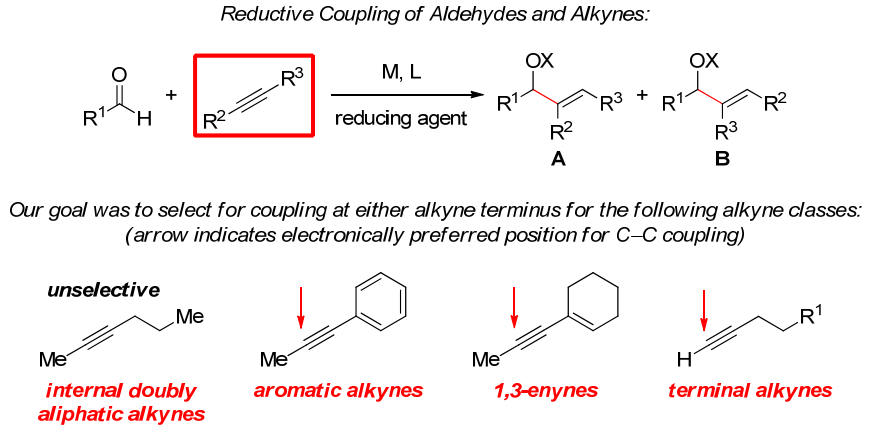
Titanium Alkoxide-Mediated Reductive Couplings:





ynamides, diynes, and 1,3- or 1,6-enynes proceed in highly regioselective reductive coupling reactions. Despite the excellent regioselectivity seen with these class of alkynes, we envisioned a general strategy for regiocontrol that overrides inherent substrate biases and would overcome the need for a pendant electronic directing group (Scheme 63).

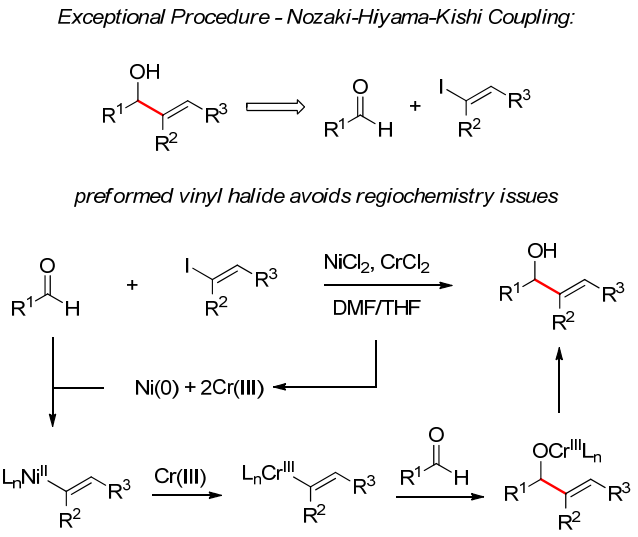
Scheme 63. *Research Goals of Achieving Regiocontrol in a Variety of Alkynes*



3.1. Methods to Attain Regioselectivity in Alkyne Addition Reactions

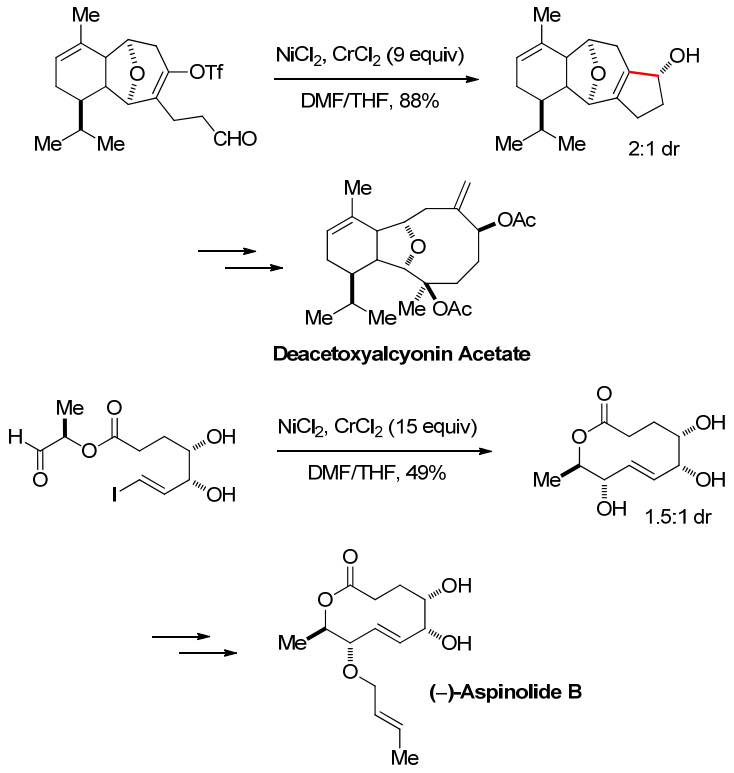
Although there are many methods available to synthesize allylic alcohols (discussed in Chapter 2, Section 2.1), almost no protocol attains the wide applicability and general utility that can be seen for the Nozaki-Hiyama-Kishi (NHK) coupling (Scheme 64). This Barbier-type addition reaction works for vinyl, alkynyl, aryl, and allyl chromium additions to aldehydes or ketones. This wide range of reactivity in NHK couplings makes this reaction a truly powerful tool for C–C bond formation. Although few methods can come close to the versatility of this transformation, there are many issues that plague the NHK reaction from becoming as widely used as Heck, Negishi, or Suzuki couplings.

Scheme 64. *Perfect Regiocontrol by the Use of Preformed Vinyl Halides*



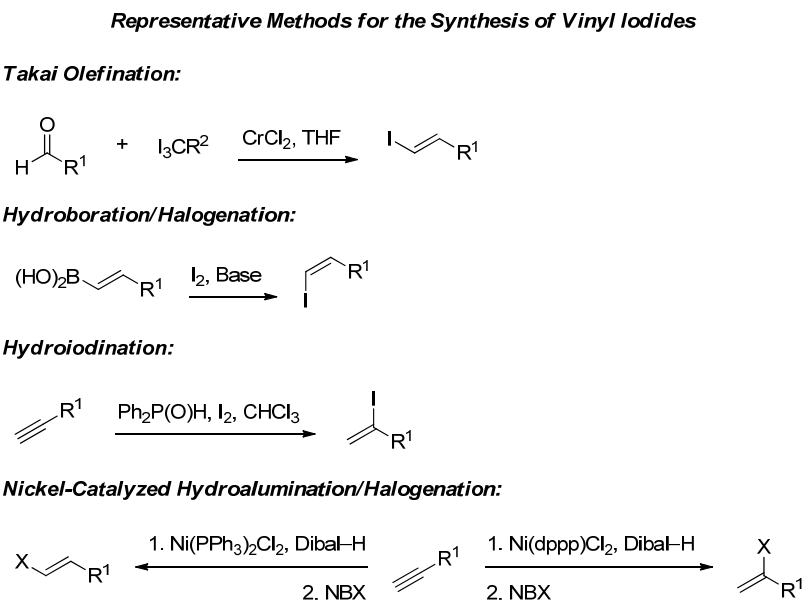
The use of a preformed vinyl halide avoids regioselectivity issues and therefore only one regiochemical outcome is possible. The dependability and utility of this type of method relies on the stereocontrolled construction of vinyl iodides, which is not always a trivial if one intends to construct a trisubstituted olefin. Another major drawback is the super stoichiometric loading of toxic chromium salts that is required, serving as a reducing and transmetallating agent (though the Fürstner modification can attenuate this by the use of Mn reducing agents).[49] The generality of this reaction suffers considerably when one combines the need to pre-synthesize a vinyl halide coupling partner with the highly toxic reagents required for the overall chemical transformation. However, the NHK reaction remains the gold standard for the synthesis of allylic alcohols due to vast substrate scope and it has been used in numerous successful total synthesis efforts (Scheme 65).[60,61]

Scheme 65. *The Nozaki-Hiyama-Kishi Coupling in Total Syntheses*



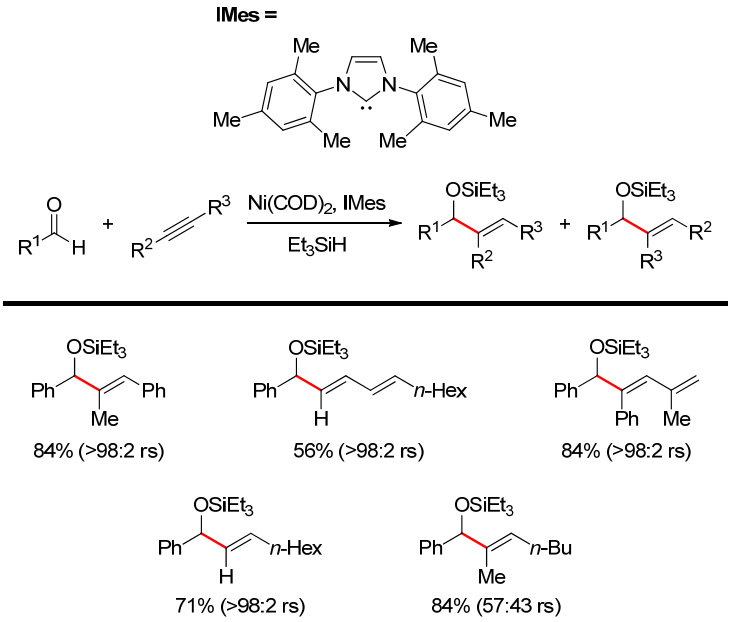
The most common method to construct linear (*E*)-vinyl halide starting materials is the Takai Olefination (Scheme 66).[49] However, many newer methods have been developed to afford linear (*Z*)-vinyl halides as well as branched vinyl halides. Recent advances in catalyst-controlled regioselective functionalization of alkynes by Hoveyda and coworkers have provided a powerful tool to access both linear (*E*)-vinyl halides and branched vinyl halides.[62] Although all these methods are impressive in their substrate tolerance, scope, and the ease in which they allow access to vinyl halides, additional synthetic steps are added when one considers their use in the NHK coupling reaction. The synthetic efficiency that is lost in NHK couplings but is inherent in the reductive coupling of aldehydes and alkynes is why this latter protocol is such a powerful and direct method to access stereodefined allylic alcohols.

Scheme 66. *Methods for the Synthesis of Vinyl Halides*

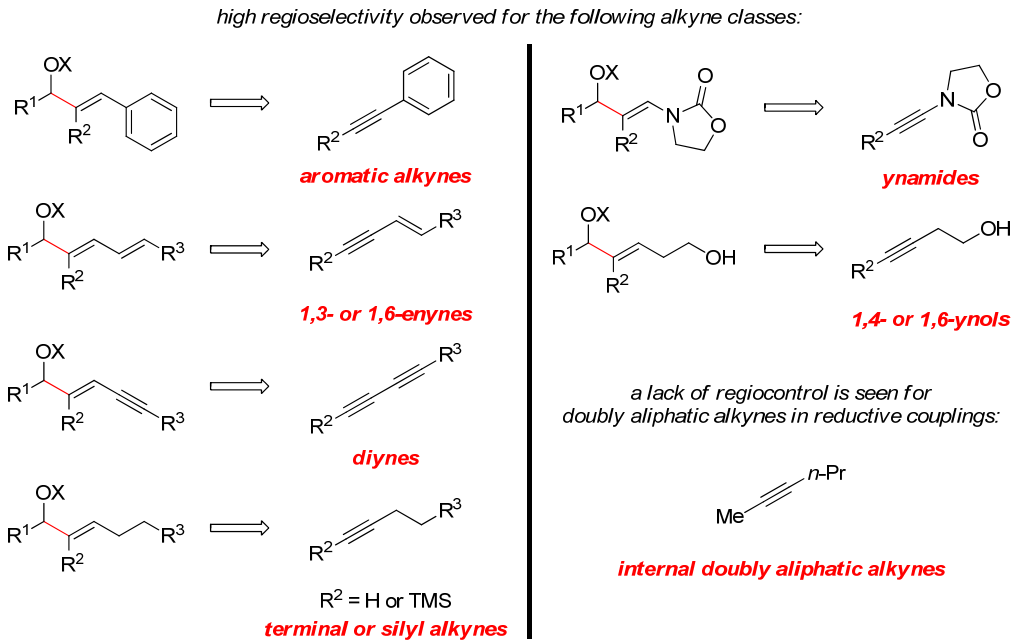


Our own work in nickel-catalyzed reductive couplings of aldehydes and alkynes illustrate the regiochemical outcomes seen with electronically biased alkynes: internal aromatic alkynes, 1,3-enynes, and terminal alkynes all proceed with exceptional regiocontrol (Scheme 67).[63] However, the opposite regioisomer cannot be obtained as these substrates are electronically biased for formation of a single isomer. Internal doubly aliphatic-substituted alkynes proceed with complete lack of selectivity (57:43 rs) and to couple such substrates with good regiocontrol remained a longstanding challenge for those in the field of reductive couplings. The ability to reverse regioselectivity for sterically and/or electronically biased alkynes would also be highly advantageous for the generality and utility of the reaction. A general overview of regioselectivity trends for commonly used alkynes in alkyne–aldehyde reductive couplings is shown (Scheme 68).

Scheme 67. *Use of NHC Ligands in Reductive Couplings*



Scheme 68. *Major Classes of Alkynes that Undergo Coupling with Regiocontrol*

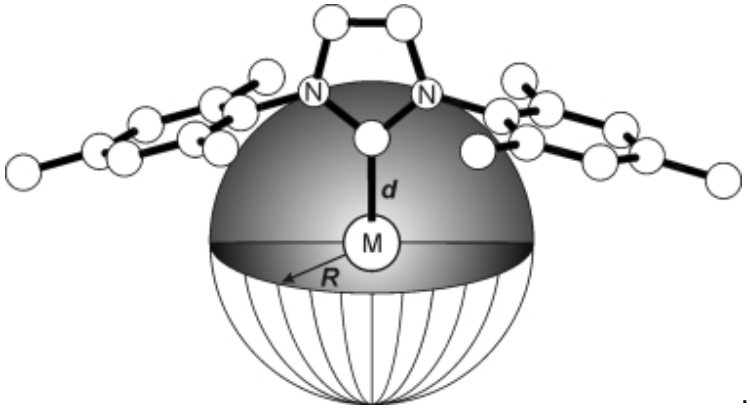


3.2. *N*-Heterocyclic Carbenes

The use of *N*-heterocyclic carbene (NHC) ligands in transition metal-catalysis has seen a great deal of development since the pioneering work of Arduengo and coworkers.[64,65] The electronic stabilization of these singlet carbenes enable them to be effective σ-donors to metal centers. In fact, carbene-metal complexes can be exceptionally stable species. One of the most famous and useful examples of a NHC-transition metal-complex is the 2nd generation Grubbs metathesis catalyst. However, NHCs have been used as ligands for a diverse range of transition metals in a variety of novel transformations. These ligands are highly versatile and are highly tunable in both sterics and electronic characteristics.

Although much is understood about phosphine ligand steric characteristics, NHC steric qualities are far less well known and much of the existing data is lacking in experimental backing. The groups of Nolan and Cavallo have extensively studied computational methods to quantify NHC sterics, most notably by defining the value $\%V_{bur}$ and making it popular in the chemical lexicon.[66] The value that is $\%V_{bur}$ is a percentage of volume within a sphere, where the radius R of that sphere measures from the metal center to the *N*-atoms of the NHC (Figure 1). However, this method of calculating an NHC steric profile is only a good initial measure of size and may be misleading for some applications because it calculates only a static equilibrium, or a snapshot of the catalyst at rest. However this is inaccurate as the *N*-aryl rings are flexible and prone to rotation as the metal binds to reagents and undergoes further interactions with these reactive species, as defined by the reaction mechanism.[67]

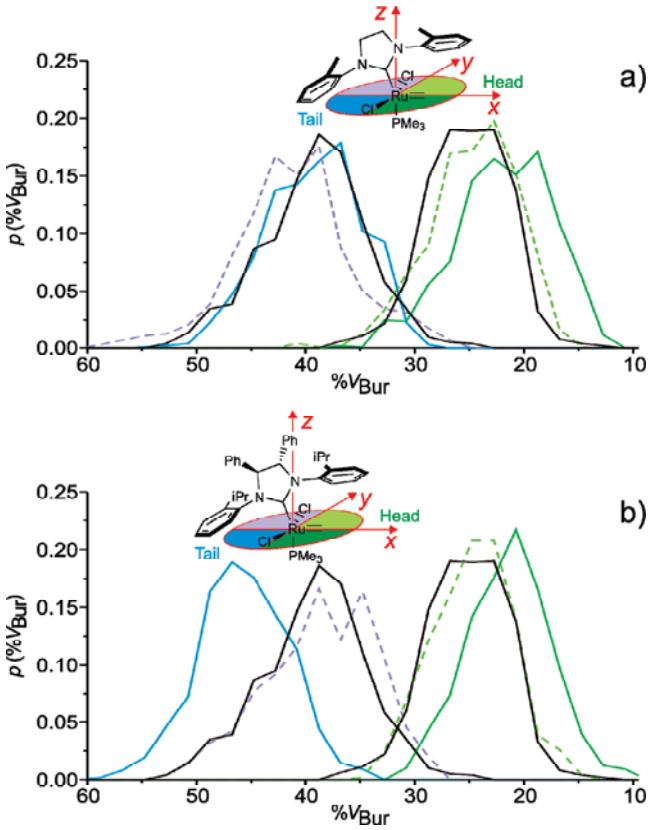
Figure 1. *The Model Used for Calculating %V_{bur}*



For these reasons, it is difficult to presume what would be considered large or small NHC ligands. The manner in which reactive species bind to an NHC-metal-catalyst changes for different reactions and different metals. For example, ruthenium-catalyzed olefin metathesis has very little in common with palladium-catalyzed cross-couplings or with nickel-catalyzed aldehyde–alkyne reductive couplings due to the dissimilar steric profiles of the catalysts used. Our ongoing collaboration with Houk is beginning to develop alternate strategies for defining sterics of NHC ligands in specific reaction classes.

Cavallo and coworkers have recently highlighted the limitations of the $\%V_{bur}$ value by calculating the sterics around a metal quadrant (Figure 2).[67] Clearly, the sterics of the ligand change considerably throughout the four quadrants around the two different metal centers (graphs **a** and **b**, Figure 2). The Cavallo group makes the argument that while $\%V_{bur}$ can be valuable for a first approximation, the reality and intricacies of ligand sterics are reaction dependent. This is something we are continuing to study for the nickel-catalyzed aldehyde–alkyne reductive coupling reaction.

Figure 2. *%V_{bur} of Quadrants Around a Metal Center*

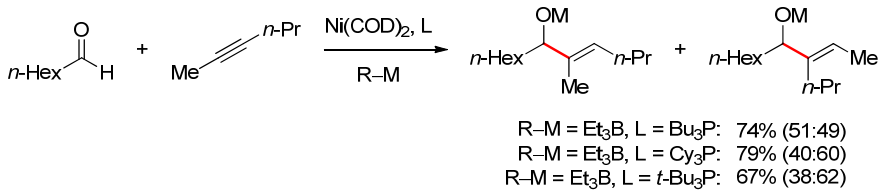


3.3. Results & Discussion

3.3.1. Development of Catalyst-Controlled Regioselectivity Studies

Earlier work related to the reductive couplings of propargyl alcohol derivatives and aldehydes, based on initial screening efforts by Dr. Mani Raj Chaulagain, revealed that phosphine ligands have a modest affect on regiochemistry of internal doubly aliphatic alkynes (Scheme 69, see Chapter 2 for more details on this initial work). From these experiments, we understood that our best chance at achieving catalyst-controlled regioselectivity was to explore a careful selection of sterically diverse NHC ligands.

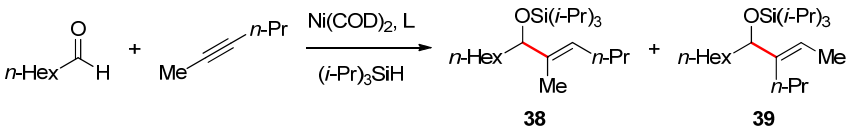
Scheme 69. *Lack of Regioselectivity using Monodentate Phosphine Ligands*



R–M = Et_3B, L = Bu_3P: 74% (51:49)
R–M = Et_3B, L = Cy_3P: 79% (40:60)
R–M = Et_3B, L = *t*-Bu_3P: 67% (38:62)

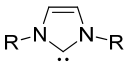
Our studies began with a careful evaluation of the regiochemical outcome derived from ligand-control (Table 2). The examples demonstrate that that **40a**, developed by Bertrand and coworkers, and **42** provide the best selectivities for **38** (entries 1 and 2), while **41b** and **±43c** provide the best selectivities for **39** (entries 9 and 10). The obvious limitation is the low yield observed for unhindered ligands (entries 1–3); however, after extensive experimentation, this was mediated by the use of base and reducing agent selection to synthetically useful levels.

Table 2. *Ligand Effects in Couplings of 2-Hexyne*

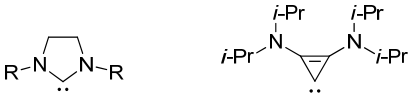


entry	L	regioselectivity (**38**:**39**)	% yield
1	**40a**	87:13	18
2	**42**	86:14	29
3	**43a**	75:25	22
4	**40b**	67:33	83
5	**41a**	61:39	73
6	**40c**	44:56	64
7	**43b**	29:71	86
8	**40d**	20:80	84
9	**41b**	7:93	85
10	**±43c**	6:94	69

L =

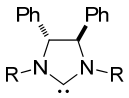


40a, R = *p*-tolyl
40b, R = mesityl
40c, R = adamantyl
40d, R = 2,6-diisopropylphenyl

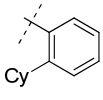


41a, R = mesityl
41b, R = 2,6-diisopropylphenyl

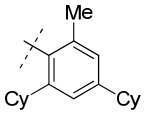
42



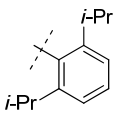
43



43a



43b

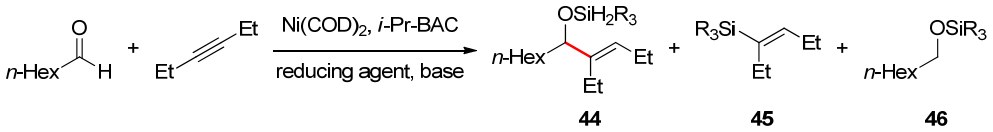


±43c

From our optimization studies for the *i*-Pr-BAC ligand (**42**),[68] we found an interesting trend of reactivity in silanes and base combinations (Table 3). Increasing the steric character of the silane reducing agent (Et vs *i*-Pr) reduces deleterious hydrosilylation byproduct formation and increases the ratio of cross-coupling product formation;

however, yields remain low (compare entries 1 and 2). Altering the electronic character of the silane, specifically changing from a mono- to dihydride silane reducing agent, increases yields slightly (compare entries 2 and 7). However, when a bulky dihydride silane and a non-reversible base such as *n*-BuLi are utilized, yields increase to a synthetically useful range (compare entries 7 and 8).

Table 3. *Optimization Study for i-Pr-BAC Ligand*



44 **45** **46**

entry	reducing agent	base	ratio of products			% yield
			44	**45**	**46**	
1	Et_3SiH	*t*-BuOK	5	24	71	<10%
2	*i*-Pr_3SiH	*t*-BuOK	61	-	39	<20%
3	*t*-Bu_3SiH	*t*-BuOK	*No Reaction*			
4	$(TMS)_3SiH$	*t*-BuOK	*Multiple Products*			
5	$(EtO)_3SiH$	*t*-BuOK	*Multiple Products*			
6	Et_2SiH_2	*t*-BuOK	*Multiple Products*			
7	*t*-Bu_2SiH_2	*t*-BuOK	86	14	-	33%
8	*t*-Bu_2SiH_2	*n*-BuLi	87	13	-	73%

3.3.2. Substrate Scope

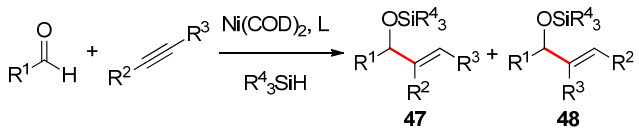
Couplings of 2-hexyne with unbranched, branched, or aromatic aldehydes are accomplished with good to excellent regioselectivity for either desired regioisomer **47** or **48** (entries 1–3, Table 4). Increased steric differences between the two alkyne substituents (Me vs *i*-Pr) is tolerated, and high regioselectivity is observed for either

isomer (entry 4). We next examined aromatic alkynes, conjugated enynes, and terminal alkynes, which uniformly provide highly selective access to regioisomer **47** using previously reported nickel-catalyzed procedures. As expected, coupling of phenyl propyne with benzaldehyde provided isomer **47** with high regioselectivity using ligand **42** (entry 5). However, the use of ligand **41b** reverses selectivity, favoring isomer **48** with 81:19 regioselectivity. As previously stated, conjugated enynes are one of the most biased alkyne classes in reductive couplings. Unsurprisingly, standard coupling with ligand **40b** provided highly selective formation of isomer **47** (entry 6). However, the use of ligand **41b** cleanly reversed regioselectivity, providing isomer **48** with excellent regiocontrol. Finally, three different terminal alkyne-aldehyde combinations were examined (entries 7–9). As anticipated, standard couplings with ligand **40b** cleanly and selectively provided the *trans*-1,2-disubstitution pattern (isomer **48**). Unfortunately, this bias could not be overcome with ligand **41b**, and isomers **47** and **48** were obtained with poor regiocontrol. However the use of ligand **43c** provided an important breakthrough, providing the 1,1-disubstitution pattern (isomer **48**) with excellent regiocontrol, ranging from 15:85 to 5:95 for the three examples studied. For a more complete analysis of ligand-controlled regioselectivity, we examined a range of NHCs using a variety of substrates (Table 5).

A substantial influence on regioselectivity can be seen based on NHC sterics where *i*-Pr-BAC (**42**) < IMes (**40b**) < IPr (**40d**) < SIPr (**41b**) ≤ Ph_2SIPr (**±43c**). From our studies, we have discovered that *i*-Pr-BAC (**42**) is the ligand of choice for internal doubly aliphatic alkynes favoring regioisomer **47**. For internal electronically biased alkynes, IMes (**40b**) provides excellent levels of regiocontrol for regioisomer **47**. For opposite regioisomer **48**, SIPr (**41b**) provides excellent selectivity for internal alkynes, but unfortunately, it is unselective for a variety of terminal alkynes. Although we were able to achieve high regiocontrol of alkyne insertion with SIPr (**41b**) using internal alkynes, we found that

large ligand regiocontrol could not be achieved for terminal alkynes to afford the *exo*-methylene product, regioisomer **48**. We realized that although the 1,2-disubstituted backbone of the ligand does not directly interact with reactive components, such substitution will likely hinder free rotation of the *N*-aryl rings, thereby locking an isopropyl moiety on both faces of the imidazolium towards the metal center (Scheme 70). This would arguably cause an increase in ligand steric bias on reactive components. The Ph_2SIPr ligand (**±43c**), fits the steric criteria mentioned above and works remarkably well for a variety of substrates in providing regiocontrol for regioisomer **48** for internal and terminal alkynes (see Scheme 71 for a detailed illustration of the best ligand-substrate combination for desired regioisomer selection).

Table 4. *Ligand-Controlled Regioselectivity Reversal*



entry	R^1	R^2	R^3	conditions, **47**:**48** (% yield)[a]	
1	*n*-Hex	Me	*n*-Pr	**A**, 88:12 (78)	**B**, 7:93 (85)
2	*c*-Hex	Me	*n*-Pr	**A**, 82:18 (75)	**B**, 5:95 (91)
3	Ph	Me	*n*-Pr	**A**, 84:16 (72)	**B**, 2:>98 (86)
4	Ph	Me	*i*-Pr	**A**, 97:3 (85)	**B**, 10:90 (89)
5	Ph	Me	Ph	**C**, >98:2 (84)[a]	**B**, 19:81 (99)
6	*n*-Hex	Me	1-*c*-Hexene	**C**, 97:3 (99)[a]	**B**, 9:91 (77)
7	Ph	H	CH_2OTBS	**C**,93:7 (88)	**D**, 15:85 (86)
8	Ph	H	*n*-Hex	**C**, 97:2 (82)	**D**, 12:88 (71)
9	*n*-Hex	H	*i*-Pr	**C**, >98:2 (74)	**D**, 5:95 (76)

[a] Conditions: **A**: L·HX = *i*-Pr-BAC (**42**), *n*-BuLi, *t*-Bu_2SiH_2; **B**: L·HX = SIPr (**41b**), *t*-BuOK, *i*-Pr_3SiH; **C**: L·HX = IMes (**40b)**, *t*-BuOK, *i*-Pr_3SiH or Et_3SiH; **D**: L·HX = Ph_2IPr (**43c)**, *n*-BuLi, Et_3SiH.

Scheme 70. *Postulated Means of Regiocontrol*

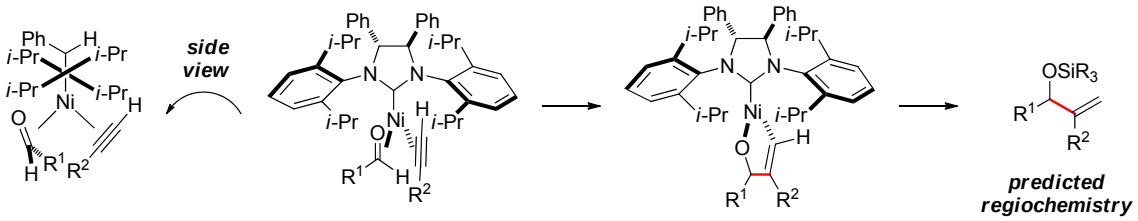
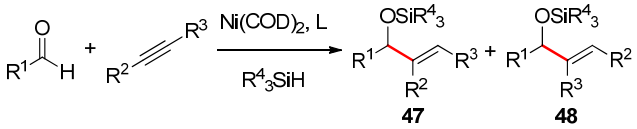


Table 5. *Ligand Steric Effects Across a Range of NHCs*



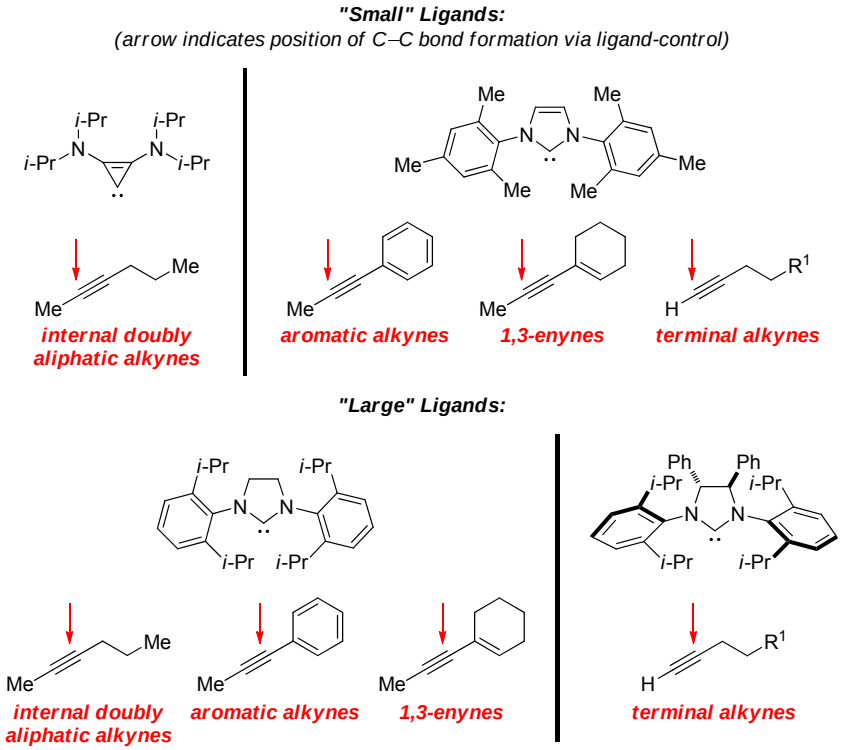
entry	R^1	R^2	R^3	conditions, **47**:**48** (% yield)[a]				
				A	**B**	**C**	**D**	**E**
1	*n*-Hex	Me	*n*-Pr	88:12 (78)	67:33 (83)	20:80 (84)	7:93 (85)	6:94 (94)
2	*c*-Hex	Me	*n*-Pr	82:18 (75)	62:38 (89)	21:79 (83)	5:95 (91)	9:91 (96)
3	Ph	Me	*n*-Pr	84:16 (72)	67:33 (98)	19:81 (95)	2:>98 (86)	2:>98 (95)
4	Ph	Me	*i*-Pr	97:3 (85)	76:24 (87)	16:84 (93)	10:90 (89)	9:91 (66)
5	Ph	Me	Ph	---	>98:2 (84)	50:50 (81)	19:81 (99)	31:69 (96)
6	*n*-Hex	Me	1-*c*-Hexene	---	97:3 (99)	---	9:91 (77)	9:91 (72)
7	*n*-Hex	H	CH_2OTBS	---	>98:2 (86)	65:35 (82)	63:37 (75)	28:72 (50)
8	Ph	H	CH_2OTBS	---	93:7 (88)	50:50 (77)	35:65 (43)	15:85 (85)
9	*n*-Hex	H	*n*-Hex	---	>98:2 (76)	70:30 (87)	69:31 (84)	28:72 (84)
10	Ph	H	*n*-Hex	---	97:3 (82)	55:45 (79)	50:50 (63)	12:88 (71)
11	*n*-Hex	H	*i*-Pr	---	>98:2 (74)	75:25 (72)	59:41 (40)	5:95 (76)

[a] Conditions: **A**: L·X = *i*-Pr-BAC (**42**), *n*-BuLi, *t*-Bu_2SiH_2;

B: L·X = IMes (**40b)**, *t*-BuOK, *i*-Pr_3SiH or Et_3SiH; **C**: L·X = IPr (**40d**), *t*-BuOK, *i*-Pr_3SiH,

D: L·X = SIPr (**41b**), *t*-BuOK, *i*-Pr_3SiH or Et_3SiH; **E**: L·X = Ph_2IPr (**±43c)**, *n*-BuLi, Et_3SiH.

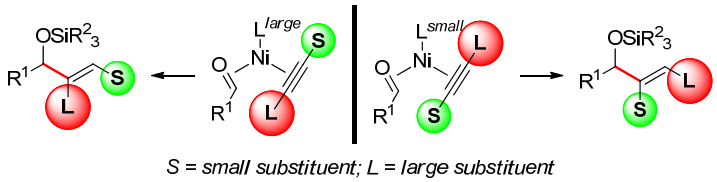
Scheme 71. *Synopsis of Optimal Alkyne–Ligand Combination for Regiocontrol*



3.4. Development of a Simple Ligand Steric Control Model for Nickel-Catalyzed Reductive Coupling of Aldehydes and Alkynes

A simple steric model is depicted below that illustrates our empirical model (Scheme 72).[69] This model was previously reported as part of a synergistic picture (Scheme 73).[42] However, this current study shows that ligand size effects are substantial and can override substrate electronic and steric biases across a broad range of alkynes. Although our predictive model is derived from empirical results, there is a theoretical underlying basis for this depiction that was discovered in the course of our ongoing collaboration with Houk and coworkers. Computational experiments show that there is a substantial correlation between experimental and predicted *in silico* calculations (Table 6).[70]

Scheme 72. *Refined Predictive Model*



Scheme 73. *Previous Predictive Model*

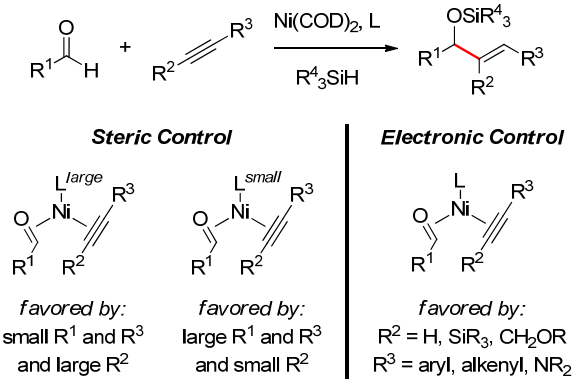
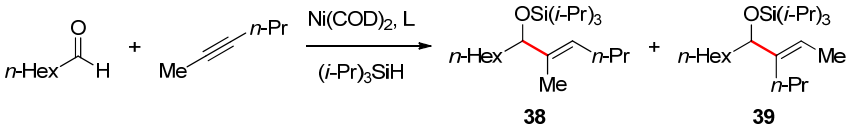


Table 6. *Theoretical Basis for Catalyst-Controlled Regioselectivity*



38 **39**

L	regioselectivity (**38**:**39**)	
	experimental	*predicted*
40a	87:13	79:21
42	86:14	64:36
40b	67:33	57:43
41a	61:39	59:41
40d	20:80	6:94
41b	7:93	4:96

Not surprisingly, Houk and coworkers have found that small NHC ligand/Ni-catalyst steric dimensions differ vastly than those of a large NHC/Ni-catalyst system (compare Figure 3 to Figure 4). However, what caught our attention was the unexpected rotation of the aryl rings of the small ligand system away from the alkyne substituent and towards the aldehyde (Figure 3). In comparison, the large ligand system has no such rotation (Figure 4). These computational findings match those recently disclosed by Cavallo and coworkers, specifically the similarities in the free rotation enjoyed by unhindered aryl substituents in Grubbs metathesis catalysts. These findings, along with our own ground state calculations, have helped our group in selecting NHC target structures for ongoing asymmetric studies (discussed in Chapter 4).

Figure 3. *Small Ligand System Transition-State Structures*

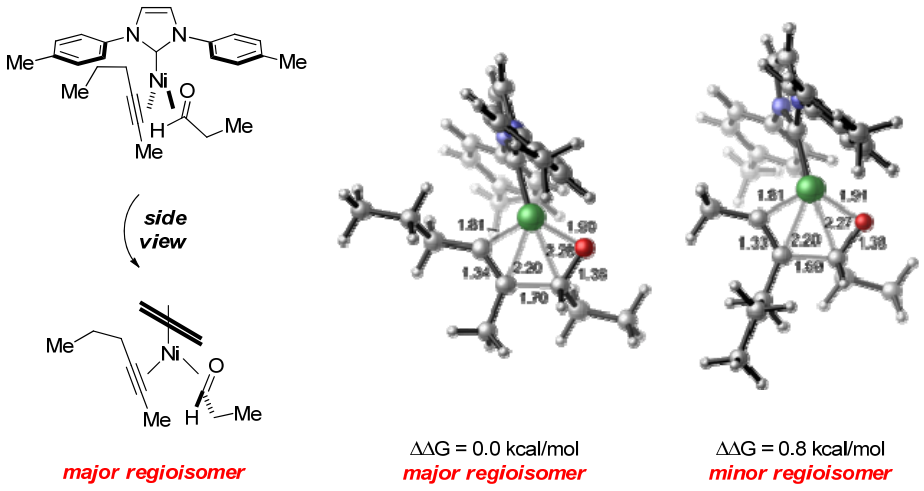
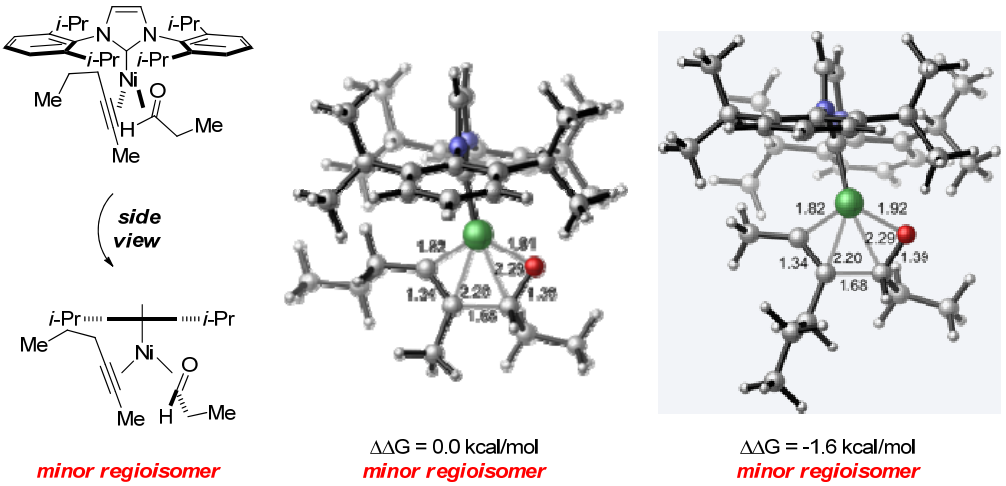


Figure 4. *Large Ligand System Transition-State Structures*



minor regioisomer

ΔΔG = 0.0 kcal/mol
minor regioisomer

ΔΔG = -1.6 kcal/mol
minor regioisomer

3.5. Conclusion

The ability to reverse alkyne regioselectivity via divergent chemical pathways is known, but to do so with high selectivity across a broad range of substrates is unprecedented. With internal alkynes that lack a strong steric or electronic bias, regioselective couplings to provide either regioisomer selectively are now possible, whereas previously reported protocols were uniformly unselective. With alkynes that possess a strong steric and/or electronic bias, such as aryl alkynes, 1,3-enynes, or terminal alkynes, only a single regioisomer was previously accessible, but our strategy now allows either regioisomer to be selectively obtained. Therefore, the ligand-based control reported herein can override even substantial substrate biases. This study thus provides the first general strategy for controlling regioselectivity in the reductive coupling of aldehydes and alkynes. Regioselectivity reversal for the range of alkynes studied herein rivals that documented for any class of alkyne 1,2-difunctionalization processes.

Chapter 4

Regio- and Enantiocontrol Strategies in the Reductive Couplings of Aldehydes and Alkynes

4. Introduction

There are many methods for the synthesis of chiral allylic alcohols but none that is currently a general method for a wide array of substrates. Most have niche applications and are highly specialized for a specific structural motif. The asymmetric reductive coupling of aldehydes and alkynes offers a great deal of versatility for the synthesis of chiral allylic alcohols. One of the last, and arguably the most difficult, remaining challenges in the field of aldehyde–alkyne multicomponent reductive couplings is the catalyst-controlled regio- and enantioselective allylic alcohol formation. The reason for this is due to the fact that one must design a catalyst that affords regiocontrol while simultaneously providing high levels of asymmetric induction. While this has proven to be an extremely difficult task in the past, the achievement of this methodology will represent the single most powerful reaction for the synthesis of stereodefined allylic alcohols to date.

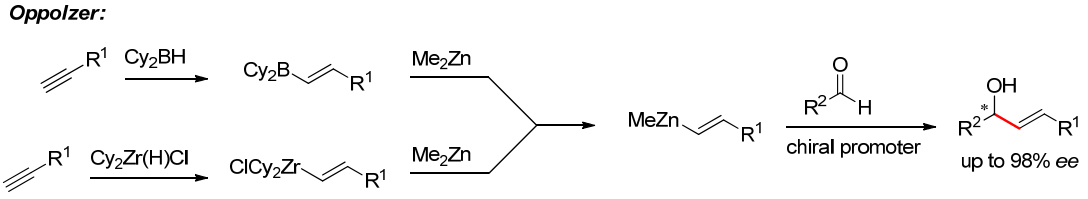
This chapter will document the ongoing efforts from our group to solve the challenges of hypothesis-driven ligand design and synthesis to afford regio- and enantioselective aldehyde–alkyne reductive couplings.

4.1. Methods for the Synthesis of Chiral Allylic Alcohols

In this section, the most important methods for chiral allylic alcohol synthesis will be described. Although many of these methods are quite powerful for a particular substitution pattern, there is no single general protocol that is best for a broad scope of substrate motifs. Particular effort will be made to cover the major substitution patterns of allylic alcohols and the limitations of the most commonly used methods.

For the synthesis of chiral linear unbranched allylic alcohols, there is probably no better method than the Oppolzer-Wipf organozinc addition to carbonyls (Scheme 74).[50] Although the reaction is limited to a substrate class of 1,2-disubstituted olefins, the reaction achieves enantioselectivities up to 98% *ee*. And since this method utilizes common commercially available reagents and reaction setup is simple and reliable, there is arguably no better protocol for these specific linear motifs.

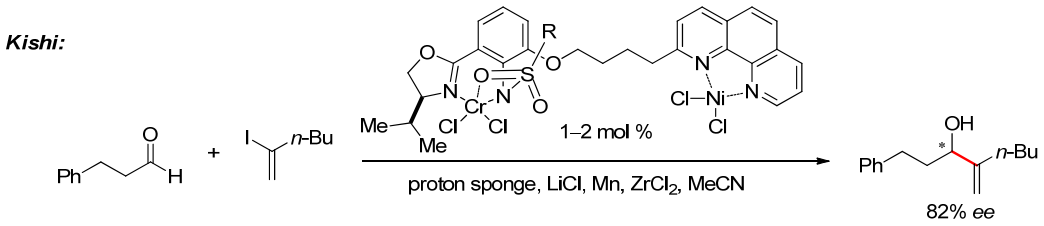
Scheme 74. *Asymmetric Methods for Linear Allylic Alcohols*



In recent years, the asymmetric Nozaki-Hiyama-Kishi (NHK) coupling reaction has seen developments in the synthesis of 1,1-disubstituted allylic alcohols by Kishi and coworkers (Scheme 75).[71] However, the noncommercial bimetallic ligands employed in this method seem to be extremely specialized for the substrates employed. Furthermore, the reagent combination that seems necessary for enantiocontrol illustrates the lengthy reaction optimization that was probably required for this methodology. Also, it is difficult to know for certain to what extent the ligand synthesis was guided by hypothesis and

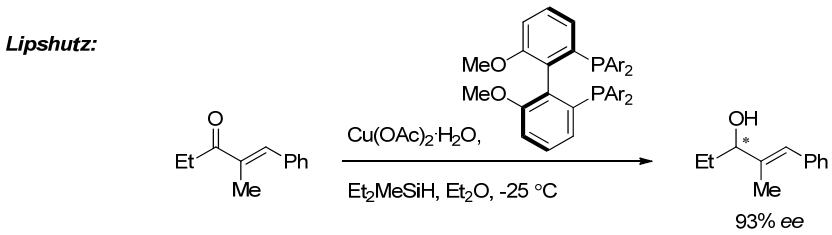
how easy it would be to modify them in order to optimize stereoselectivity. For synthetic chemists, the question of general applicability and predictability of a reaction is definitely something of an activation barrier when choosing a method. This especially applies to a protocol that requires ligands that may entail laborious synthetic tailoring for a specific substrate combination. All these negative factors work to drastically reduce the generality of this asymmetric transformation and it remains to be seen how widely this method is adopted by general chemical community.

Scheme 75. *The Asymmetric NHK Coupling for 1,1-Disubstitued Allylic Alcohols*



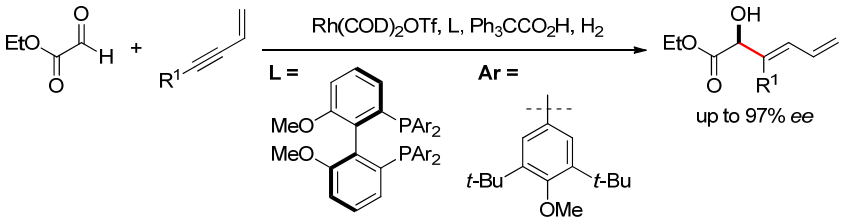
A recent contribution from Lipshutz and coworkers is the enantioselective 1,2-reduction of α,β-unsaturated carbonyls to produce chiral allylic alcohols (Scheme 76).[72] Although the substrates studied in this report were limited in scope, this may have been more due to the obvious ease in which certain staring materials can be accessed. Upon further improvements of this methodology, this reaction could prove to be quite powerful.

Scheme 76. *An Asymmetric Silane-Mediated 1,2-Reduction for Internal Allylic Alcohols*



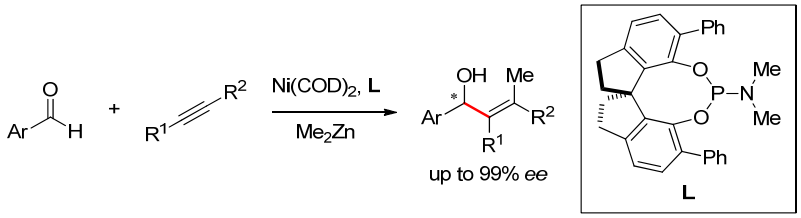
There have been several reports of transition metal–catalyzed asymmetric aldehyde–alkyne cross-couplings but few compare to the high enantioselectivities obtained in rhodium-catalyzed hydrogen-mediated variant reported by Krische and coworkers (Scheme 77).[8] However, this reaction is seemingly limited to α-keto aldehydes and electronically biased 1,3-enynes. This method may become more general in the future with reagent modifications but currently it remains highly specialized in scope. An intramolecular variant has also been reported by Krische and workers with equally high levels of asymmetric induction, however, the substrate scope is limited by the apparent necessity of substructures that benefit from a Thorpe-Ingold effect.

Scheme 77. *An Asymmetric Rhodium-Catalyzed Aldehyde–Alkyne Coupling*



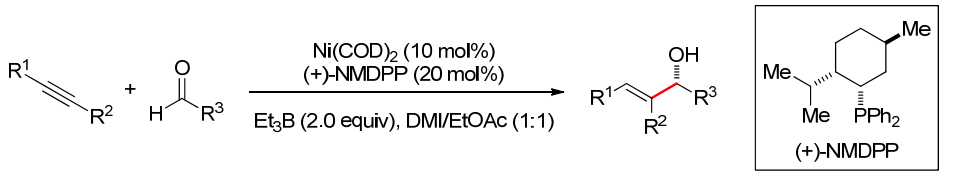
A highly enantioselective nickel-catalyzed aldehyde–alkyne alkylative coupling process has been accomplished using chiral spiro phosphoramidite ligands by Zhou and coworkers (Scheme 78).[73] Enantioselectivities range from 85–99% *ee*. However, only aromatic aldehydes are reported in this communication, arguably due to the low asymmetric induction that might be seen when aliphatic aldehydes are employed (by far the more useful aldehyde class from a synthetic utility perspective). Furthermore, only electronically biased or symmetric alkynes were utilized so regioselectivity issues are not addressed in this report.

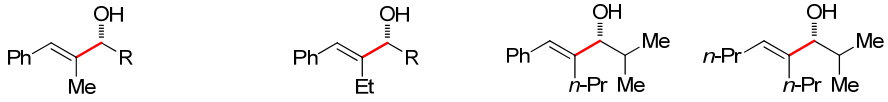
Scheme 78. *An Asymmetric Aldehyde–Alkyne Alkylative Coupling*



Jamison and coworkers have reported an asymmetric nickel-catalyzed Et_3B-mediated reductive coupling (Scheme 79).[36] Enantioselectivities range from 42–92% *ee* and the protocol is best suited for internal aromatic alkynes and branched aldehydes. Asymmetric induction drops quite dramatically if aldehyde or alkyne selection deviates from the optimized substrate combination. Interestingly, the enantioselectivities and product motifs are quite comparable to those seen in the copper-catalyzed silane-mediated 1,2-reduction method reported by Lipshutz and coworkers.

Scheme 79. *Chiral Phosphines in Asymmetric Reductive Couplings*





R = *i*-Pr: 95% (90% ee)
R = *n*-Pr: 82% (65% ee)
R = *c*-Hex: 97% (90% ee)
R = Ph: 79% (91:9 rs, 73% ee)

R = *c*-Hex: 78% (89% ee)
R = *i*-Pr: 95% (90% ee)

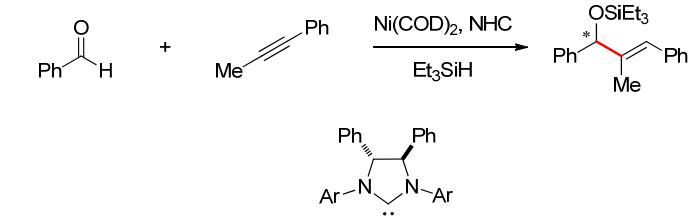
74% (92% ee)

35% (42% ee)

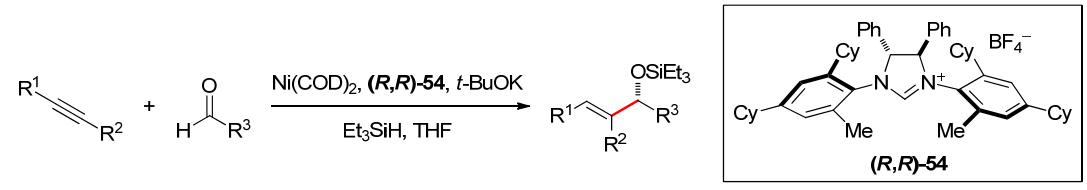
Our group reported an asymmetric nickel-catalyzed silane-mediated aldehyde–alkyne reductive coupling procedure using chiral NHC ligands.[37] These studies were inspired by the asymmetric ring-closing metathesis methods disclosed by

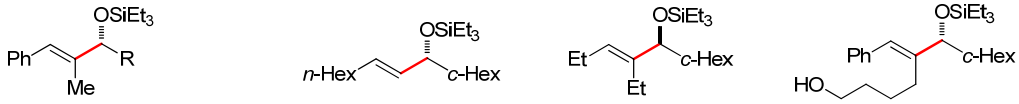
Grubbs and coworkers in which they utilize chiral NHC ligands. Various C_2-symmetric NHCs were synthesized and screened for optimal reactivity and enantioselectivity (Scheme 80). The NHC ligands **52** and **54** performed quite well. Ultimately, ligand **54** was chosen for a broader study due to the higher yields and enantioselectivities seen for a larger variety of substrate combinations. Enantioselectivities range from 65–85% ee and we used this as a benchmark for continuing studies.

Scheme 80. *Chiral NHCs in Asymmetric Reductive Couplings*



NHC	Yield	*ee*
49	50%	27%
50	50%	29%
51	40%	45%
52	60%	72%
53	79%	30%
54	98%	78%





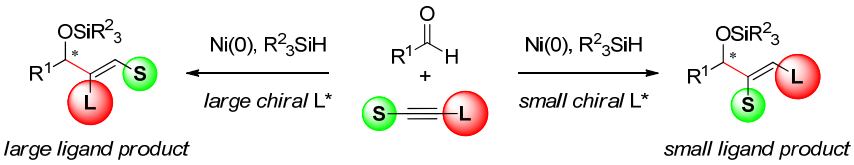
[a] **(*S*,*S*)-54** was used to obtain this stereoisomer.

4.2. Results and Discussion

4.2.1. Chiral Ligand Design

Enantiocontrol in nickel-catalyzed aldehyde–alkyne reductive couplings has been a long-term project of interest for our research group, one that my colleague and collaborator Grant J. Sormunen has been working to solve since the beginning of his doctoral studies in the Montgomery group. After the conclusion of various regioselectivity studies that I was involved with, my last project was to assist in the realization of a nickel catalyzed enantio- and regioselective reductive coupling of aldehydes and alkynes (Scheme 81).

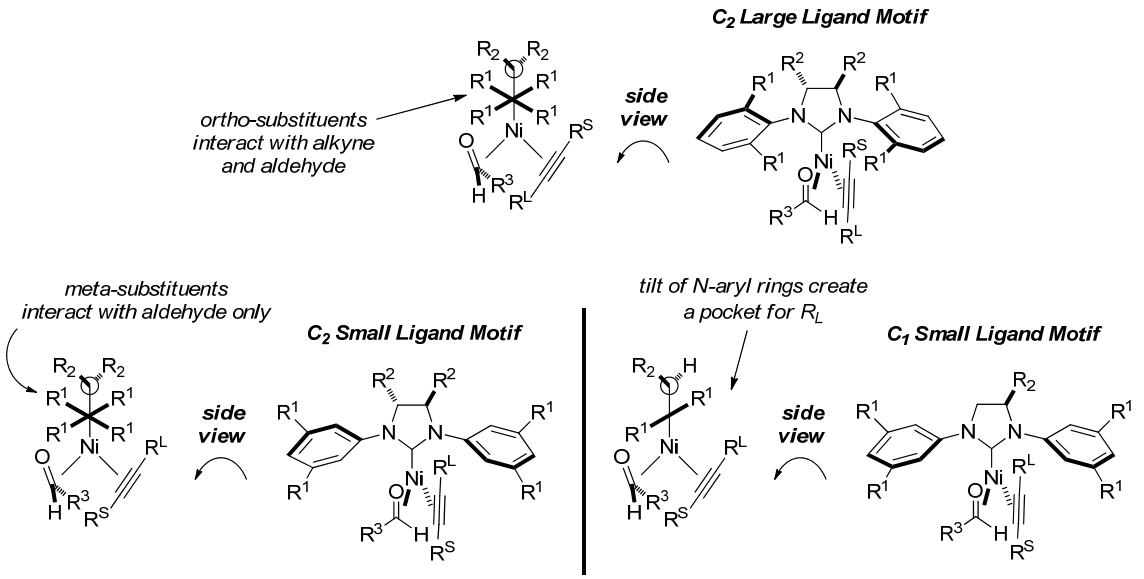
Scheme 81. *Research Goals for an Enantio- and Regioselective Reductive Coupling*



Based on our collaboration with Houk and coworkers, we realized that we could use different chiral NHC motifs to achieve our goals (Scheme 82). We realized that we needed to explore both C_1- and C_2-symmetric NHC ligands. The choice of the C_1 ligands was based on the parallel tilt orientation that we had seen in the transition-state structures of small NHC ligands in our past regioselectivity studies. In these systems, the single chiral center of the NHC backbone will bias the tilt in a particular direction, creating a pocket for the large alkyne substituent and inducing chirality by interacting with the aldehyde. For the C_2 ligands, Houk had informed us that *meta*-substituents on the *N*-aryl rings of an NHC interact exclusively with an aldehyde (prior to metallacycle formation), whereas the *ortho*-substituents impact alkyne regioselectivity as well as

aldehyde binding. By this analysis, we decided on two small ligand frameworks and one large ligand motif.

Scheme 82. *NHC Frameworks for Inducing Asymmetry and Regiocontrol*

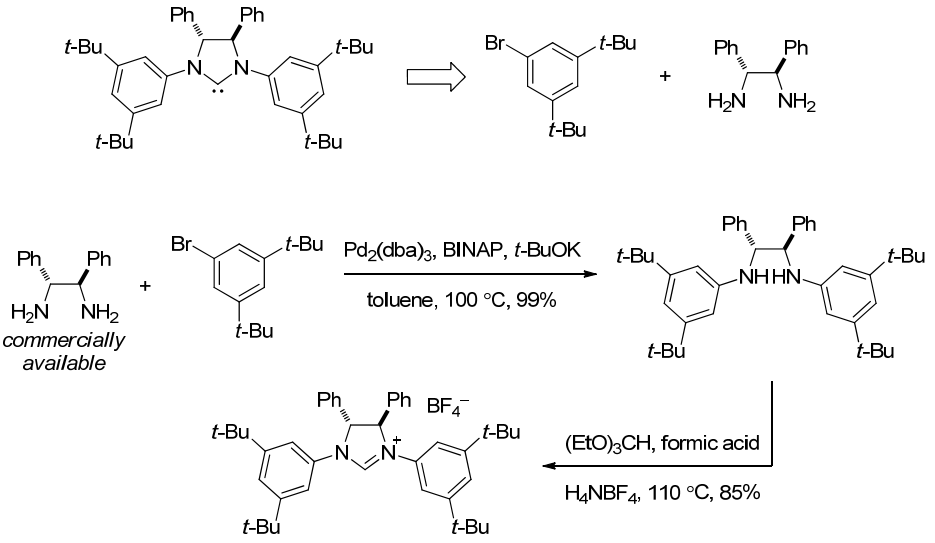


Various strategies for the synthesis of chiral NHC ligands have been disclosed, and contributions on expedient syntheses have come from various research groups, including our own. We have utilized much of this chemistry in both prior and ongoing studies, and some of this work has been published in our 2007 communication on asymmetric aldehyde–alkyne reductive couplings. Therefore, only representative syntheses of C_2 and C_1 ligands are shown in this section in order to avoid repetition.

The most commonly used chiral diamine for the synthesis of chiral C_2 NHCs is 1,2-diphenylethane diamine, due to the commercial availability of both enantiomers (Scheme 83). This diamine can undergo palladium-catalyzed Buchwald-Hartwig *N*-arylation chemistry to produce the aniline product. Next, the diamine can be cyclized to produce the free carbene precursor. In just two synthetic steps, the tetrafluoroborate salt of an

NHC can be obtained in good overall yield. This is the most expeditious method to produce chiral NHCs and is highly amenably for the generation of various analogs.

Scheme 83. *An Example of a C_2 NHC Synthesis*

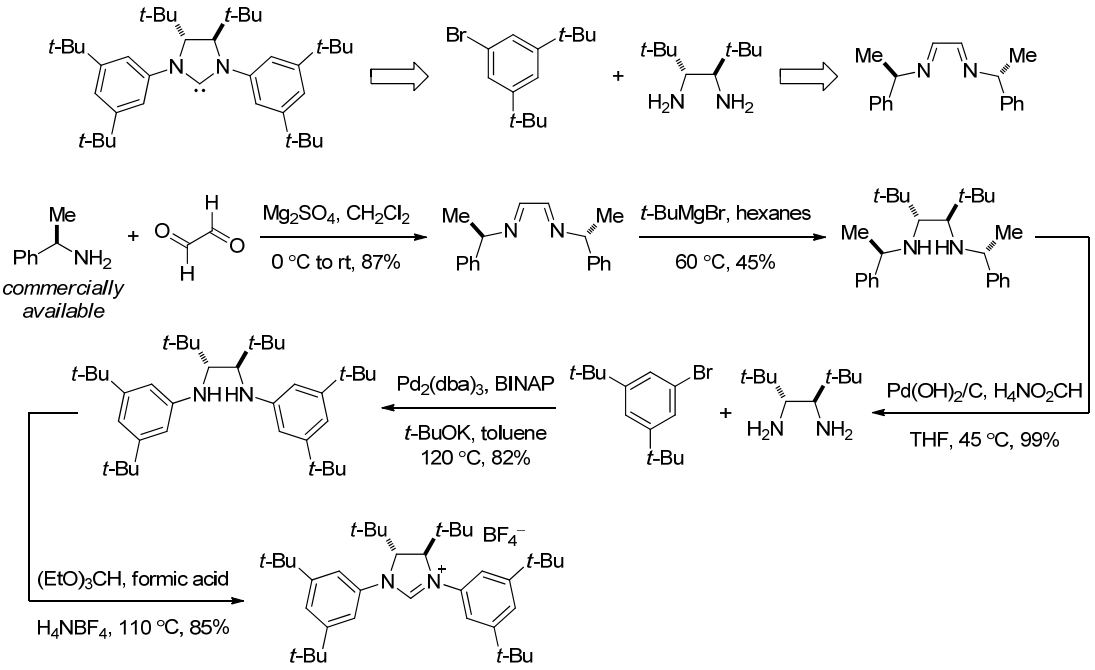


Another chiral C_2 symmetric ligand scaffold that was of interest is based on the 1,2-di-*tert*-butylethane backbone (Scheme 84).[74] Even though the final sequence to produce the free carbene precursor is identical to the earlier 1,2-diphenylethane C_2 symmetric ligand, the overall ligand synthesis is much longer due to the lack of commercial availability of the diamine itself. The sequence begins with the condensation of a chiral α-methylbenzyl amine with glyoxal. The resulting diimine undergoes diastereoselective Grignard addition of *t*-BuMgBr to produce a diamine. Following a benzyl deprotection reaction, an *N*-arylation/cyclization sequence is employed to produce the chiral free carbene precursor.

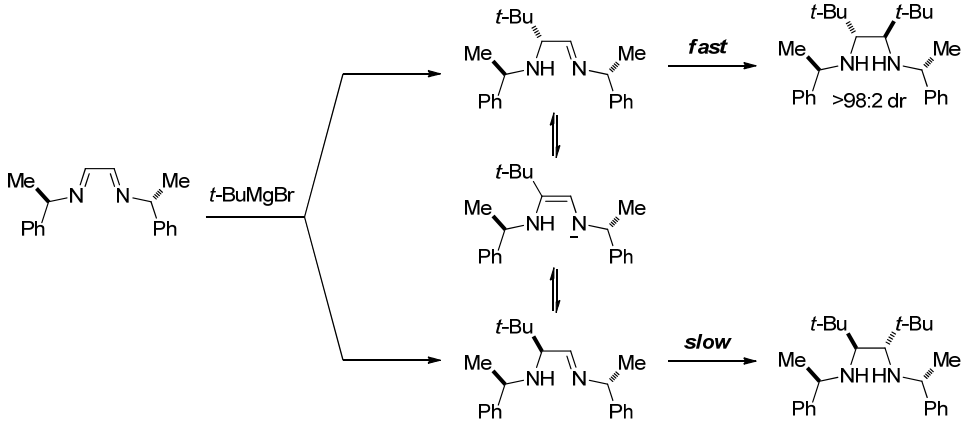
The most powerful aspect of the Grignard addition chemistry is the ability to control diastereoselectivity by means of a dynamic kinetic resolution (DKR) (Scheme 85). The DKR allows almost any Grignard reagent to be successfully reacted with control of

stereochemistry in the resulting product. This is undoubtedly the protocol of choice if resolution methods of racemic diamines are not readily viable. In fact, for large scale syntheses, resolution methods would be the more efficient and cost-effective route.

Scheme 84. *The Synthesis of Another Type of C_2 Symmetric NHC Ligand*

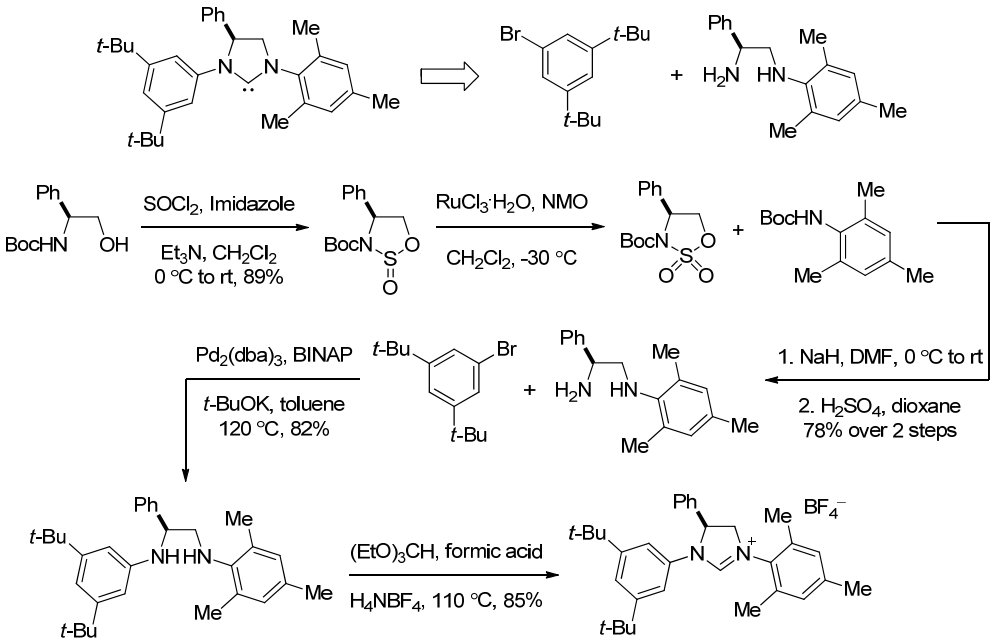


Scheme 85. *Postulated Dynamic Kinetic Resolution*



The final class of NHC ligand we were interested in synthesizing were chiral C_1 symmetric NHCs inspired by work of Hoveyda and coworkers (Scheme 86).[75] These ligands have proven to be extremely effective for a range of transition metal–catalyzed transformations and we were interested to see how similar ligands would function in nickel-catalyzed aldehyde–alkyne reductive couplings. Amino acid-derived Boc-protected 1,2-aminoalcohols can be cyclized by reaction with thionyl chloride. Ruthenium-catalyzed oxidation of the *O*-sulfoxide protecting group to an *O*-sulfone leaving group is followed by an S_N2 displacement reaction/global deprotection reaction. Palladium-catalyzed *N*-arylation/cyclization produces the free carbene precursor.

Scheme 86. *An Example of a C_1 NHC Ligand Synthesis*

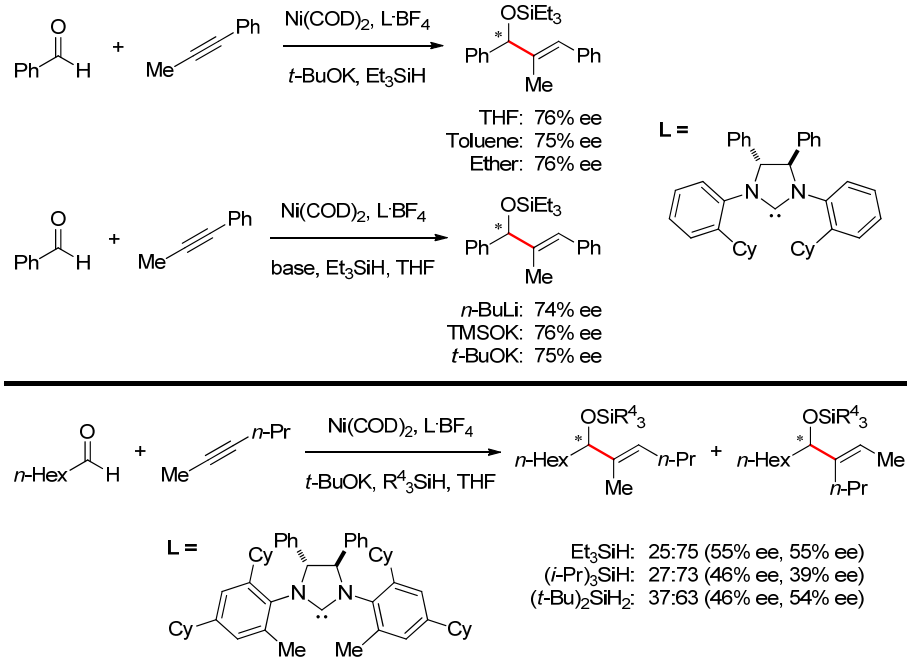


4.2.2. Enantio- and Regiocontrol using Chiral NHCs

Optimization studies performed by Dr. Mani R. Chaulagain and Grant J. Sormunen had shown that solvent, silane, and base selection had little effect on asymmetric induction (Scheme 87). From these studies, we realized that we could interchange

reagent combinations without loss of enantioselectivity. This is an important consideration as "small" ligands seem to require the use of *t*-Bu_2SiH_2 while "large" ligands can operate under standard conditions using Et_3SiH.

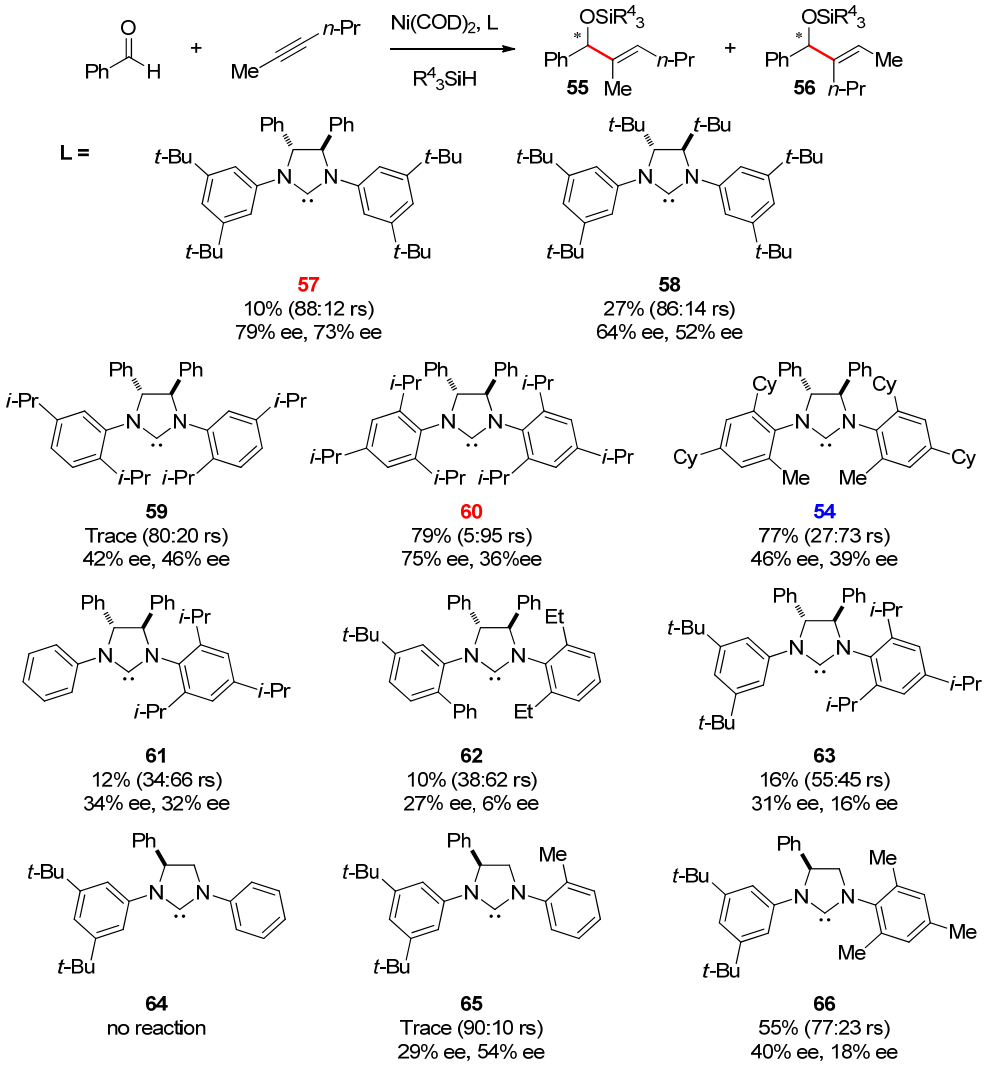
Scheme 87. *Unpublished Optimization Studies*



We decided to begin our enantio- and regioselectivity studies using 2-hexyne as internal alkynes with aliphatic substituents are arguably the most difficult substrate for stereoselective addition reactions (Scheme 88). Generally, enantioselectivities were low for a broad range of chiral C_1 and C_2 NHCs. However, two ligands stand out as impressive first generation leads for both small and large chiral NHC ligands (**57** and **60**). As a benchmark exampple, the chiral ligand **54** from our 2007 report affords a mixture of regioisomers **55**:**56** in 27:73 regioselectivity with 46% *ee* and 39% *ee*, respectively. Ligand **57** was the best small ligand studied, favoring **55** in 88:12

regioselectivity and 79% *ee*. Ligand **60** was the best large chiral ligand, favoring isomer **56** in 95:5 regioselectivity and 36% *ee*.

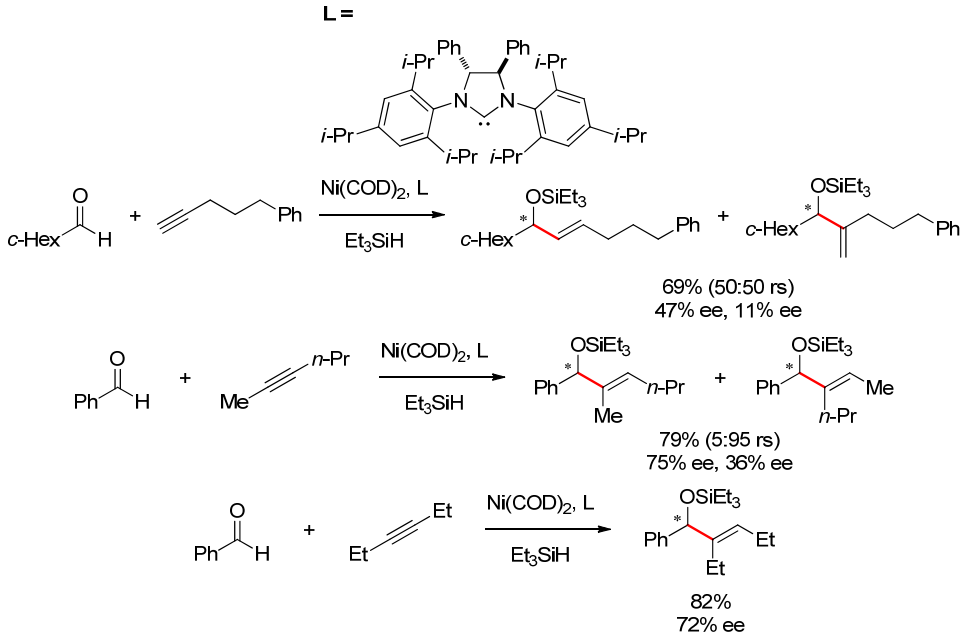
Scheme 88. *Results of Chiral NHC Screening Efforts*



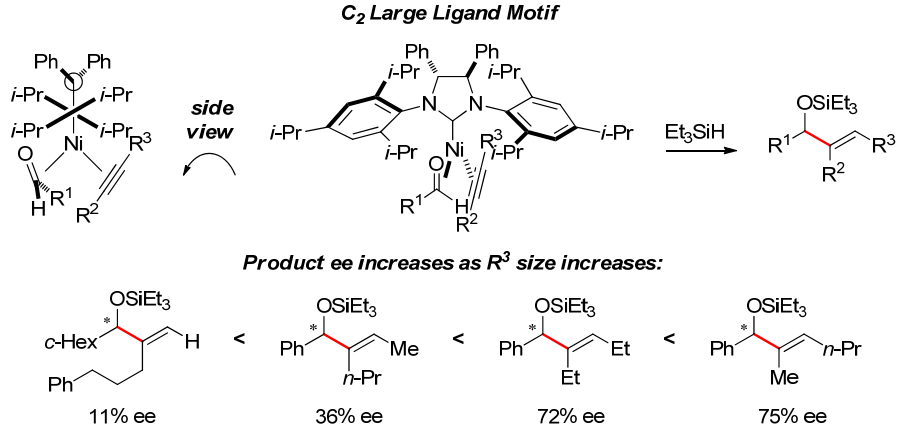
From the data collected, it can be seen that the asymmetric induction of regioisomer **55** is almost always considerably higher than **56** across the range of NHCs studied. We suspected that the reason for this divergence of enantioselectivities was due to the lack of steric interaction of the methyl group on the alkyne terminus with the catalyst in the

metallacycle formation step. To study this, we tested a range of alkynes using NHC **56** (Scheme 89). The level of asymmetric induction is clearly based on the choice of alkyne, specifically the size of R^3 in the enantio- and regioselectivity determining metallacycle formation transition-state (Scheme 90). As the size of R^3 increases, the level of asymmetric induction is enhanced.

Scheme 89. *Experiments to Study Trends*

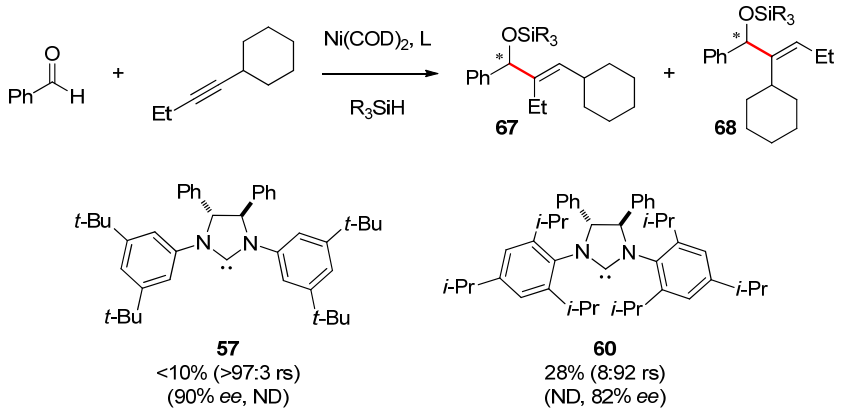


Scheme 90. *Trends of Asymmetric Induction of the Product Based on Alkyne Sterics*



Recent results from Grant J. Sormunen add further evidence to suggest an alkyne–catalyst interaction is vital for high levels of asymmetry in the resulting allylic alcohol product (Scheme 91). Although the basis of this phenomenon is unclear, we believe that increased alkyne sterics cause a larger rotation of the *N*-aryl rings of the NHC, thereby resulting in a heightened aldehyde–catalyst interaction which could increase asymmetric induction. Essentially there is an *indirect* interaction between the alkyne substituents and the aldehyde *through* the catalyst system. Using a biased alkyne with extended steric characteristics at both termini, ligand **57** produced isomer **67** in >97:3 regioselectivity and 90% *ee*. Ligand **60** reverses selectivity to favor **68** in 92:8 regioselectivity and of 82% *ee*. While yields are low, they could be raised by alternate carbene generation methods. It is important to note that to date, this is the best example of catalyst controlled enantio- and regiocontrol in the transition metal-catalyzed reductive coupling.

Scheme 91. *An Illustration of the Importance of Extended Branching in Alkynes*



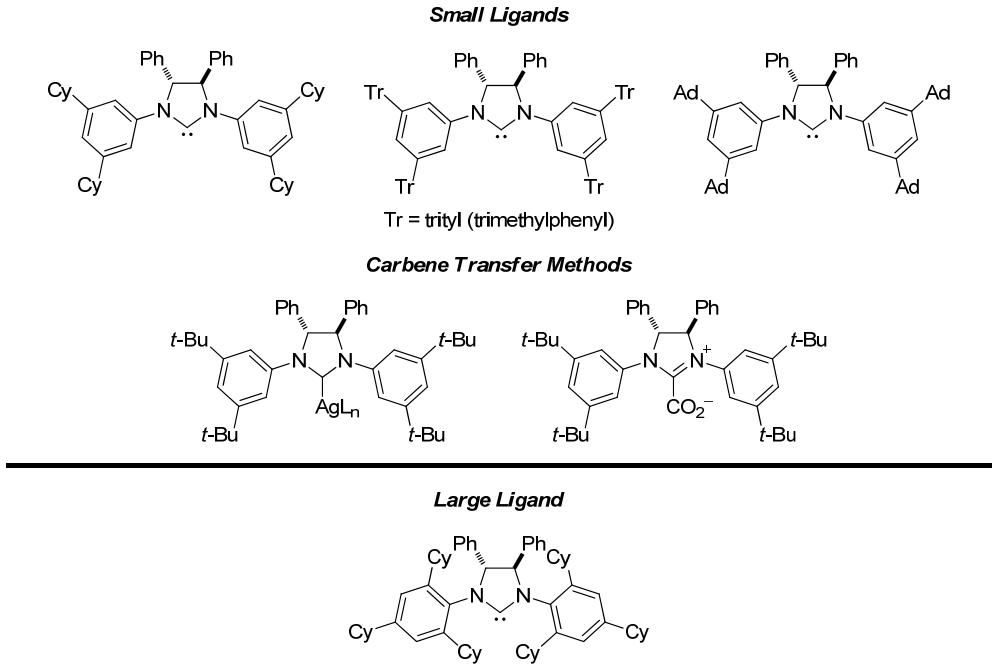
4.3. Future Directions for Enantio- and Regiocontrol Studies

There is an apparent necessity for an alkyne–catalyst–aldehyde interaction to achieve high levels of asymmetric induction of the resulting allylic alcohol (as discussed

in the previous section). If we wish to make the method general for a large class of alkynes, we need to extend the sterics of the ligands (Scheme 92). For the small ligand motifs, this translates to larger or more extended groups at the *meta*-position of the *N*-aryl groups. Furthermore, a careful and extensive study will need to be performed to find the optimal carbene transfer method if we hope to increase yields for the small NHC ligands (such as silver and CO_2 transfer methods). For the large ligand motifs, a simple 2,4,6-cyclohexyl substitution may be adequate to achieve our goal. However, the main difficulty in achieving such a substitution pattern is the challenge in achieving palladium-catalyzed *N*-arylations for highly hindered aryl halides. It may well be worth devising a racemic synthesis of the corresponding aniline and resolving the enantiomers by addition of chiral amino acids. Again, this is a long term project that may require a level of expertise not easily achieved in a short amount of time.

For the immediate future, any graduate student that continues this project should keep in mind that the best strategy for progress is to get an initial “hit” as quickly as possible. Optimization of yield and elegant ligand syntheses are of little importance if the enantio- and regiocontrol aspects are not encouraging. I believe that the years of work Grant J. Sormunen has expended on this project and my own assistance on for the past few months has solved many important and longstanding issues that previously existed. We have a clear indication of which ligand frameworks to improve upon in the future. The most difficult and tedious aspects of this project have, in my opinion, been resolved.

Scheme 92. *Future Directions*



4.4. Conclusion

In summary, an effective and direct means of enantio- and regioselective aldehyde–alkyne reductive couplings has been described. However, improvements to the current method will be necessary, specifically: (1) careful and hypothesis-derived ligand alterations to improve asymmetric induction; and (2) overall yield improvement will provide a highly effective procedure. From an extensive hypothesis-driven screening effort, we have found second generation NHC motifs that may perform at an even higher level of stereoselectivity. When fully realized, this protocol will become an important and powerful method for the construction of internal chiral allylic alcohols.

Chapter 5

Experimental Supporting Information

5. General Experimental Details

Unless otherwise noted, all reactions were conducted in flame-dried or oven dried (120 °C) glassware with magnetic stirring under an atmosphere of dry nitrogen. Solvents were purified under nitrogen using a solvent purification system (Innovative Technology, inc., Model # SPS-400-3 and PS-400-3). Aldehydes and alkynes were distilled prior to use. Silanes were passed through alumina. $Ni(COD)_2$ (Strem Chemicals, Inc.), all *N*-heterocyclic carbene salts, and *t*-BuOK (Aldrich) were stored and weighed in an inert atmosphere glovebox.

Analytical thin layer chromatography (TLC) was performed on Kieselgel 60 F254 (250 μm silica gel) glass plates and compounds were visualized with UV light, iodine, *p*-anisaldehyde stain, ceric ammonium molybdate stain, or aqueous $KMnO_4$ solution. Flash column chromatography was performed using Kieselgel 60 (230-400 mesh) silica gel. Eluent mixtures are reported as v:v percentages of the minor constituent in the major constituent. All compounds purified by column chromatography were sufficiently pure for use in further experiments unless otherwise indicated.

^1H NMR spectra were measured at 400 MHz on a Varian Mercury 400 instrument or at 500 MHz on a Varian Unity 500 instrument. The proton signal of the residual, nondeuterated solvent (δ 7.24 for $CHCl_3$) was used as an internal reference for ^1H NMR

spectra. ^{13}C NMR spectra were completely heterodecoupled and measured at 125 or 100 MHz. Residual chloroform (δ 77.0) was used as an internal reference. High resolution mass spectra were recorded on a VG 70-250-s spectrometer manufactured by Micromass Corp. (Manchester UK) at the University of Michigan Mass Spectrometry Laboratory.

5.1. General Procedures

5.1.1. General Procedure A for the $Ni(COD)_2$/NHC-Promoted Reductive Coupling of Silyl(propargyl)ethers:

To a solid mixture of $Ni(COD)_2$ (12 mol%), IMes·HCl salt (10 mol%), and *t*-BuOK (10 mol%) was added THF (0.125 M). The resulting solution was stirred for 5 min at rt until the solution turned dark blue in appearance. The propargyl alcohol derivative (1.0 equiv), aldehyde (1.1 equiv), and triisopropylsilane (2.0 equiv) were added sequentially and the reaction mixture was allowed to stir until starting materials were consumed. The reaction mixture was filtered through silica gel eluting with 50% EtOAc/hexanes. The solvent was removed *in vacuo*, and the crude residue was purified via flash chromatography on silica gel to afford the desired product.

5.1.2. General Procedure B for Palladium-Catalyzed Allylic Reductions to Form External Olefins:

To a solid mixture of $Pd_2(dba)_3·CHCl_3$ (5 mol%) and ammonium formate (2.0 equiv) was added THF (0.2 M). To the resulting solution was added PBu_3 (20 mol%) and the reaction mixture was stirred for 10 min. The allylic acetate was added to the reaction vessel and heated to 65 °C for 48 h. The reaction was then quenched with H_2O and extracted with diethyl ether three times. The organic layer was dried with $MgSO_4$, filtered, and concentrated. The crude residue was purified via flash chromatography to afford the desired products.

5.1.3. General Procedure C for Palladium-Catalyzed Allylic Reductions to Form 1,3-Dienes:

To a solid mixture of $Pd_2(dba)_3·CHCl_3$ (5 mol%), 1,1'-bis(diphenylphosphino)ferrocene (dppf) (20 mol%) was added DMF (0.2 M). To the resulting solution was added formic acid (1.2 equiv) and triethylamine (2.0 equiv) and

stirred for 10 min. The allylic acetate was added to the reaction vessel and heated to 80 °C for 48 h. The reaction mixture was then quenched with satd. ammonium chloride solution and extracted with ether three times. The organic layer was dried with $MgSO_4$, filtered, and concentrated. The crude residue was purified via flash chromatography to afford the desired products.

5.1.4. General Procedure D for Deoxygenation via SO_3·Py S_N2 Displacement Protocol:

To a SO_3·Py (1.5 equiv) in THF (0.1 M) was added the allylic alcohol at 0 °C for 3 h. To the reaction mixture was added $LiAlH_4$ (6.0 equiv) and stirred at 0 °C for 1 h, and then the reaction mixture was then allowed to warm to rt. The reaction was then quenched with 15% NaOH solution at 0 °C, diluted with diethyl ether, and then filtered through celite. The filtrate was then dried with $MgSO_4$, filtered, and concentrated. The crude residue was purified via flash chromatography to afford the desired products.

5.1.5. General Procedure E for the Ni(COD)$_2$/*i*-Pr-BAC-Promoted Reductive Coupling of Alkynes, Aldehydes, and Di-*tert*-butylsilane:

To a solid mixture of $Ni(COD)_2$ (22 mol %), *i*-Pr-BAC·HBF_4 salt (20 mol %) was added THF (0.25 M). To the resulting solution was added *n*-BuLi (2.5 M in hexanes) (20 mol %). The resulting solution was stirred for 5 min at rt until the solution turned dark red in appearance. The alkyne (1.0 equiv), aldehyde (1.0 equiv), di-*tert*-butylsilane (1.2 equiv), and THF (0.25 M) were added via syringe pump addition over 60 minutes and the reaction mixture was allowed to stir until starting materials were consumed. The reaction mixture was filtered through silica gel eluting with 50% EtOAc/hexanes. The solvent was removed *in vacuo*, and the crude residue was purified via flash chromatography on silica gel to afford the desired product.

5.1.6. General Procedure F for the $Ni(COD)_2$/SIPr-Promoted Reductive Coupling of Alkynes, Aldehydes, and Triisopropylsilane:

To a solid mixture of $Ni(COD)_2$ (12 mol %), SIPr·HCl salt (10 mol %), and *t*-BuOK (10 mol %) was added THF (0.125 M). The resulting solution was stirred for 5 min at rt until the solution turned dark brown in appearance. The alkyne (1.0 equiv), aldehyde (1.0 equiv), and triisopropylsilane (2.0 equiv) were added sequentially, and the reaction mixture was allowed to stir until starting materials were consumed. The reaction mixture was filtered through silica gel eluting with 50% EtOAc/hexanes. The solvent was removed *in vacuo*, and the crude residue was purified via flash chromatography on silica gel to afford the desired product.

5.1.7. General Procedure G for the $Ni(COD)_2$/IMes-Promoted Reductive Coupling of Alkynes, Aldehydes, and Triisopropylsilane:

To a solid mixture of $Ni(COD)_2$ (12 mol %), IMes·HCl salt (10 mol %), and *t*-BuOK (10 mol %) was added THF (0.125 M). The resulting solution was stirred for 5 min at rt until the solution turned dark blue in appearance. The alkyne derivative (1.0 equiv), aldehyde (1.0 equiv), and triisopropylsilane (2.0 equiv) were added sequentially, and the reaction mixture was allowed to stir until starting materials were consumed. The reaction mixture was filtered through silica gel eluting with 50% EtOAc/hexanes. The solvent was removed *in vacuo*, and the crude residue was purified via flash chromatography on silica gel to afford the desired product.

5.1.8. General Procedure H for the $Ni(COD)_2$/Ph_2SIPr-Promoted Reductive Coupling of Alkynes, Aldehydes, and Triethylsilane:

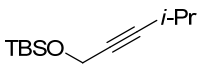
To a solid mixture of $Ni(COD)_2$ (12 mol %), Ph_2SIPr·HBF_4 salt (10 mol %) was added THF (0.2 M). To the resulting solution was added *n*-BuLi (2.5 M in hexanes) (10 mol %). The resulting solution was stirred for 5 min at rt until the solution turned dark red in

appearance. Triethylsilane (2.0 equiv) was then added to the reaction mixture. The alkyne (1.2 equiv), aldehyde (1.0 equiv), and THF (0.2 M) were added via syringe pump addition over 30 minutes and the reaction mixture was allowed to stir until starting materials were consumed. The reaction mixture was filtered through silica gel eluting with 50% EtOAc/hexanes. The solvent was removed *in vacuo*, and the crude residue was purified via flash chromatography on silica gel to afford the desired product.

5.2. Spectral Characterization

5.2.1. Chapter 2 Starting Propargyl Alcohol Derivatives

***t*-Butyldimethyl(4-methylpent-2-ynyloxy)silane**:



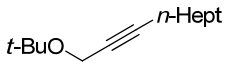
^{1}H NMR (400 MHz, $CDCl_3$): δ 4.26 (d, *J* = 1.6 Hz, 2H), 2.53 (septt, *J* = 7.2 Hz, 2.0 Hz, 1H), 1.12 (d, *J* = 6.8 Hz, 6H), 0.88–0.86 (m, 9H), 0.09–0.08 (m, 6H). **^{13}C NMR (100 MHz, $CDCl_3$):** δ 90.8, 77.9, 51.9, 25.9, 25.8, 22.8, 20.5, 18.3, -5.1. **IR (thin film):** v 2960, 2930, 2858 1463 cm^{-1}. **HRMS Chemical Ionization (*m/z*):** $[M–H]^+$ calcd for $C_{12}H_{23}OSi$, 211.1518; found 211.1521.

1-Methoxydec-2-yne:



^{1}H NMR (400 MHz, $CDCl_3$): δ 4.03 (t, *J* = 2.4 Hz, 2H), 3.32 (s, 3H), 2.17 (tt, *J* = 7.6 Hz, 2.0 Hz, 2H), 1.47 (quint, *J* = 7.2, 2H), 1.38–1.18 (m, 8H), 0.84 (t, *J* = 6.8 Hz, 3H). **^{13}C NMR (100 MHz, $CDCl_3$):** δ. 87.1, 75.6, 60.1, 57.2, 31.7, 28.8 28.7, 28.6, 22.6, 18.7, 14.0. **IR (thin film):** v 2928, 2855, 1465 cm^{-1}. **HRMS Chemical Ionization (*m/z*):** $[M–H]^+$ calcd for $C_{11}H_{19}O$, 167.1436; found 167.1436.

1-*t*-Butoxydec-2-yne:

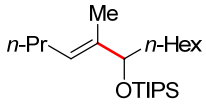


^{1}H NMR (400 MHz, $CDCl_3$): δ 4.05 (t, *J* = 2.0 Hz, 2H), 2.18 (tt, *J* = 7.2 Hz, 2.0 Hz, 2H), 1.53–1.41 (m, 4H), 1.37–1.24 (m, 6H), 1.21 (s, 9H), 0.86 (t, *J* = 6.8 Hz, 3H). **^{13}C NMR (100 MHz, $CDCl_3$):** δ 85.4, 77.4, 73.8, 50.7, 31.7, 28.8, 28.7, 28.5, 27.4, 22.5, 18.8, 14.0. **IR (thin film):** v 2973, 2930, 2857, 1466 cm^{-1}. **HRMS Chemical Ionization (*m/z*):** $[M+H]^+$ calcd for $C_{14}H_{27}O$, 211.2062; found 211.2066.

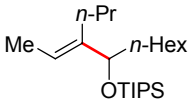
5.2.2. Chapter 2 Nickel-Catalyzed Reductive Coupling Substrates

5.2.2.1. Scheme 52 Entries

(*E*)-triisopropyl(5-methyldodec-4-en-6-yloxy)silane. *Major Regioisomer:*



(*E*)-triisopropyl(4-propylundec-3-en-5-yloxy)silane. *Minor Regioisomer:*



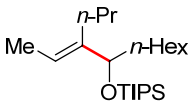
Scheme 52, Entry 1: Following Procedure A, $Ni(COD)_2$ (19.6 mg, 0.071 mmol), IMes·HCl salt (20.3 mg, 0.059 mmol), *t*-BuOK (6.7 g, 0.059 mmol), triisopropylsilane (0.24 mL, 1.19 mmol), 2-hexyne (50 mg, 0.59 mmol), 1-heptanal (75 g, 0.66 mmol) gave a crude residue which was purified via flash chromatography (100% hexanes) to afford two regioisomers in a 67:33 selectivity (175 mg, 83% yield): Major (117 g, 0.33 mmol, 55% yield); Minor (58 mg, 0.16 mmol, 28% yield).

Major Regioisomer: **^{1}H NMR (500 MHz, $CDCl_3$):** δ 5.26 (t, *J* = 7 Hz, 1H), 4.04 (t, *J* = 6.5 Hz, 1H), 2.00 (dq, *J* = 14.0 Hz, 7.0 Hz, 1H), 1.96 (dq, *J* = 14.0 Hz, 7.0 Hz, 1H), 1.54–1.49 (m, 2H), 1.37 (m, 2H), 1.31–1.12 (m, 6H), 1.19–1.15 (m, 2H), 1.06–1.01 (m, 21H), 0.90 (t, *J* = 7.5 Hz, 3H), 0.88 (t, *J* = 7.0 Hz, 3H). **^{13}C NMR (125 MHz, $CDCl_3$):** δ 137.1, 126.0, 78.9, 36.1, 31.9, 29.6, 29.4, 25.5, 22.8, 22.7, 18.14, 18.10, 14.1, 13.9, 12.4, 10.7. **IR (thin film):** ν 2932, 2866, 1464 cm^{-1}. **HRMS Chemical Ionization (*m/z*):** $[M+H]^+$ calcd for $C_{22}H_{47}OSi$, 355.3396; found 355.3382.

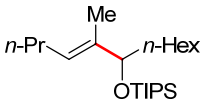
Minor Regioisomer: **^{1}H NMR (500 MHz, $CDCl_3$):** δ 5.37 (q, *J* = 7.0 Hz, 1H), 4.09 (t, *J* = 6.5 Hz, 1H), 1.98 (m, 2H), 1.61 (d, *J* = 7.0 Hz, 3H), 1.55–1.51 (m, 2H), 1.42 (m, 2H), 1.31–1.22 (m, 6H), 1.19–1.15 (m, 2H), 1.07–1.01 (m, 21H), 0.93 (t, *J* = 7.0 Hz, 3H), 0.88 (t, *J* = 7.0 Hz, 3H). **^{13}C NMR (125 MHz, $CDCl_3$):** δ 142.0, 120.7, 78.1, 36.7, 31.9, 29.5, 28.9, 25.1, 22.74, 22.68, 18.15, 18.14, 14.9, 14.1, 13.0, 12.5. **IR (thin film):** ν 2932,

2866, 1465 cm^{-1}. **HRMS Chemical Ionization (*m/z*):** $[M–H]^+$ calcd for $C_{22}H_{45}OSi$, 353.3240; found 353.3234.

(*E*)-triisopropyl(4-propylundec-3-en-5-yloxy)silane. *Major Regioisomer:*



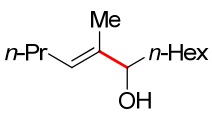
(*E*)-triisopropyl(5-methyldodec-4-en-6-yloxy)silane. *Minor Regioisomer:*



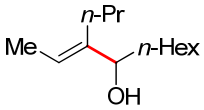
Scheme 52, Entry 2: Following Procedure A, $Ni(COD)_2$ (19.6 mg, 0.071 mmol), IPr·HCl salt (25.3 mg, 0.059 mmol), *t*-BuOK (6.7 g, 0.059 mmol), triisopropylsilane (0.24 mL, 1.19 mmol), 2-hexyne (50 mg, 0.59 mmol), 1-heptanal (75 g, 0.66 mmol) gave a crude residue which was purified via flash chromatography (100% hexanes) to afford two regioisomers in a 80:20 selectivity (177 mg, 84% yield): Major (118 mg, 0.33 mmol, 56% yield); Minor (59 mg, 0.17 mmol, 28% yield).

Spectral data as previously reported for Scheme 52, Entry 1.

(*E*)-5-methyldodec-4-en-6-ol. *Major Regioisomer:*



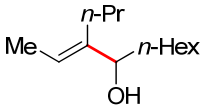
(*E*)-4-ethylideneundecan-5-ol. *Minor Regioisomer:*



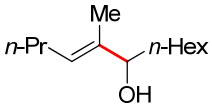
Scheme 52, Entry 3: Following a modified Procedure A, $Ni(COD)_2$ (16.4 mg, 0.059 mmol), PBu_3 (24.0 mg, 0.12 mmol, Et_3B (0.17 mL, 1.19 mmol), 2-hexyne (50 mg, 0.59 mmol), 1-heptanal (75 g, 0.66 mmol) gave a crude residue which was purified via flash chromatography (100% hexanes) to afford a mixture of two regioisomers in a 51:49 selectivity (87 mg, 74% yield): Major (44.4 mg, 0.22 mmol, 38% yield); Minor (42.6 mg, 0.21 mmol, 36% yield).

^{1}H NMR (500 MHz, $CDCl_3$): δ 5.45 (q, *J* = 7.0 Hz, 0.5H), 5.34 (t, *J* = 7.0 Hz, 0.5H), 3.96–3.92 (m, 1H), 2.02–1.80 (m, 2H), 1.06 (d, *J* = 7.0 Hz, 1.5H), 1.56 (s, 1.5H), 1.52–1.15 (m, 13H), 0.91–0.83 (m, 6H). **^{13}C NMR (125 MHz, $CDCl_3$):** δ 142.9, 137.2, 126.7, 120.7, 78.1, 76.96, 35.7, 34.8, 31.81, 31.80, 29.5. 29.26, 29.21, 26.0, 25.8, 22.8, 22.64, 22.59, 22.58, 14.5, 14.0, 13.8, 13.1, 11.0. **IR (thin film):** v 3347, 2958, 2930, 2859, 1466 cm^{-1}. **HRMS Electron Ionization (*m/z*):** $[M]^+$ calcd for $C_{13}H_{26}O$, 198.1984; found 198.1983.

(*E*)-4-ethylideneundecan-5-ol. *Major Regioisomer:*



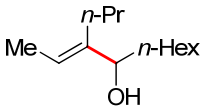
(*E*)-5-methyldodec-4-en-6-ol. *Minor Regioisomer:*



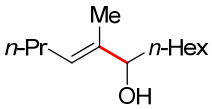
Scheme 52, Entry 4: Following a modified Procedure A, $Ni(COD)_2$ (16.4 mg, 0.059 mmol), PCy_3 (24.0 mg, 0.12 mmol, Et_3B (0.17 mL, 1.19 mmol), 2-hexyne (50 mg, 0.59 mmol), 1-heptanal (75 g, 0.66 mmol) gave a crude residue which was purified via flash chromatography (100% hexanes) to afford a mixture of two regioisomers in a 60:40 selectivity (93 mg, 79% yield): Major (56 mg, 0.28 mmol, 47% yield); Minor (37 mg, 0.19 mmol, 32% yield).

Spectral data as previously reported for Scheme 52, Entry 3.

(*E*)-4-ethylideneundecan-5-ol. *Major Regioisomer:*



(*E*)-5-methyldodec-4-en-6-ol. *Minor Regioisomer:*

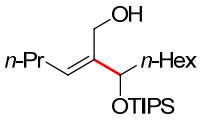


Scheme 52, Entry 5: Following a modified Procedure A, $Ni(COD)_2$ (16.4 mg, 0.059 mmol), P(*t*-Bu)$_3$ (24.0 mg, 0.12 mmol, Et_3B (0.17 mL, 1.19 mmol), 2-hexyne (50 mg, 0.59 mmol), 1-heptanal (75 g, 0.66 mmol) gave a crude residue which was purified via flash chromatography (100% hexanes) to afford a mixture of two regioisomers in a 62:38 selectivity (79 mg, 67% yield): Major (49 mg, 0.25 mmol, 42% yield); Minor (30 mg, 0.19 mmol, 25% yield).

Spectral data as previously reported for Scheme 52, Entry 3.

5.2.2.2. Table 1 Entries

(*E*)-2-butylidene-3-(triisopropylsilyloxy)nonan-1-ol. *Major Regioisomer:*



(*E*)-3-propyl-4-(triisopropylsilyloxy)dec-2-en-1-ol. *Minor Regioisomer:*

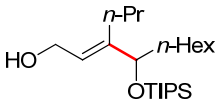


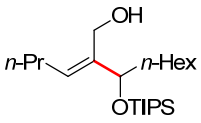
Table 1, Entry 1: Following Procedure A, $Ni(COD)_2$ (34 mg, 0.12 mmol), IMes·HCl salt (35 mg, 0.10 mmol), *t*-BuOK (12 mg, 0.10 mmol), triisopropylsilane (0.42 mL, 2.0 mmol), 2-hexyn-1-ol (100 mg, 1.0 mmol), 1-heptanal (128 mg, 1.1 mmol) gave a crude residue which was purified via flash chromatography (10% EtOAc/Hexanes) to afford two

regioisomers in a 80:20 selectivity (339 mg, 92% yield): Major (273 mg, 0.74 mmol, 74% yield); Minor (66 mg, 0.18 mmol, 18% yield).

Major Regioisomer: **^{1}H NMR (500 MHz, C_6D_6):** δ 5.36 (t, *J* = 7.5 Hz, 1H), 4.33 (d, *J* = 12.0 Hz, 1H), 4.28 (dd, *J* = 8.5 Hz, 5 Hz, 1H), 4.26 (d, *J* = 12.0 Hz, 1H), 2.59 (s, 1H), 2.02 (m, 1H), 1.96 (m, 1H), 1.91–1.82 (m, 1H), 1.79–1.72 (m, 1H), 1.36–1.18 (m, 10H), 1.12–1.07 (m, 21H) 0.87 (t, *J* = 7.5 Hz, 3H), 0.84 (t, *J* = 7.5 Hz, 3H). **^{13}C NMR (100 MHz, C_6D_6):** δ 139.6, 130.5, 79.8, 58.2, 36.9, 32.3, 29.69, 29.67, 25.9, 23.3, 23.0, 18.35, 18.34, 14.3, 14.0, 12.7. **IR (thin film):** v 3442, 2931, 2866, 1464 cm^{-1}. **HRMS Chemical Ionization (*m/z*):** $[M–H]^+$ calcd for $C_{22}H_{45}O_2Si$, 369.3189; found 369.3191.

Minor Regioisomer : **^{1}H NMR (500 MHz, $CDCl_3$):** δ 5.55 (t, *J* = 6.5 Hz, 1H), 4.22–4.13 (m, 3H), 1.99 (m, 2H), 1.55–1.51 (m, 2H), 1.41–1.33 (m, 3H), 1.21–1.12 (m, 8H), 1.06–1.01 (m, 21H), 0.90 (t, *J* = 7.0 Hz, 3H), 0.85 (t, *J* = 7.0 Hz, 3H). **^{13}C NMR (125 MHz, $CDCl_3$):** δ 144.8, 125.0, 76.8, 59.3, 36.4, 31.8, 29.5, 29.4, 24.6, 23.7, 22.6, 18.14, 18.11, 14.7, 14.1, 12.4. **IR (thin film):** v 3320, 2933, 2867, 1464 cm^{-1}. **HRMS Chemical Ionization (*m/z*):** $[M–H]^+$ calcd for $C_{22}H_{45}O_2Si$, 369.3181; found 369.3195.

(*E*)-2-butylidene-3-(triisopropylsilyloxy)nonan-1-ol. *Major Regioisomer:*



(*E*)-3-propyl-4-(triisopropylsilyloxy)dec-2-en-1-ol. *Minor Regioisomer:*

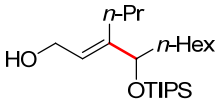
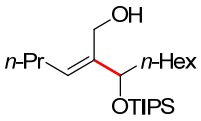


Table 1, Entry 2: Following Procedure A, $Ni(COD)_2$ (34 mg, 0.12 mmol), IPr·HCl salt (44 mg, 0.10 mmol), *t*-BuOK (12 mg, 0.10 mmol), triisopropylsilane (0.42 mL, 2.0 mmol), 2-hexyn-1-ol (100 mg, 1.0 mmol), 1-heptanal (128 mg, 1.1 mmol) gave a crude residue which was purified via flash chromatography (10% EtOAc/Hexanes) to afford two regioisomers in a 67:33 regioselectivity (294 g, 78% yield): Major (196 mg, 0.52 mmol, 52% yield); Minor (98 mg, 0.26mmol, 26% yield).

Spectral data as previously reported for Table 1, Entry 1.

(*E*)-2-butylidene-3-(triisopropylsilyloxy)nonan-1-ol. *Major Regioisomer:*



(*E*)-3-propyl-4-(triisopropylsilyloxy)dec-2-en-1-ol. *Minor Regioisomer:*

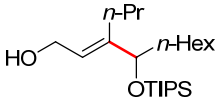
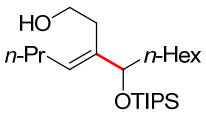


Table 1, Entry 3: Following a modified Procedure A, $Ni(COD)_2$ (28 mg, 0.10 mmol), PCy_3 (57 mg, 0.20 mmol), triisopropylsilane (0.42 mL, 2.0 mmol), 2-hexyn-1-ol (100 mg, 1.0 mmol), 1-heptanal (128 mg, 1.1 mmol) gave a crude residue which was purified via flash chromatography (10% EtOAc/Hexanes) to afford two regioisomers in a 67:33 regioselectivity (302 g, 80% yield): Major (200 mg, 0.59 mmol, 53% yield); Minor (102 mg, 0.27 mmol, 27% yield).

Spectral data as previously reported for Table 1, Entry 1.

(*E*)-4-propyl-5-(triisopropylsilyloxy)undec-3-en-1-ol:



(*E*)-3-butylidene-4-(triisopropylsilyloxy)decan-1-ol:

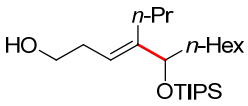
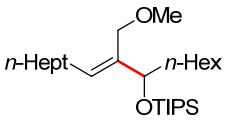


Table 1, Entry 4: Following Procedure A, $Ni(COD)_2$ (19.6 mg, 0.071 mmol), IMes·HCl salt (20.3 mg, 0.059 mmol), *t*-BuOK (6.7 g, 0.059 mmol), triisopropylsilane (0.24 mL, 1.19 mmol), 3-heptyn-1-ol (67 mg, 0.59 mmol), 1-heptanal (75 g, 0.66 mmol) gave a crude residue which was purified via flash chromatography (10% EtOAc/Hexanes) to afford two regioisomers in a 50:50 selectivity (188 mg, 0.49 mmol, 82% yield).

^{1}H NMR (500 MHz, $CDCl_3$): δ 5.38 (t, *J* = 7.0 Hz, 1H), 4.08 (dd, *J* = 10.0 Hz, 5.0 Hz, 1H), 3.71–3.65 (m, 1H), 3.57–3.51 (m, 1H), 3.42 (dd, *J* = 9.0 Hz, 3.0 Hz, 1H), 2.47 (dt, *J* = 14.0 Hz, 4.5 Hz, 1H), 2.17 (ddd, *J* = 14.5 Hz, 9.0 Hz, 5.5 Hz, 1H), 2.02 (dd, *J* = 7.5 Hz, 2.0 Hz, 1H), 1.99 (dd, *J* = 7.0 Hz, 2.0 Hz, 1H), 1.72–1.64 (m, 1H), 1.60–1.54 (m, 2H), 1.41–1.32 (m, 2H), 1.30–1.16 (m, 7H), 1.07–1.03 (m, 21H), 0.89 (t, *J* = 7.0 Hz, 3H), 0.85 (t, *J* = 7.0 Hz, 3H). **^{13}C NMR (100 MHz, $CDCl_3$):** δ 137.8, 132.0, 79.8, 62.4, 35.5, 31.8, 29.7, 29.5, 29.1, 25.3, 22.8, 22.6, 18.05, 18.0, 14.0, 13.8, 12.4. **IR (thin film):** v 3337, 2929, 1464 cm^{-1}. **HRMS Electrospray (*m/z*):** $[M+Na]^+$ calcd for $C_{23}H_{48}O_2SiNa$, 407.3321; found 407.3327.

^{1}H NMR (500 MHz, $CDCl_3$): δ 5.28 (t, *J* = 7.5 Hz, 1H), 4.12 (t, *J* = 6.5 Hz, 1H), 3.62 (q, *J* = 6.5 Hz, 2H), 2.37–2.25 (m, 2H), 1.99–1.95 (m, 2H), 1.54–1.50 (m, 2H), 1.42–1.36 (m, 2H), 1.30–1.20 (m, 9H), 1.04–1.00 (m, 21H), 0.91 (t, *J* = 7.0 Hz, 3H), 0.85 (t, *J* = 7.0 Hz, 3H). **^{13}C NMR (100 MHz, $CDCl_3$):** δ 144.6, 121.6, 77.4, 62.7, 36.4, 31.9, 31.2, 29.44, 29.36, 24.8, 23.2, 22.6, 18.13, 18.11, 14.9, 14.1, 12.4. **IR (thin film):** v 3326, 2931, 2866, 1465 cm^{-1}. **HRMS Electrospray(*m/z*):** $[M+Na]^+$ calcd for $C_{23}H_{48}O_2SiNa$, 407.3321; found 407.3318.

(*E*)-triisopropyl[8-(methoxymethyl)hexadec-8-en-7-yloxy]silane. *Major Regioisomer:*



(*E*)-triisopropyl(8-(2-methoxyethylidene)pentadecan-7-yloxy)silane.

Minor Regioisomer:

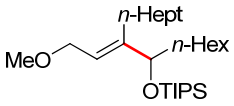


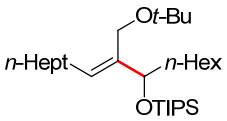
Table 1, Entry 5: Following Procedure A, $Ni(COD)_2$ (19.6 mg, 0.071 mmol), IMes·HCl salt (20.3 mg, 0.059 mmol), *t*-BuOK (6.7 g, 0.059 mmol), triisopropylsilane (0.24 mL, 1.19 mmol), 1-methoxydec-2-yne (100 mg, 0.59 mmol), 1-heptanal (75 g, 0.66 mmol) gave a crude residue which was purified via flash chromatography (100% hexanes) to afford two regioisomers in a 75:25 selectivity (149 mg, 57% yield): Major (112 mg, 0.25 mmol, 43% yield); Minor (37 mg, 0.08 mmol, 14% yield).

Major Regioisomer: **^{1}H NMR (400 MHz, $CDCl_3$):** δ 5.54 (t, *J* = 7.2 Hz, 1H), 4.18 (t, *J* = 6.0 Hz, 1H), 3.91 (d, *J* = 10.8 Hz, 1H), 3.88 (d, *J* = 10.8 Hz, 1H), 3.27 (s, 3H), 2.11 (m, 2H), 1.60–1.50 (m, 2H), 1.37–1.15 (m, 18H), 1.06–0.99 (m, 21H), 0.88–0.83 (m, 6H). **^{13}C NMR (100 MHz, $CDCl_3$):** δ 137.3, 131.8, 76.4, 67.2, 58.1, 36.8, 31.9, 29.7, 29.4, 29.3, 29.2, 27.5, 24.8, 22.67, 22.64, 18.1, 14.1, 12.4. **IR (thin film):** v 2929, 2865, 1464 cm^{-1}. **HRMS Electrospray (*m/z*):** $[M+Na]^+$ calcd for $C_{27}H_{56}O_2SiNa$, 463.3947; found 463.3952.

Minor Regioisomer: **^{1}H NMR (400 MHz, $CDCl_3$):** δ 5.45 (t, *J* = 6.8 Hz, 1H), 4.14 (t, *J* = 6.0 Hz, 1H), 3.98 (d, *J* = 6.8 Hz, 2H), 3.30 (s, 3H), 2.00–1.96 (m, 2H), 1.56–1.48 (m, 2H), 1.36–1.11 (m, 18H), 1.07–0.98 (m, 21H), 0.89–0.83 (m, 6H). **^{13}C NMR (100 MHz, $CDCl_3$):** δ 145.0, 122.8, 77.1, 68.8, 57.8, 36.4, 31.9, 31.8, 30.3, 30.1, 29.4, 29.1, 18.15, 18.12, 14.09, 14.07, 12.4. **IR (thin film):** v 2928, 2865, 1464 cm^{-1}. **HRMS electrospray (*m/z*):** $[M+Na]^+$ calcd for $C_{27}H_{56}O_2SiNa$, 463.3947; found 463.3933.

(*E*)-[8-(*tert*-butoxymethyl)hexadec-8-en-7-yloxy]triisopropylsilane.

Major Regioisomer:



(*E*)-[8-(2-*tert*-butoxyethylidene)pentadecan-7-yloxy]triisopropylsilane.

Minor Regioisomer:

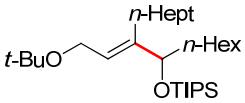
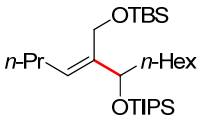


Table 1, Entry 6: Following Procedure A, $Ni(COD)_2$ (19.6 mg, 0.071 mmol), IMes·HCl salt (20.3 mg, 0.059 mmol), *t*-BuOK (6.7 g, 0.059 mmol), triisopropylsilane (0.24 mL, 1.19 mmol), 2-decyn-1-ol (125 g, 0.59 mmol), 1-heptanal (75 g, 0.66 mmol) gave a crude residue which was purified via flash chromatography (100% hexanes) to afford two regioisomers in a 75:25 selectivity (215 mg, 75% yield): Major (161 mg, 0.33 mmol, 56% yield); Minor (54 mg, 0.11 mmol, 19% yield).

Major Regioisomer: **^{1}H NMR (400 MHz, $CDCl_3$):** δ 5.46 (t, *J* = 7.2 Hz, 1H), 4.17 (t, *J* = 5.6 Hz, 1H), 3.83 (s, 2H), 2.08 (q, *J* = 7.2 Hz, 2H), 1.58–1.50 (m, 2H), 1.35–1.20 (m, 18 H), 1.17 (s, 9H), 1.02–0.99 (m, 21H), 0.88–0.83 (m, 6H). **^{13}C NMR (100 MHz, $CDCl_3$):** δ 138.5, 130.6, 72.4, 56.1, 37.0, 31.9, 29.7, 29.5, 29.34, 29.25, 27.5, 27.4, 24.9, 22.7, 18.16, 18.15, 14.1, 12.5. **IR (thin film):** v 2926, 2865, 1465 cm^{-1}. **HRMS electrospray (*m/z*):** $[M+Na]^+$ calcd for $C_{30}H_{62}O_2SiNa$, 505.4417; found 505.4405.

Minor Regioisomer: **^{1}H NMR (400 MHz, $CDCl_3$):** δ 5.40 (t, *J* = 6.4 Hz, 1H), 4.09 (t, *J* = 6.4 Hz, 1H), 3.94 (d, *J* = 6.0 Hz, 2H), 1.96 (m, 2H), 1.54–1.49 (m, 2H), 1.31–1.15 (m, 27 H), 1.06–0.98 (m, 21H), 0.88–0.83 (m, 6H). **^{13}C NMR (100 MHz, $CDCl_3$):** δ 142.8, 125.3, 77.8, 72.8, 58.6, 36.7, 31.9, 31.8, 30.3, 30.0, 29.4, 29.1, 27.7, 27.2, 25.2, 22.7, 22.6, 18.1, 14.08, 14.07, 12.4. **IR (thin film):** ν 2927, 2864, 1465 cm^{-1}. **HRMS electrospray (*m/z*):** $[M+Na]^+$ calcd for $C_{30}H_{62}O_2SiNa$, 505.4417; found 505.4408.

(*E*)-6-butylidene-7-hexyl-9,9-diisopropyl-2,2,3,3,10-pentamethyl-4,8-dioxa-3,9-disilaundecane. *Major Regioisomer:*



(*E*)-8-hexyl-10,10-diisopropyl-2,2,3,3,11-pentamethyl-7-propyl-4,9-dioxa-3,10-disiladodec-6-ene. *Minor Regioisomer:*

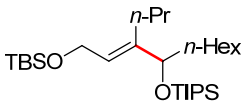
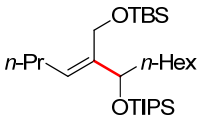


Table 1, Entry 7: Following Procedure A, $Ni(COD)_2$ (15.6 mg, 0.057 mmol), IMes·HCl salt (16 mg, 0.047 mmol), *t*-BuOK (5.3 mg, 0.047 mmol), triisopropylsilane (0.19 mL, 0.94 mmol), *t*-butyl(hex-2-ynyloxy)dimethylsilane (100 mg, 0.47 mmol), 1-heptanal (59 g, 0.52 mmol) gave a crude residue which was purified via flash chromatography (100% Hexanes) to afford two regioisomers in a 87:13 selectivity (171 mg, 75% yield): Major (139.6 mg, 0.31 mmol, 66% yield); Minor (21.4 mg, 0.044 mmol, 9% yield).

Major Regioisomer: **^{1}H NMR (500 MHz, $CDCl_3$):** δ 5.47 (t, *J* = 7.5 Hz, 1H), 4.29–4.27 (m, 1H), 4.18 (d, *J* = 11.0 Hz, 1H), 4.10 (d, *J* = 11.0 Hz, 1H), 2.10 (m, 2H), 1.63–1.54 (m, 2H), 1.40 (q, *J* = 7.5 Hz, 2H), 1.31–1.17 (m, 8H), 1.08–1.02 (m, 21H), 0.93–0.86 (m, 15H), 0.07–0.06 (m, 6H). **^{13}C NMR (100 MHz, $CDCl_3$):** δ 139.7, 129.1, 75.8, 57.7, 36.9, 32.0, 29.5, 25.9, 24.8, 23.0, 22.7, 18.22, 18.16, 14.1, 13.9, 12.5, -5.5. **IR (thin film):** v 2930, 2865, 1463 cm^{-1}. **HRMS Electrospray (*m/z*):** $[M+Na]^+$ calcd for $C_{28}H_{60}O_2Si_2Na$, 507.4030; found 507.4026.

Minor Regioisomer: **^{1}H NMR (400 MHz, $CDCl_3$):** δ 5.43 (t, *J* = 6.0 Hz, 1H), 4.19 (m, 2H), 4.01 (t, *J* = 6.0 Hz, 1H), 1.94–1.90 (m, 2H), 1.51–1.49 (m, 2H), 1.34 (m, 2H), 1.25–1.16 (m, 8H), 1.02–0.99 (m, 21H), 0.89–0.82 (m, 15H), 0.03-0.02 (m, 6H). **^{13}C NMR (100 MHz, $CDCl_3$):** δ 141.8, 126.6, 77.1, 59.8, 36.4, 31.8, 29.5, 29.4, 25.9, 24.8, 23.3, 22.6, 18.2, 18.1, 14.7, 14.0, 12.4, -5.2. **IR (thin film):** v 2956, 2928, 2864, 1463cm^{-1}. **HRMS Electrospray (*m/z*):** $[M+Na]^+$ calcd for $C_{28}H_{60}O_2Si_2Na$, 507.4030; found 507.4020.

(*E*)-6-butylidene-7-hexyl-9,9-diisopropyl-2,2,3,3,10-pentamethyl-4,8-dioxa-3,9-disilaundecane. *Major Regioisomer:*



(*E*)-8-hexyl-10,10-diisopropyl-2,2,3,3,11-pentamethyl-7-propyl-4,9-dioxa-3,10-disiladodec-6-ene. *Minor Regioisomer:*

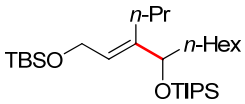
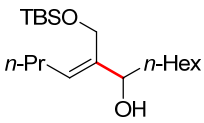


Table 1, Entry 8: Following Procedure A, $Ni(COD)_2$ (19.6 mg, 0.071 mmol), IPr·HCl salt (25.3 mg, 0.059 mmol), *t*-BuOK (6.7 g, 0.059 mmol), triisopropylsilane (0.24 mL, 1.19 mmol), *t*-butyl(hex-2-ynyloxy)dimethylsilane (127 mg, 0.59 mmol), 1-heptanal (75 g, 0.66 mmol) gave a crude residue which was purified via flash chromatography (100% hexanes) to afford two regioisomers in a 71:29 selectivity (249 mg, 86% yield): Major (178 mg, 0.37 mmol, 61% yield); Minor (71 mg, 0.15 mmol, 25% yield).

Spectral data as previously reported for Table 1, Entry 7.

(*E*)-5-[(*tert*-butyldimethylsilyloxy)methyl]dodec-4-en-6-ol. *Major Regioisomer:*



(*E*)-4-(2-(*tert*-butyldimethylsilyloxy)ethylidene)undecan-5-ol. *Minor Regioisomer:*

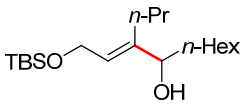
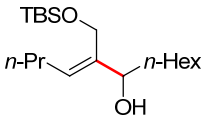


Table 1, Entry 9: Following a modified Procedure A, $Ni(COD)_2$ (16.4 mg, 0.060 mmol), PBu_3 (24.1 mg, 0.12 mmol), Et_3B (0.17 mL, 1.2 mmol), *t*-butyl(hex-2-ynyloxy)dimethylsilane (127 mg, 0.60 mmol), 1-heptanal (68 g, 0.60 mmol) gave a crude residue which was purified via flash chromatography (100% Hexanes) to afford two regioisomers in a 57:43 selectivity (128 mg, 65% yield): Major (73 mg, 0.22 mmol, 37% yield); Minor (55 mg, 0.17 mmol, 28% yield).

Major Regioisomer: **^{1}H NMR (500 MHz, $CDCl_3$):** δ 5.44 (t, *J* = 7.6 Hz, 1H), 4.34 (d, *J* = 11.6 Hz, 1H), 4.26 (d, *J* = 12.0 Hz, 1H), 4.01 (q, *J* = 6.8 Hz, 1H), 3.04 (d, *J* = 6.4 Hz, 1H), 2.00 (m, 2H), 1.67–1.52 (m, 2H), 1.41–1.16 (m, 10H), 0.91–0.84 (m, 15H), 0.09 (s, 3H), 0.08 (s, 3H). **^{13}C NMR (100 MHz, $CDCl_3$):** δ 138.4, 129.4, 77.6, 59.7, 35.9, 31.8, 29.4, 29.3, 26.0, 25.8, 22.8, 22.6, 18.1, 14.1, 13.7, -5.54, -5.56. **IR (thin film):** v 3412, 2957, 2930, 2858, 1464 cm^{-1}. **HRMS Electrospray (*m/z*):** $[M+Na]^+$ calcd for $C_{19}H_{40}O_2SiNa$, 351.2695; found 351.2698.

Minor Regioisomer: **^{1}H NMR (500 MHz, $CDCl_3$):** δ 5.52 (t, *J* = 6.0, 1H), 4.21 (m, 2H), 3.99 (t, *J* = 6.4 Hz, 1H), 1.97 (m, 2H), 1.52–1.47 (m, 2H), 1.31–1.21 (m, 3H), 0.91–0.84 (m, 15H), 0.05 (s, 6H). **^{13}C NMR (100 MHz, $CDCl_3$):** δ 143.4, 126.1, 76.2, 59.9, 35.6, 31.8, 30.0, 29.2, 25.96, 25.90, 23.3, 22.6, 18.4, 14.5, 14.1, -5.1. **IR (thin film):** v 3368, 2957, 2930, 2858, 1464 cm^{-1}. **HRMS Electrospray (*m/z*):** $[M+Na]^+$ calcd for $C_{19}H_{40}O_2SiNa$, 351.2695; found 351.2702.

(*E*)-5-((*tert*-butyldimethylsilyloxy)methyl)dodec-4-en-6-ol. *Major Regioisomer:*



(*E*)-4-(2-(*tert*-butyldimethylsilyloxy)ethylidene)undecan-5-ol. *Minor Regioisomer:*

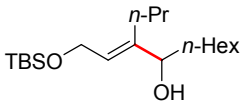


Table 1, Entry 10: Following a modified Procedure A, $Ni(COD)_2$ (16.4 mg, 0.060 mmol), PCy_3 (34 mg, 0.12 mmol), Et_3B (0.17 mL, 1.2 mmol), *t*-butyl(hex-2-ynyloxy)dimethylsilane (127 mg, 0.60 mmol), 1-heptanal (68 g, 0.60 mmol) gave a crude residue which was purified via flash chromatography (100% Hexanes) to afford two regioisomers in a 58:42 selectivity (143 mg, 73% yield): Major (83 mg, 0.25 mmol, 42% yield); Minor (60 mg, 0.18 mmol, 31% yield).

Spectral data as previously reported for Table 1, Entry 9.

(*E*)-5-((*tert*-butyldimethylsilyloxy)methyl)dodec-4-en-6-ol. *Major Regioisomer:*



(*E*)-4-(2-(*tert*-butyldimethylsilyloxy)ethylidene)undecan-5-ol. *Minor Regioisomer:*

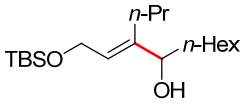
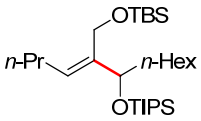


Table 1, Entry 11: Following a modified Procedure A, $Ni(COD)_2$ (16.4 mg, 0.060 mmol), $P(t\text{-}Bu)_3$ (34 mg, 0.12 mmol), Et_3B (0.17 mL, 1.2 mmol), *t*-butyl(hex-2-ynyloxy)dimethylsilane (127 mg, 0.60 mmol), 1-heptanal (68 g, 0.60 mmol) gave a crude residue which was purified via flash chromatography (100% Hexanes) to afford two regioisomers in a 53:47 selectivity (140 mg, 71% yield): Major (80 mg, 0.24 mmol, 38% yield); Minor (60 mg, 0.18 mmol, 33% yield).

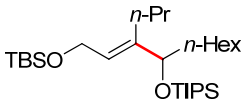
Spectral data as previously reported for Table 1, Entry 9.

5.2.2.3. Scheme 54 Entries

(*E*)-6-butylidene-7-hexyl-9,9-diisopropyl-2,2,3,3,10-pentamethyl-4,8-dioxa-3,9-disilaundecane. *Major Regioisomer:*



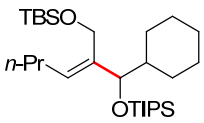
(*E*)-8-hexyl-10,10-diisopropyl-2,2,3,3,11-pentamethyl-7-propyl-4,9-dioxa-3,10-disiladodec-6-ene. *Minor Regioisomer:*



Scheme 54, Entry 1: Following Procedure A, $Ni(COD)_2$ (15.6 mg, 0.057 mmol), IMes·HCl salt (16 mg, 0.047 mmol), *t*-BuOK (5.3 mg, 0.047 mmol), triisopropylsilane (0.19 mL, 0.94 mmol), *t*-butyl(hex-2-ynyloxy)dimethylsilane (100 mg, 0.47 mmol), 1-heptanal (59 mg, 0.52 mmol) gave a crude residue which was purified via flash chromatography (100% Hexanes) to afford two regioisomers in a 87:13 selectivity (171 mg, 75% yield): Major (139.6 mg, 0.31 mmol, 65.6% yield); Minor (21.4 mg, 0.044 mmol, 9.4% yield).

Spectral data as previously reported for Table 1, Entry 7.

(*E*)-6-butylidene-7-cyclohexyl-9,9-diisopropyl-2,2,3,3,10-pentamethyl-4,8-dioxa-3,9-disilaundecane. *Major Regioisomer:*

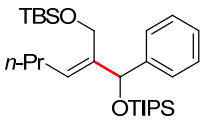


Scheme 54, Entry 2: Following Procedure A, $Ni(COD)_2$ (15.6 mg, 0.057 mmol), IMes·HCl salt (16 mg, 0.047 mmol), *t*-BuOK (5.3 mg, 0.047 mmol), triisopropylsilane (0.19 mL, 0.94 mmol), *t*-butyl(hex-2-ynyloxy)dimethylsilane (100 mg, 0.47 mmol),

cyclohexanescarbaldehyde (58 mg, 0.52 mmol) gave a crude residue which was purified via flash chromatography (100% Hexanes) to afford a single regioisomer in a >98:2 isolated selectivity (87:13 crude) (198 mg, 0.41 mmol, 87% yield).

^{1}H NMR (400 MHz, $CDCl_3$): δ 5.39 (t, *J* = 7.2 Hz, 1H), 4.12 (d, *J* = 11.2 Hz, 1H), 4.06 (d, *J* = 11.2 Hz, 1H), 3.95 (d, *J* = 6.8 Hz, 1H), 2.07 (dq, *J* = 14.4 Hz, 7.2 Hz, 2H), 1.89 (d, *J* = 12.4 Hz, 1H), 1.74–1.60 (m, 4H), 1.49 – 1.34 (m, 3H), 1.18–1.06 (m, 3H), 1.04–1.02 (m, 21H), 0.92–0.89 (m, 5H), 0.88 (s, 9H), 0.52 (s, 6H). **^{13}C NMR (100 MHz, $CDCl_3$):** δ 139.2, 131.1, 81.7, 58.1, 43.1, 30.0, 29.9, 29.2, 27.1, 26.9, 26.8, 26.1, 23.2, 18.54, 18.51, 18.4, 14.3, 13.0, -5.31, -5.38. **IR (thin film):** v 2928, 2711, 1463 cm^{-1}. **HRMS Electrospray (*m/z*):** $[M+Na]^+$ calcd for $C_{28}H_{58}O_2Si_2Na$, 505.3873; found 505.3860.

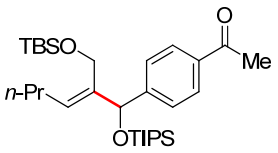
(*E*)-6-butylidene-9,9-diisopropyl-2,2,3,3,10-pentamethyl-7-phenyl-4,8-dioxa-3,9-disilaundecane. *Major Regioisomer:*



Scheme 54, Entry 3: Following Procedure A, $Ni(COD)_2$ (15.6 mg, 0.057 mmol), IMes·HCl salt (16 mg, 0.047 mmol), *t*-BuOK (5.3 mg, 0.047 mmol), triisopropylsilane (0.19 mL, 0.94 mmol), *t*-butyl(hex-2-ynyloxy)dimethylsilane (100 mg, 0.47 mmol), benzaldehyde (55 mg, 0.52 mmol) gave a crude residue which was purified via flash chromatography (100% Hexanes) to afford a single regioisomer in a >98:2 isolated selectivity (91:9 crude) (191 mg, 0.40 mmol, 85% yield).

^{1}H NMR (400 MHz, $CDCl_3$): δ 7.35–7.33 (m, 2H), 7.26–7.22 (m, 2H), 7.18–7.16 (m, 1H), 5.89 (t, *J* = 7.6 Hz, 1H), 5.40 (s, 1H), 4.21 (d, *J* = 11.6 Hz, 1H), 3.65 (d, *J* = 11.6 Hz, 1H), 2.05 (m, 2H), 1.41 (sext, *J* = 6.8 Hz, 2H), 1.09–1.03 (m, 3H), 1.01 (d, *J* = 6.8 Hz, 9H), 0.96 (d, *J* = 6.8 Hz, 9H), 0.90 (t, *J* = 7.2 Hz, 3H), 0.86 (s, 9H), -0.3 (s, 3H), -0.06 (s, 3H). **^{13}C NMR (100 MHz, $CDCl_3$):** δ 144.6, 141.0, 127.9, 126.89, 126.87, 126.0, 75.5, 58.3, 29.7, 26.1, 23.3, 18.4, 18.3, 18.2, 14.1, 12.5, -5.3, -5.4. **IR (thin film):** v 3063, 3028, 2956, 2865, 1463 cm^{-1}. **HRMS Electrospray (*m/z*):** $[M+Na]^+$ calcd for $C_{28}H_{52}O_2Si_2Na$, 499.3404; found 499.3405.

(*E*)-1-[4-(6-butylidene-3,3-diisopropyl-2,9,9,10,10-pentamethyl-4,8-dioxa-3,9-disilaundecan-5-yl)phenyl]ethanone. *Major Regioisomer:*

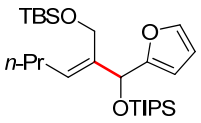


Scheme 54, Entry 4: Following Procedure A, $Ni(COD)_2$ (19.6 mg, 0.071 mmol), IMes·HCl salt (20.3 mg, 0.059 mmol), *t*-BuOK (6.7 g, 0.059 mmol), triisopropylsilane (0.24 mL, 1.19 mmol), *t*-butyl(hex-2-ynyloxy)dimethylsilane (127 mg, 0.59 mmol) and 4-acetylbenzealdehyde (98 mg, 0.66 mmol) gave a crude residue which was purified via flash chromatography (5% EtOAc/hexanes) to afford a single regioisomer in a >98:2 isolated selectivity (91:9 crude) (258 mg, 0.50 mmol, 83% yield).

^{1}H NMR (400 MHz, $CDCl_3$): δ 7.87–7.84 (m, 2H), 7.45–7.43 (m, 2H), 5.88 (t, *J* = 7.2 Hz, 1H), 5.45 (s, 1H), 4.21 (d, *J* = 11.6 Hz, 1H), 3.65 (d, *J* = 12.0 Hz, 1H), 2.56 (s, 3H), 2.12–1.96 (m, 2H), 1.44–1.35 (m, 2H), 1.11–1.02 (m, 3H), 1.00 (d, *J* = 6.8 Hz, 9H), 0.96 (d, *J*

= 6.8 Hz, 9H), 0.88 (t, *J* = 7.2 Hz, 3H), 0.82 (s, 9H), -0.04 (s, 3H), -0.07 (s, 3H). **^{13}C NMR (100 MHz, $CDCl_3$):** δ 198.0, 150.1, 140.1, 135.7, 128.0, 126.7, 126.6, 75.0, 57.9, 29.4, 26.6, 25.8, 22.9, 18.02, 17.96, 13.8, 12.2, -5.59, -5.64. **IR (thin film):** v 2946, 2865, 2713, 1927, 1687, 1606 cm^{-1}. **HRMS Electrospray (*m/z*):** $[M+Na]^+$ calcd for $C_{30}H_{54}O_3Si_2Na$, 541.3509; found 541.3495.

(*E*)-6-butylidene-7-(furan-2-yl)-9,9-diisopropyl-2,2,3,3,10-pentamethyl-4,8-dioxa-3,9-disilaundecane. *Major Regioisomer:*

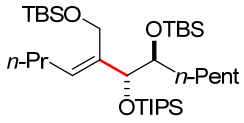


Scheme 54, Entry 5: Following Procedure A, $Ni(COD)_2$ (15.6 mg, 0.057 mmol), IMes·HCl salt (16 mg, 0.047 mmol), *t*-BuOK (5.3 mg, 0.047 mmol), triisopropylsilane (0.19 mL, 0.94 mmol), *t*-butyl(hex-2-ynyloxy)dimethylsilane (100 mg, 0.47 mmol), furaldehyde (50 mg, 0.52 mmol) gave a crude residue which was purified via flash chromatography (100% hexanes) to afford a single regioisomer in a >98:2 isolated selectivity (91:9 crude) (180 mg, 0.39 mmol, 82% yield).

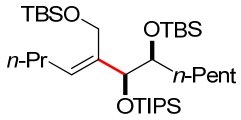
^{1}H NMR (500 MHz, $CDCl_3$): δ 7.30–7.29 (m, 1H), 6.26–6.25 (m, 1H), 6.143–6.135 (m, 1H), 5.89 (t, *J* = 7.6 Hz, 1H), 5.43 (s, 1H), 4.26 (d, *J* = 12.0 Hz, 1H), 3.80 (d, *J* = 11.6 Hz, 1H), 2.12 (dq, *J* = 14.0 Hz, 6.8 Hz, 1H), 2.08 (dq, *J* = 14.0 Hz, 6.8 Hz, 1H), 1.44–1.39 (m, 2H), 1.13–1.04 (m, 3H), 1.02–0.99 (m, 18H), 0.90 (t, *J* = 7.2 Hz, 3H), 0.84 (s, 9H), -0.03 (s, 3H), -0.05 (s, 3H) . **^{13}C NMR (100 MHz, $CDCl_3$):** δ 156.5, 141.3, 137.9, 127.7, 109.9, 106.5, 69.0, 58.3, 29.5, 25.8, 22.9, 18.2, 18.0, 17.9, 13.8, 12.3, -5.60, -5.64. **IR**

(thin film): ν 2957, 2866, 1464 cm^{-1}. **HRMS Electrospray (*m/z*):** $[M+Na]^+$ calcd for $C_{26}H_{50}O_3Si_2Na$, 489.3196; found 489.3198.

±(5*S*,6*R*,*E*)-7-butylidene-2,2,3,3,10,10,11,11-octamethyl-5-pentyl-6-(triisopropylsilyloxy)-4,9-dioxa-3,10-disiladodecane. *Major Diastereomer:*



±(5*S*,6*S*,*E*)-7-butylidene-2,2,3,3,10,10,11,11-octamethyl-5-pentyl-6-(triisopropylsilyloxy)-4,9-dioxa-3,10-disiladodecane. *Minor Diastereomer:*



Scheme 54, Entry 6: Following Procedure A, $Ni(COD)_2$ (15.6 mg, 0.057 mmol), IMes·HCl salt (16 mg, 0.047 mmol), *t*-BuOK (5.3 mg, 0.047 mmol), triisopropylsilane (0.19 mL, 0.94 mmol), *tert*-butyl(hex-2-ynyloxy)dimethylsilane (100 mg, 0.47 mmol), (±)-2-(*tert*-butyldimethylsilyloxy)heptanal (127 mg, 0.52 mmol) gave a crude residue which was purified via flash chromatography (100% hexanes) to afford a single regioisomer (215 mg, 74% yield, 75:25 dr): Major diastereomer (160 mg, 0.26 mmol, 55% yield); Minor diastereomer (55 mg, 0.090 mmol, 19% yield).

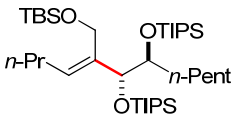
Major Regioisomer: **^{1}H NMR (500 MHz, $CDCl_3$):** δ 5.57 (t, *J* = 7.5 Hz, 1H), 4.34 (d, *J* = 0.5 Hz, 1H), 4.25 (d, *J* = 12.0 Hz, 1H), 4.07 (d, *J* = 12.0 Hz, 1H), 3.67 (td, *J* = 6.0 Hz, 2.5

Hz, 1H), 2.13 (dq, *J* = 14.5 Hz, 7.0 Hz, 1H), 2.13 (dq, *J* = 14.5 Hz, 7.0 Hz, 1H), 1.46–1.40 (m, 5H), 1.30–1.20 (m, 5H), 1.08–1.06 (m, 21H), 0.94–0.87 (m, 24H), 0.08 (s, 6H), 0.06 (s, 3H), 0.05 (s, 3H). **^{13}C NMR (125 MHz, $CDCl_3$):** δ 138.3, 130.0, 78.6, 76.6, 59.7, 32.3, 32.0, 30.0, 26.1, 26.0, 25.8, 23.0, 22.7, 18.3, 14.1, 14.0, 12.7, -3.8, -4.6, -5.4, -5.3. **IR (thin film):** v 2952, 2926, 2865, 2353, 1464 cm^{-1}. **HRMS Electrospray (*m/z*):** $[M+Na]^+$ calcd for $C_{34}H_{74}O_3Si_3Na$, 637.4844; found 637.4844.

Minor Regioisomer: **^{1}H NMR (500 MHz, $CDCl_3$):** δ 5.62 (t, *J* = 7.5 Hz, 1H), 4.46 (d, *J* = 4.0 Hz, 1H), 4.27 (d, *J* = 11.0 Hz, 1H), 4.11 (d, *J* = 11.0 Hz, 1H), 3.72 (ddd, *J* = 7.0 Hz, 4.0 Hz, 3.0 Hz, 1H), 2.15 (m, 1H), 2.10 (m, 1H), 1.56–1.50 (m, 1H), 1.42–1.36 (m, 3H), 1.31–1.14 (m, 6H), 1.14–1.02 (m, 21H), 0.93–0.86 (m, 24H), 0.09 (s, 3H), 0.06 (s, 3H), 0.04 (s, 6H). **^{13}C NMR (125 MHz, $CDCl_3$):** δ 137.4, 130.0, 76.4, 75.1, 59.2, 32.2, 31.5, 29.7, 26.0, 25.9, 25.7, 23.1, 22.7, 18.2, 14.1, 14.0, 12.5, -3.7, -4.8, -5.3, -5.4. **IR (thin film):** v 2957, 2864, 2360, 1463, 1388cm^{-1}. **HRMS Electrospray (*m/z*):** $[M]^+$ calcd for $C_{34}H_{74}O_3Si_3$, 637.4844; found 637.4831.

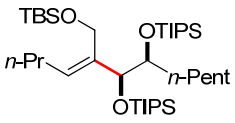
±(7*R*,8*S*,*E*)-6-butylidene-10,10-diisopropyl-2,2,3,3,11-pentamethyl-8-pentyl-7-(triisopropylsilyloxy)-4,9-dioxa-3,10-disiladodecane.

Major Regioisomer & Major Diastereomer:



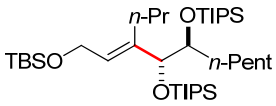
±(7*S*,8*S*,E)-6-butylidene-10,10-diisopropyl-2,2,3,3,11-pentamethyl-8-pentyl-7-(triisopropylsilyloxy)-4,9-dioxa-3,10-disiladodecane.

Major Regioisomer & Minor Diastereomer:



(8*R*,9*S*,*E*)-11,11-diisopropyl-2,2,3,3,12-pentamethyl-9-pentyl-7-propyl-8-(triisopropylsilyloxy)-4,10-dioxa-3,11-disilatridec-6-ene.

Minor Regioisomer (Anti Diastereomer):



Scheme 54, Entry 7: Following Procedure A, $Ni(COD)_2$ (15.6 mg, 0.057 mmol), IMes·HCl salt (16 mg, 0.047 mmol), *t*-BuOK (5.3 mg, 0.047 mmol), triisopropylsilane (0.19 mL, 0.94 mmol), *tert*-butyl(hex-2-ynyloxy)dimethylsilane (100 mg, 0.47 mmol), (±)-2-(triisopropylsilyloxy)heptanal (148 mg, 0.52 mmol) gave a crude residue which was purified via flash chromatography (100% hexanes) to afford a two regioisomers in a 92:8 selectivity (218 mg, 75% yield): Major regioisomer (199 mg, 0.32 mmol, 69% yield, 75:25 dr); Minor regioisomer (19 mg, 0.031 mmol, 6% yield, >98:2 dr).

Major Regioisomer & Major Diastereomer: **^{1}H NMR (400 MHz, $CDCl_3$):** δ 5.53 (t, *J* = 7.6 Hz, 1H), 4.36 (s, 1H), 4.26 (d, *J* = 12.0 Hz, 1H), 4.03 (d, *J* = 12.0 Hz, 1H), 3.81 (ddd, *J* = 7.2 Hz, 4.0 Hz, 2.0 Hz, 1H), 2.08 (m, 2H), 1.60–1.15 (m, 10H), 1.08–0.99 (m, 42H),

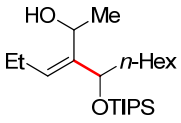
0.88–0.82 (m, 15H), 0.02 (s, 3H), 0.00 (s, 3H). **^{13}C NMR (100 MHz, $CDCl_3$):** δ 138.1, 130.2, 78.5, 76.9, 59.6, 33.4, 32.5, 30.1, 25.97, 25.94, 23.0, 22.7, 18.34, 18.32, 18.28, 14.09, 14.07, 12.9, 12.7, -5.5, -5.6. **IR (thin film):** v 2944, 2859, 2716, 1463, 1388 cm^{-1}. **HRMS Electrospray (*m/z*):** $[M+Na]^+$ calcd for $C_{37}H_{80}O_3Si_3Na$, 679.5313; found 679.5287.

Major Regioisomer & Minor Diastereomer: **^{1}H NMR (400 MHz, $CDCl_3$):** δ 5.64 (t, *J* = 7.2, 1H), 4.51 (d, *J* = 3.6 Hz, 1H), 4.23 (d, *J* = 11.2 Hz, 1H), 4.10 (d, *J* = 11.2 Hz, 1H), 3.87 (dt, *J* = 6.8 Hz, 4.4 Hz, 1H), 2.10 (dq, *J* = 14.4 Hz, 7.2 Hz, 1H), 2.06 (dq, *J* = 14.4 Hz, 7.2 Hz, 1H), 1.59–1.12 (m, 10H), 1.02–0.98 (m, 42H), 0.90–0.81 (m, 15H), 0.00 (s, 3H), -0.02 (s, 3H). **^{13}C NMR (100 MHz, $CDCl_3$):** δ 137.6, 130.1, 76.5, 76.0, 59.2, 33.4, 32.6, 29.8, 25.9, 25.6, 23.1, 22.7, 18.4, 18.28, 18.25, 14.09, 14.07, 12.9, 12.6, -5.4, -5.5. **IR (thin film):** v 2945, 2870, 2723, 1464 cm^{-1}. **HRMS Electrospray (*m/z*):** $[M+Na]^+$ calcd for $C_{37}H_{80}O_3Si_3Na$, 679.5313; found 679.5298.

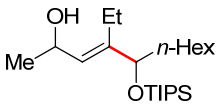
Minor Regioisomer (Anti Diastereomer): **^{1}H NMR (400 MHz, $CDCl_3$):** δ 5.55 (t, *J* = 6.0 Hz, 1H), 4.23 (s, 1H), 4.20–4.14 (m, 2H), 3.77 (ddd, *J* = 6.4 Hz, 4.4 Hz, 1.2 Hz, 1H), 2.04 (ddd, *J* = 13.6 Hz, 11.6 Hz, 5.6 Hz, 1H), 1.88 (ddd, *J* = 13.6 Hz, 11.6 Hz, 5.2 Hz, 1H), 1.64–1.13 (m, 10H), 1.04–0.99 (m, 42H), 0.88–0.81 (m, 15H), 0.01 (s, 6H). **^{13}C NMR (100 MHz, $CDCl_3$):** δ 140.5, 127.1, 80.1, 76.5, 59.9, 32.9, 32.5, 31.5, 26.2, 25.9, 22.9, 22.6, 18.35, 18.31, 18.27, 14.7, 14.1, 12.83, 12.76, -5.22, -5.25. **IR (thin film):** v 2945, 2867, 2726, 1464, 1388 cm^{-1}. **HRMS electrospray (*m/z*):** $[M+Na]^+$ calcd for $C_{37}H_{80}O_3Si_3Na$, 679.5313; found 679.5327.

5.2.2.4. Scheme 57 Entries

(*E*)-4-ethyl-5-(triisopropylsilyloxy)undec-3-en-2-ol. *Major Regioisomer:*



(*E*)-3-propylidene-4-(triisopropylsilyloxy)decan-2-ol. *Minor Regioisomer:*



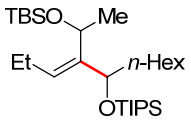
Scheme 57, Entry 1: Following Procedure A, $Ni(COD)_2$ (19.6 mg, 0.071 mmol), IMes·HCl salt (20.3 mg, 0.059 mmol), *t*-BuOK (6.7 g, 0.059 mmol), triisopropylsilane (0.24 mL, 1.19 mmol), hex-3-yn-2-ol (59 mg, 0.60 mmol), 1-heptanal (75 mg, 0.66 mmol) gave a crude residue which was purified via flash chromatography (100% hexanes) to afford two regioisomers in a 57:43 selectivity (198 mg, 89% yield): Major (112 g, 0.30 mmol, 50% yield, 50:50 dr); Minor (86 mg, 0.23 mmol, 39% yield, 67:33 dr).

Major Regioisomer: **^{1}H NMR (500 MHz, $CDCl_3$):** δ 5.13 (t, *J* = 7.2 Hz, 1H), 5.11 (t, *J* = 7.6 Hz, 1H), 4.82 (q, *J* = 6.8 Hz, 1H), 4.65–4.58 (m, 2H), 4.19–4.15 (m, 2H), 2.61 (d, *J* = 8.0 Hz, 1H, OH), 2.12–1.90 (m, 4H), 1.81–1.66 (m, 3H), 1.59–1.52 (m, 1H), 1.33 (d, *J* = 6.8 Hz, 3H), 1.30 (d, *J* = 6.8 Hz, 3H), 1.28–1.14 (m, 16H), 1.06–1.00 (m, 42H), 0.95 (t, *J* = 7.6 Hz, 3H), 0.94 (t, *J* = 7.6 Hz, 3H), 0.85 (t, *J* = 6.8 Hz, 3H), 0.84 (t, *J* = 6.8 Hz, 3H). **^{13}C NMR (100 MHz, $CDCl_3$):** δ 142.2, 140.1, 131.3, 129.2, 82.3, 79.0, 67.7, 66.8, 37.6,

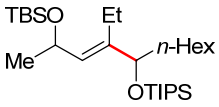
36.6, 31.9, 31.8, 29.2, 29.1, 26.0, 25.7, 24.7, 24.1, 22.6, 21.1, 20.8, 18.2, 18.1, 18.0, 14.3, 14.05, 14.03, 13.9, 12.4, 12.2. **IR (thin film):** v 3483 (bs), 2932, 2867, 1463 cm^{-1}. **HRMS Electrospray (*m/z*):** $[M+Na]^+$ calcd for $C_{22}H_{46}O_2SiNa$, 393.3165; found 393.3165.

Minor Regioisomer: **^{1}H NMR (400 MHz, $CDCl_3$):** δ 5.36 (d, *J* = 8.8 Hz, 1H), 5.31 (d, *J* = 8.8 Hz, 2H), 4.63–4.57 (m, 3H), 4.13–4.08 (m, 3H), 2.17–1.98 (m, 6H), 1.57–1.50 (m, 6H), 1.29–1.13 (m, 42H), 1.06–0.98 (m, 63H), 0.88–0.83 (m, 9H). **^{13}C NMR (100 MHz, $CDCl_3$):** δ 144.4, 144.3, 130.3, 129.8, 77.3, 76.5, 64.5, 64.3, 36.4, 36.3, 31.8, 29.4, 29.3, 24.8, 24.6, 23.7, 23.5, 22.62, 22.61, 20.1, 19.8, 18.14, 18.13, 18.10, 17.7, 15.3, 15.2, 14.1, 12.4, 12.3. **IR (thin film):** v 3344 (bs), 2933, 2866, 1465 cm^{-1}. **HRMS Electrospray (*m/z*):** $[M+Na]^+$ calcd for $C_{22}H_{46}O_2SiNa$, 393.3165; found 393.3156.

(*E*)-7-hexyl-9,9-diisopropyl-2,2,3,3,5,10-hexamethyl-6-propylidene-4,8-dioxa-3,9-disilaundecane. *Major Regioisomer:*



(*E*)-7-ethyl-8-hexyl-10,10-diisopropyl-2,2,3,3,5,11-hexamethyl-4,9-dioxa-3,10-disiladodec-6-ene. *Minor Regioisomer:*

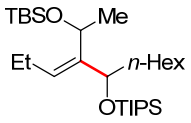


Scheme 57, Entry 2: Following Procedure A, $Ni(COD)_2$ (19.6 mg, 0.071 mmol), IMes·HCl salt (20.3 mg, 0.059 mmol), *t*-BuOK (6.7 mg, 0.059 mmol), triisopropylsilane (0.24 mL, 1.19 mmol), *t*-butyl(hex-3-yn-2-yloxy)dimethylsilane (127 mg, 0.60 mmol), 1-heptanal (75 mg, 0.66 mmol) gave a crude residue which was purified via flash chromatography (100% hexanes) to afford two regioisomers in a 77:23 selectivity (247 mg, 85% yield): Major (190 mg, 0.39 mmol, 68% yield, 50:50 dr); Minor (57 mg, 0.12 mmol, 21% yield, 67:33 dr).

Major Regioisomer: **^{1}H NMR (400 MHz, $CDCl_3$):** δ 5.39 (t, *J* = 7.2 Hz, 1H), 5.33 (t, *J* = 7.6 Hz, 1H), 4.61 (q, *J* = 6.4 Hz, 1H), 4.55 (q, *J* = 6.4 Hz, 1H), 4.48 (t, *J* = 4.0 Hz, 1H), 4.26 (t, *J* = 5.2 Hz, 1H), 2.30–2.13 (m, 2H), 2.20–2.00 (m, 2H), 2.68–1.48 (m, 4H), 1.28–1.21 (m, 34H), 1.06–1.03 (m, 36H), 0.96 (t, *J* = 7.6 Hz, 3H), 0.95 (t, *J* = 7.6 Hz, 3H), 0.89–0.84 (m, 18H), 0.06 (s, 3H), 0.05 (s, 3H), 0.01 (s, 3H), 0.00 (m, 3H). **^{13}C NMR (100 MHz, $CDCl_3$):** δ 142.5, 142.4, 129.2, 126.6, 74.4, 72.3, 67.0, 65.9, 37.3, 36.6, 32.1, 32.0, 29.6, 29.5, 25.8, 24.64, 24.5, 23.1, 22.74, 22.71, 21.0, 20.8, 18.3, 18.23. **IR (thin film):** v 2930, 2865, 1463 cm^{-1}. **HRMS Electrospray (*m/z*):** $[M+Na]^+$ calcd for $C_{28}H_{60}O_2Si_2Na$, 507.4030; found 507.4028.

Minor Regioisomer: **^{1}H NMR (500 MHz, $CDCl_3$):** δ 5.34 (d, *J* = 8.8 Hz, 1H), 5.29 (d, *J* = 8.4 Hz, 2H), 4.60–4.52 (m, 3H), 4.12–4.07 (m, 3H), 2.06–1.98 (m, 6H), 1.58–1.49 (m, 6H), 1.28–1.17 (m, 60H), 1.04–1.01 (m, 54H), 0.87–0.83 (m, 27H), 0.04–-0.01 (18H). **^{13}C NMR (100 MHz, $CDCl_3$):** δ 140.3, 140.0, 132.2, 131.4, 77.9, 76.5, 65.5, 65.4, 36.7, 36.4, 31.9, 30.9, 30.4, 29.40, 29.36 25.8, 25.3, 25.0, 24.9, 24.8, 22.6, 19.9, 19.5, 18.19, 18.16, 18.1, 14.8, 14.7, 14.1, 12.42, 12.38, -4.51, -4.6. **IR (thin film):** v 2930, 2865, 1464 cm^{-1}. **HRMS Electrospray (*m/z*):** $[M+Na]^+$ calcd for $C_{28}H_{60}O_2Si_2Na$, 507.4030; found 507.4027.

(*E*)-7-hexyl-9,9-diisopropyl-2,2,3,3,5,10-hexamethyl-6-propylidene-4,8-dioxa-3,9-disilaundecane. *Major Regioisomer:*

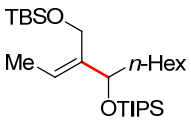


Scheme 57, Entry 3: Following Procedure A, $Ni(COD)_2$ (19.6 mg, 0.071 mmol), IMes·HCl salt (20.3 mg, 0.059 mmol), *t*-BuOK (6.7 mg, 0.059 mmol), triisopropylsilane (0.24 mL, 1.19 mmol), *t*-butyl(hex-3-yn-2-yloxy)dimethylsilane (127 mg, 0.60 mmol), 1-heptanal (75 mg, 0.66 mmol) gave a crude residue which was purified via flash chromatography (100% hexanes) to afford a single regioisomer in a >98:2 selectivity (223 g, 0.46 mmol, 77% yield).

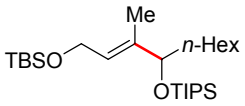
Spectral data as previously reported for Scheme 57, Entry 2.

5.2.2.5. Scheme 58 Entries

(*E*)-8-hexyl-10,10-diisopropyl-2,2,3,3,7,11-hexamethyl-4,9-dioxa-3,10-disiladodec-6-ene. *Major Regioisomer:*



(*E*)-6-ethylidene-7-hexyl-9,9-diisopropyl-2,2,3,3,10-pentamethyl-4,8-dioxa-3,9-disilaundecane. *Minor Regioisomer:*



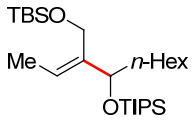
Scheme 58, Entry 1: Following Procedure A, $Ni(COD)_2$ (19.6 mg, 0.071 mmol), IMes·HCl salt (20.3 mg, 0.059 mmol), *t*-BuOK (6.7 g, 0.059 mmol), triisopropylsilane (0.24 mL, 1.19 mmol), (but-2-ynyloxy)(*tert*-butyl)dimethylsilane (110 mg, 0.59 mmol), 1-heptanal (75 g, 0.66 mmol) gave a crude residue which was purified via flash chromatography (100% Hexanes) to afford two regioisomers in a 69:31 selectivity (232 mg, 85% yield): Major (160 mg, 0.35 mmol, 59% yield); Minor (72 mg, 0.16 mmol, 26% yield)

Major Regioisomer: **^{1}H NMR (400 MHz, $CDCl_3$):** δ 5.51 (q, *J* = 7.2 Hz, 1H), 4.24 (t, *J* = 6.0 Hz, 1H), 4.17 (d, *J* = 11.2 Hz, 1H), 4.09 (d, *J* = 11.2 Hz, 1H), 1.66 (d, *J* = 6.8 Hz, 3H), 1.59–1.51 (m, 2H), 1.26–1.17 (m, 8H), 1.05–0.99 (m, 21H), 0.88–0.84 (m, 12H), 0.05 (s, 6H). **^{13}C NMR (100 MHz, $CDCl_3$):** δ 140.7, 123.1, 75.8, 57.5, 36.9, 32.0, 29.6, 25.9, 24.8, 22.7, 18.3, 18.15, 18.12, 14.1, 12.9, 12.4, -5.5. **IR (thin film):** ν 2930, 2865, 1464 cm^{-1}. **HRMS Electrospray (*m/z*):** $[M+Na]^+$ calcd for $C_{26}H_{56}O_2Si_2Na$, 479.3717; found 479.3714.

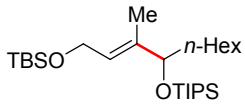
Minor Regioisomer: **^{1}H NMR (400 MHz, $CDCl_3$):** δ 5.40 (t, *J* = 6.0 Hz, 1H), 4.19 (d, *J* = 6.0 Hz, 2H), 4.05 (t, *J* = 6.4Hz, 1H), 1.54 (s, 3H), 1.53–1.46 (m, 2H), 1.26–1.20 (m, 8H), 1.04–0.99 (m, 21H), 0.88–0.84 (m, 12H), 0.04 (s, 6H). **^{13}C NMR (100 MHz, $CDCl_3$):** δ 137.9, 125.9, 78.1, 60.0, 36.0, 31.9, 29.4, 25.9, 25.3, 22.6, 18.3, 18.11, 18.08, 14.1,

12.4, 11.1, -5.2. **IR (thin film):** v 2931, 2865, 1464 cm^{-1}. **HRMS Electrospray (*m/z*):** $[M+Na]^+$ calcd for $C_{26}H_{56}O_2Si_2Na$, 479.3717; found 479.3731.

(*E*)-8-hexyl-10,10-diisopropyl-2,2,3,3,7,11-hexamethyl-4,9-dioxa-3,10-disiladodec-6-ene. *Major Regioisomer:*



(*E*)-6-ethylidene-7-hexyl-9,9-diisopropyl-2,2,3,3,10-pentamethyl-4,8-dioxa-3,9-disilaundecane. *Minor Regioisomer:*

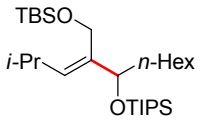


Scheme 58, Entry 2: Following Procedure A, $Ni(COD)_2$ (19.6 mg, 0.071 mmol), IPr·HCl salt (25.3 mg, 0.059 mmol), *t*-BuOK (6.7 g, 0.059 mmol), triisopropylsilane (0.24 mL, 1.19 mmol), (but-2-ynyloxy)(*tert*-butyl)dimethylsilane (110 mg, 0.59 mmol), 1-heptanal (75 g, 0.66 mmol) gave a crude residue which was purified via flash chromatography (100% Hexanes) to afford two regioisomers in a 90:10 selectivity (240 mg, 88% yield): Major (216 mg, 0.47 mmol, 79% yield); Minor (24 mg, 0.053 mmol, 6% yield)

Spectral data as previously reported for Scheme 58, Entry 1.

5.2.2.6. Scheme 59 Entries

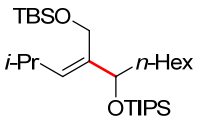
(*E*)-7-hexyl-9,9-diisopropyl-2,2,3,3,10-pentamethyl-6-(2-methylpropylidene)-4,8-dioxa-3,9-disilaundecane. *Major Regioisomer:*



Scheme 59, Entry 1: Following Procedure A, $Ni(COD)_2$ (15.6 mg, 0.057 mmol), IMes·HCl salt (16 mg, 0.047 mmol), *t*-BuOK (5.3 mg, 0.047 mmol), triisopropylsilane (0.19 mL, 0.94 mmol), *t*-butyldimethyl(4-methylpent-2-ynyloxy)silane (100 mg, 0.47 mmol), 1-heptanal (59 mg, 0.52 mmol) gave a crude residue which was purified via flash chromatography (100% Hexanes) to afford a single regioisomer in a >98:2 isolated selectivity (90:10 crude) (160 mg, 0.33 mmol, 70% yield).

^{1}H NMR (400 MHz, $CDCl_3$): δ 5.22 (d, *J* = 9.6 Hz, 1H), 4.19 (dd, *J* = 6.8 Hz, 4.8 Hz, 1H), 4.13 (d, *J* = 11.2 Hz, 1H), 4.06 (d, *J* = 11.2 Hz, 1H), 2.64 (dsept, *J* = 10.0 Hz, 6.8 Hz, 1H), 1.63–1.46 (m, 2H), 1.26–1.18 (m, 8H), 1.03–0.99 (m, 21H), 0.94 (d, *J* = 6.8 Hz, 3H), 0.91 (d, *J* = 6.4 Hz, 3H), 0.85–0.83 (m, 12H), 0.04–0.03 (m, 6H). **^{13}C NMR (100 MHz, $CDCl_3$):** δ 137.2, 137.1, 76.1, 57.9, 37.0, 32.3, 29.7, 27.1, 26.1, 25.0, 23.6, 23.3, 22.9, 18.38, 18.36, 14.4, 12.6, -5.3. **IR (thin film):** ν 2930, 2866, 1464 cm^{-1}. **HRMS Electrospray (*m/z*):** $[M+Na]^+$ calcd for $C_{28}H_{60}O_2Si_2Na$, 507.4030; found 507.4019.

(*E*)-7-hexyl-9,9-diisopropyl-2,2,3,3,10-pentamethyl-6-(2-methylpropylidene)-4,8-dioxa-3,9-disilaundecane. *Major Regioisomer:*

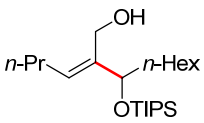


Scheme 59, Entry 2: Following Procedure A, $Ni(COD)_2$ (15.6 mg, 0.057 mmol), IMes·HCl salt (16 mg, 0.047 mmol), *t*-BuOK (5.3 mg, 0.047 mmol), triisopropylsilane (0.19 mL, 0.94 mmol), *t*-butyldimethyl(4-methylpent-2-ynyloxy)silane (100 mg, 0.47 mmol), 1-heptanal (59 mg, 0.52 mmol) gave a crude residue which was purified via flash chromatography (100% Hexanes) to afford one regioisomer in a >20:1 selectivity (171 mg, 0.35 mmol, 75% yield).

Spectral data as previously reported for Scheme 59, Entry 1.

5.2.2.7. Scheme 60 Entries

(*E*)-2-butylidene-3-(triisopropylsilyloxy)nonan-1-ol:

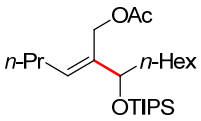


(*E*)-6-butylidene-7-hexyl-9,9-diisopropyl-2,2,3,3,10-pentamethyl-4,8-dioxa-3,9-disilaundecane (200 mg, 0.41 mmol), PPTS/TsOH (4:1, 30 mol%), and THF/H_2O (20:1, 0.2 M) were added and the reaction mixture was stirred for several hours until

consumption of the starting material by TLC analysis. The reaction was then quenched by the addition of saturated bicarbonate solution and extracted with EtOAc three times. The organic layer was washed with H2O and brine. The crude residue was purified via flash chromatography (10% EtOAc/hexanes) to afford (*E*)-2-butylidene-3-(triisopropylsilyloxy)nonan-1-ol (144 mg, 0.39 mmol, 94% yield).

Spectral data as previously reported for Table 1, Entry 1.

(*E*)-2-butylidene-3-(triisopropylsilyloxy)nonyl acetate:

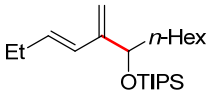


(*E*)-2-butylidene-3-(triisopropylsilyloxy)nonan-1-ol (144 mg, 0.39 mmol), acetic anhydride (3.0 equiv), Pyidine (5.0 equiv), and CH_2Cl_2 (0.2 M) were added and stirred until consumption of starting material. The reaction was then quenched by the addition of saturated bicarbonate solution and extracted with EtOAc three times. The organic layer was washed with H_2O and brine. The crude residue was purified via flash chromatography (10% EtOAc/hexanes) to afford (*E*)-2-butylidene-3-(triisopropylsilyloxy)nonyl acetate (158 mg, 0.38 mmol, 99% yield).

^{1}H NMR (500 MHz, $CDCl_3$): δ 5.59 (t, *J* = 7.6 Hz, 1H), 4.64 (d, *J* = 12.0 Hz, 1H), 4.54 (d, *J* = 12.0 Hz, 1H), 4.17 (t, *J* = 6.8 Hz, 1H), 2.07 (dddd, *J* = 7.2 Hz, 7.2 Hz, 7.2 Hz, 2.4 Hz, 2H), 2.00 (s, 3H), 1.56–1.5 (m, 2H), 1.41–1.33 (m, 2H), 1.28–1.15 (m, 8H), 1.04–0.97 (m, 21H), 0.88 (t, *J* = 7.2 Hz, 3H), 0.85 (t, *J* = 7.2 Hz, 3H). **^{13}C NMR (100 MHz, $CDCl_3$):** δ

171.0, 135.5, 133.6, 76.5, 58.8, 36.8, 31.8, 29.6, 29.3, 24.8, 22.66, 22.58, 20.9, 18.03, 18.02, 14.0, 13.7, 12.3. **IR (thin film):** ν 2933, 2866,1743, 1464 cm^{-1}. **HRMS electrospray (*m/z*):** $[M+Na]^+$ calcd for $C_{24}H_{48}O_3SiNa$, 435.3270; found 435.3252.

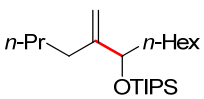
(*E*)-triisopropyl(5-methylenedodec-3-en-6-yloxy)silane:



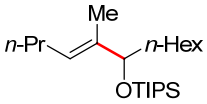
Scheme 60, Product C: Following Procedure C, $Pd_2(dba)_3{\cdot}CHCl_3$ (14 mg, 0.0135 mmol), 1,1'-bis(diphenylphosphino)ferrocene (dppf) (30 mg, 0.054 mmol), triethylamine (74 µL, 0.53 mmol), (*E*)-2-butylidene-3-(triisopropylsilyloxy)nonyl acetate (110 mg, 0.27 mmol) gave a crude reside which was purified via flash chromatography (100% hexanes) to afford **13** (89 mg, 0.25 mmol, 95% yield, >98:2).

^{1}H NMR (500 MHz, $CDCl_3$): δ 5.96 (dd, *J* = 16.0 Hz, 0.5 Hz, 1H), 5.85 (dt, *J* = 16.0, 6.5 Hz, 1H), 4.98 (d, *J* = 6.0 Hz, 2H), 4.42 (t, *J* = 6.0 Hz, 1H), 2.08 (quintet, *J* = 7.0 Hz, 2H), 1.68–1.50 (m, 3H), 1.15 m, 7H), 1.09–0.94 (m, 18H), 0.91–0.82 (m, 6H). **^{13}C NMR (125 MHz, $CDCl_3$):** δ 148.7, 132.4, 128.0, 111.9, 73.8, 37.2, 31.9, 29.4, 26.3, 24.6, 22.7, 22.6, 18.1, 14.1, 13.6, 12.4. **IR (thin film):** ν 2932, 2867, 1464 cm^{-1}. **HRMS Chemical Ionization (*m/z*):** $[M+H]^+$ calcd for $C_{22}H_{45}OSi$, 353.3240; found 353.3227.

Triisopropyl(5-methylenedodecan-6-yloxy)silane. *Major:*



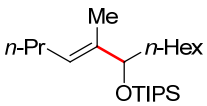
(*E*)-triisopropyl(5-methyldodec-4-en-6-yloxy)silane. *Minor:*



Scheme 60, Product A: Following Procedure B, $Pd_2(dba)_3 \cdot CHCl_3$ (13 mg, 0.013 mmol), ammonium formate (31 mg, 0.49 mmol), PBu_3 (12.1 µL, 0.049 mmol), (*E*)-2-butylidene-3-(triisopropylsilyloxy)nonyl acetate (100 mg, 0.24 mmol) gave a crude reside which was purified via flash chromatography (100% hexanes) to afford two products in a 88:12 selectivity (65 mg, 0.19 mmol, 77% yield): Major (**14**) (57 mg, 0.162 mmol, 68% yield); Minor (**15**) (8 mg, 0.089 mmol, 9% yield).

^{1}H NMR (500 MHz, $CDCl_3$): δ 4.92 (s, 1H), 4.79 (s, 1H), 4.18 (t, *J* = 6.5 Hz, 1H), 2.07 (ddd, *J* = 16.0 Hz, 9.5 Hz, 6.0 Hz, 1H), 1.91 (ddd, *J* = 16.0 Hz, 9.5 Hz, 6.0 Hz, 1H), 1.54–1.52 (m, 2H), 1.48–1.40 (m, 2H), 1.37–1.33 (m, 2H), 1.31–1.15 (m, 8H), 1.08–1.00 (m, 21H), 0.92 (t, *J* = 7.5 Hz, 3H), 0.88 (t, *J* = 8 Hz, 3H). **^{13}C NMR (100 MHz, $CDCl_3$):** δ 151.3, 109.2, 76.9, 36.2, 31.9, 29.9, 29.7, 29.4, 24.7, 22.8, 22.6, 18.1, 14.09, 14.07, 12.4. **IR (thin film):** v 2932, 2867, 1465 cm^{-1}. **HRMS Chemical Ionization (*m/z*):** $[M–H]^+$ calcd for $C_{22}H_{45}OSi$, 355.3396; found 355.3381.

(*E*)-triisopropyl(5-methyldodec-4-en-6-yloxy)silane:

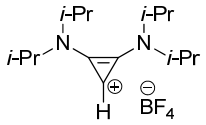


Scheme 60, Product B: Following Procedure D, (*E*)-2-butylidene-3-(triisopropylsilyloxy)nonan-1-ol (100 mg, 0.27 mmol), SO_3·Py (1.5 equiv), $LiAlH_4$ (6.0 equiv) gave a crude residue which was purified via flash chromatography (100% hexanes) to afford (*E*)-triisopropyl(5-methyldodec-4-en-6-yloxy)silane (79 mg, 0.22 mmol, 82% yield).

Spectral data as previously reported for Scheme 52, Entry 1.

5.2.3. Chapter 3 Ligands for Nickel-Catalyzed Reductive Couplings

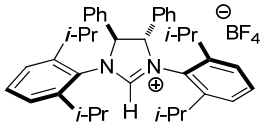
2,3-Bis(diisopropylamino)cycloprop-2-en-1-ylium tetrafluoroborate (42·HBF_4/*i*-Pr-BAC·HBF_4):



42·HBF_4/*i*-Pr-BAC·HBF_4: This compound was previously reported as the $HBPh_4$ salt.

^{1}H NMR (400 MHz, $CDCl_3$): δ 7.41 (s, 1H), 3.97 (sept, *J* = 6.0 Hz, 2H), 3.79 (sept, *J* = 6.8 Hz, 2H), 1.31 (app t, *J* = 6.8 Hz, 24H). **^{13}C NMR (100 MHz, $CDCl_3$):** δ 133.6, 99.1, 56.9, 48.9, 20.61, 20.52. **IR (thin film):** ν 3123, 2985, 2941, 2881, 1881, 1572 cm^{-1}. **HRMS Electrospray (*m/z*):** $[M–BF_4]^+$ calcd for $C_{15}H_{29}N_2$, 237.2331; found 237.2337.

(±)-(4*R*,5*R*)-1,3-Bis(2,6-diisopropylphenyl)-4,5-diphenyl-4,5-dihydro-1H-imidazol-3-ium tetrafluoroborate (43c·HBF_4):



43c·HBF_4: (±)-(1*S*,2*S*)-N^1,N^2-Bis(2,6-diisopropylphenyl)-1,2-diphenylethane-1,2-diamine[2] (0.580 g, 0.940 mmol), ammonium tetrafluoroborate (98 mg, 0.94 mmol), triethylorthoformate (1.11 g, 7.52 mmol), and formic acid (1 drop) were placed in a dry 25 mL round-bottom flask with a reflux condenser under nitrogen. The reaction was then heated to 120 ˚C with stirring for 24 h. The reaction was allowed to cool to rt and then concentrated under high vacuum. The reaction mixture was then purified by column chromatography (SiO_2, 0.5% methanol/99.5% dichloromethane) followed by washing with EtOAc to afford **5c·HBF_4** (0.530 g, 0.84 mmol, 89% yield) as a pale yellow solid.

^{1}H NMR (400 MHz, $(D_3C)_2SO$): δ 9.79 (s, 1H), 7.51–7.39 (m, 14H), 7.19–7.14 (m, 2H), 6.25 (s, 2H), 3.29 (sept, *J* = 6.8 Hz, 2H), 2.74 (sept, *J* = 7.2 Hz, 2H), 1.66 (d, *J* = 6.8 Hz, 6H), 1.31 (d, *J* = 6.4 Hz, 6H), 1.04 (d, *J* = 6.8 Hz, 6H), 0.50 (d, *J* = 6.4 Hz, 6H). **^{13}C NMR (100 MHz, $(D_3C)_2SO$):** δ 159.0, 147.1, 146.2, 131.5, 130.6, 129.7, 129.3, 129.1, 125.1, 124.6, 72.8, 29.3, 29.0, 25.38, 25.34, 23.5, 21.7. **IR (thin film):** v 3064, 3035, 2966, 2931, 2872, 1614, 1583 cm^{-1}. **HRMS Electrospray (*m/z*):** $[M–BF_4]^+$ calcd for $C_{39}H_{47}N_2$, 543.3839; found 543.3743.

5.2.4. Chapter 3 Nickel-Catalyzed Reductive Couplings Substrates

5.2.4.1. Table 4 Entries

(*E*)-5-Methyldodec-4-en-6-ol. *Major Regioisomer:*

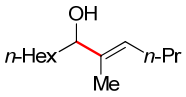


Table 4, Entry 1, Regioisomer 47: Following Procedure E, $Ni(COD)_2$ (37 mg, 0.14 mmol), *i*-Pr-BAC·HBF_4 salt (39 mg, 0.12 mmol), *n*-BuLi (2.5 M in hexanes) (49 μL, 0.12 mmol), di-*tert*-butylsilane (105 mg, 0.73 mmol), 2-hexyne (50 mg, 0.59 mmol), 1-heptanal (68 mg, 0.59 mmol) gave a crude residue which was purified via flash chromatography (100 % hexanes) to afford a single regioisomer in a 88:12 isolated regioselectivity (88:12 crude regioselectivity) (156 mg, 0.46 mmol, 78% yield). This compound was subsequently subjected to *n*-tetrabutylammonium fluoride deprotection for characterization purposes.

Spectral data as previously reported for Scheme 52, Entry 3.

(*E*)-[(4-Ethylideneundecan-5-yl)oxy]triisopropylsilane. *Major Regioisomer:*

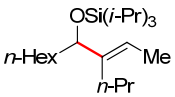


Table 4, Entry 1, Regioisomer 48: Following Procedure F, $Ni(COD)_2$ (20 mg, 0.073 mmol), SIPr·HCl salt (25 mg, 0.059 mmol), *t*-BuOK (6.7 mg, 0.059 mmol), triisopropylsilane (0.24 mL, 1.18 mmol), 2-hexyne (50 mg, 0.59 mmol), 1-heptanal (68 mg, 0.59 mmol) gave a crude residue which was purified via flash chromatography (100% hexanes) to afford a single regioisomer in a >98:2 isolated regioselectivity (93:7 crude regioselectivity) (179 mg, 0.51 mmol, 85% yield).

Spectral data as previously reported for Scheme 52, Entry 1.

(*E*)-1-Cyclohexyl-2-methylhex-2-en-1-ol. *Major Regioisomer:*

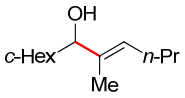


Table 4, Entry 2, Regioisomer 47: Following Procedure E, $Ni(COD)_2$ (37 mg, 0.14 mmol), *i*-Pr-BAC·HBF_4 salt (39 mg, 0.12 mmol), *n*-BuLi (2.5 M in hexanes) (49 μL, 0.12 mmol), di-*tert*-butylsilane (105 mg, 0.73 mmol), 2-hexyne (50 mg, 0.59 mmol), cyclohexylcarboxaldehyde (68 mg, 0.59 mmol) gave a crude residue which was purified via flash chromatography (100 % hexanes) in a 82:18 isolated regioselectivity (82:18 crude regioselectivity) (150 mg, 0.44 mmol, 75% yield). This compound was subsequently subjected to *n*-tetrabutylammonium fluoride deprotection for characterization purposes.

^{1}H NMR (400 MHz, $CDCl_3$): δ 5.30 (t, *J* = 7.2 Hz, 1H), 3.59 (d, *J* = 8.0 Hz, 1H), 1.97 (app q, *J* = 7.2 Hz, 2H), 1.76–1.60 (m, 3H), 1.55 (s, 3H), 1.45–1.31 (m, 4H), 1.25–1.08 (m, 4H), 1.02 (s, 1H), 0.96–0.79 (m, 2H), 0.87 (t, *J* = 7.2 Hz, 3H). **^{13}C NMR (100 MHz,**

$CDCl_3$): δ 136.1, 128.1, 83.3, 40.5, 29.56, 29.55, 29.3, 26.5, 26.2, 26.0, 22.7, 13.8, 11.1. **IR (thin film):** ν 3430, 2944, 2867, 1461 cm^{-1}. **MS (EI) (*m/z*):** $[M+Na]^+$ calcd for $C_{13}H_{24}ONa$, 219.2; found 219.2.

(*E*)-[(1-Cyclohexyl-2-ethylidenepentyl)oxy]triisopropylsilane. *Major Regioisomer:*

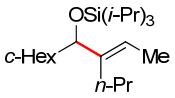
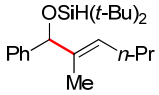


Table 4, Entry 2, Regioisomer 48: Following Procedure F, $Ni(COD)_2$ (20 mg, 0.073 mmol), SIPr·HCl salt (25 mg, 0.059 mmol), *t*-BuOK (6.7 mg, 0.059 mmol), triisopropylsilane (0.24 mL, 1.18 mmol), 2-hexyne (50 mg, 0.59 mmol), cyclohexylcarboxaldehyde (68 mg, 0.59 mmol) gave a crude residue which was purified via flash chromatography (100% hexanes) to afford a single regioisomer in a >98:2 isolated regioselectivity (95:5 crude regioselectivity) (191 mg, 0.54 mmol, 91% yield).

^{1}H NMR (400 MHz, $CDCl_3$): δ 5.28 (q, *J* = 7.2 Hz, 1H), 3.78 (d, *J* = 7.2 Hz, 1H), 2.01–1.88 (m, 2H), 1.74–1.53 (m, 6H), 1.41–1.27 (m, 3H), 1.22–1.09 (m, 4H), 1.05–1.02 (m, 21H), 0.92 (t, *J* = 7.2 Hz, 3H), 0.88–0.81 (m, 3H). **^{13}C NMR (100 MHz, $CDCl_3$):** δ 141.5, 121.7, 83.2, 42.7, 30.3, 29.8, 29.1, 26.8, 26.5, 26.4, 22.6, 18.30, 18.27, 15.1, 13.0, 12.8. **IR (thin film):** ν 2925, 2864, 1464 cm^{-1}. **HRMS (EI) (*m/z*):** $[M]^+$ calcd for $C_{22}H_{44}OSi$, 352.3161; found 352.3160.

(*E*)-Di-*tert*-butyl[(2-methyl-1-phenylhex-2-en-1-yl)oxy]silane. *Major Regioisomer:*



(*E*)-Di-*tert*-butyl[(2-ethylidene-1-phenylpentyl)oxy]silane. *Minor Regioisomer:*

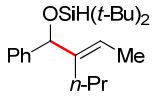


Table 4, Entry 3, Regioisomer 47: Following Procedure E, $Ni(COD)_2$ (37 mg, 0.14 mmol), *i*-Pr-BAC·HBF_4 salt (39 mg, 0.12 mmol), *n*-BuLi (2.5 M in hexanes) (49 μL, 0.12 mmol), di-*tert*-butylsilane (105 mg, 0.73 mmol), 2-hexyne (50 mg, 0.59 mmol), benzaldehyde (63 mg, 0.59 mmol) gave a crude residue which was purified via flash chromatography (100 % hexanes) to afford a mixture of regioisomers in a 85:15 isolated regioselectivity (84:16 crude regioselectivity) (143 mg, 0.43 mmol, 72% yield).

^{1}H NMR (400 MHz, $CDCl_3$): δ 7.39–7.34 (m, 2H), 7.32–7.27 (m, 2H), 7.23–7.19 (m, 1H), 5.77 (q, *J* = 6.8 Hz, 0.15H), 5.64 (t, *J* = 7.2 Hz, 0.85H), 5.19 (s, 0.85H), 5.15 (s, 0.15 H), 4.07 (s, 0.85H), 4.02 (s, 0.15H), 2.03 (m, 2H), 1.88–1.62 (m, 1H), 1.46–1.39 (m, 4H), 1.08–1.01 (m, 10H), 0.94–0.93 (m, 9H), 0.91–0.88 (m, 2H). **^{13}C NMR (100 MHz, $CDCl_3$):** δ 143.39, 143.33, 141.9, 136.8, 128.8, 127.2, 126.8, 126.7, 126.6, 126.1, 120.6, 83.5, 82.2, 29.6, 29.1, 27.40, 27.36, 27.29, 27.25, 22.7, 22.1, 20.3, 20.1, 20.0, 19.9, 14.5, 13.9, 13.1, 11.3. **IR (thin film):** ν 3087, 3063, 3028, 2962, 2930, 1891, 1858, 2090, 1493, 1470 cm^{-1}. **HRMS (EI) (*m/z*):** $[M]^+$ calcd for $C_{21}H_{36}OSi$, 332.2535; found 332.2522.

(*E*)-[(2-Ethylidene-1-phenylpentyl)oxy]triisopropylsilane. *Major Regioisomer:*

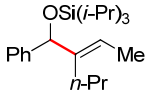


Table 4, Entry 3, Regioisomer 48: Following Procedure F, $Ni(COD)_2$ (20 mg, 0.073 mmol), SIPr·HCl salt (25 mg, 0.059 mmol), *t*-BuOK (6.7 mg, 0.059 mmol), triisopropylsilane (0.24 mL, 1.18 mmol), 2-hexyne (50 mg, 0.59 mmol), benzaldehyde (63 mg, 0.59 mmol) gave a crude residue which was purified via flash chromatography (100 % hexanes) to afford a single regioisomer in a >98:2 isolated regioselectivity (95:5 crude regioselectivity) (171 mg, 0.51 mmol, 86% yield).

^{1}H NMR (400 MHz, $CDCl_3$): δ 7.45–7.41 (m, 2H), 7.34–7.29 (m, 2H), 7.25–7.21 (m, 1H), 5.80 (q, *J* = 6.8 Hz, 1H), 5.24 (s, 1H), 2.00–1.86 (m, 2H), 1.69 (d, *J* = 7.2 Hz, 3H), 1.20–1.04 (m, 23H), 0.83 (t, *J* = 7.6 Hz, 3H). **^{13}C NMR (100 MHz, $CDCl_3$):** δ 144.5, 143.1, 127.7, 126.6, 126.3, 120.0, 79.4, 28.7, 22.3, 18.07, 18.04, 14.6, 13.1, 12.4. **IR (thin film):** v 3085, 3061, 3026, 2958, 2891, 2866, 1492, 1464 cm^{-1}. **HRMS (EI) (*m/z*):** $[M]^+$ calcd for $C_{22}H_{38}OSi$, 346.2692; found 346.2683.

(*E*)-Di-*tert*-butyl[(2,4-dimethyl-1-phenylpent-2-en-1-yl)oxy]silane.

Major Regioisomer:

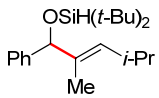


Table 4, Entry 4, Regioisomer 47: Following Procedure E, $Ni(COD)_2$ (37 mg, 0.14 mmol), *i*-Pr-BAC·HBF_4 salt (39 mg, 0.12 mmol), *n*-BuLi (2.5 M in hexanes) (49 μL, 0.12 mmol), di-*tert*-butylsilane (105 mg, 0.73 mmol), 4-methylpent-2-yne (50 mg, 0.59 mmol), benzaldehyde (63 mg, 0.59 mmol) gave a crude residue which was purified via flash chromatography (100 % hexanes) to afford a single regioisomer in a >98:2 isolated regioselectivity (97:3 crude regioselectivity) (168 mg, 0.51 mmol, 85% yield).

^{1}H NMR (400 MHz, $CDCl_3$): δ 7.35 (m, 2H), 7.28 (m, 2H), 7.19 (m, 1H), 5.43 (d, *J* = 9.2 Hz, 1H), 5.12 (s, 1H), 4.04 (s, 1H), 2.49 (septd, *J* = 9.2 Hz, 6.8 Hz, 1H), 1.37 (d, *J* = 1.6 Hz, 3H), 1.02 (s, 9H), 0.98 (d, *J* = 6.8 Hz, 3H), 0.96 (d, *J* = 6.8 Hz, 3H), 0.92 (s, 9H). **^{13}C NMR (100 MHz, $CDCl_3$):** δ 143.3, 135.1, 134.2, 127.7, 126.5, 126.0, 83.5, 27.4, 27.3, 26.9, 22.87, 22.84, 20.4, 19.8, 11.1. **IR (thin film):** v 3087, 3064, 3028, 1962, 2930, 2892, 2858, 2091, 1493, 1470 cm^{-1}. **HRMS (EI) (*m/z*):** $[M]^+$ calcd for $C_{21}H_{36}OSi$, 332.2535; found 332.2528.

(*E*)-Triisopropyl[(2-isopropyl-1-phenylbut-2-en-1-yl)oxy]silane. *Major Regioisomer:*

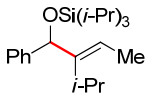


Table 4, Entry 4, Regioisomer 48: Following Procedure F, $Ni(COD)_2$ (20 mg, 0.073 mmol), SIPr·HCl salt (25 mg, 0.059 mmol), *t*-BuOK (6.7 mg, 0.059 mmol), triisopropylsilane (0.24 mL, 1.18 mmol), 4-methylpent-2-yne (50 mg, 0.59 mmol), benzaldehyde (63 mg, 0.59 mmol) gave a crude residue which was purified via flash chromatography (100 % hexanes) to afford a single regioisomer in a >98:2 isolated regioselectivity (90:10 crude regioselectivity) (183 mg, 0.53 mmol, 89% yield).

^{1}H NMR (400 MHz, $CDCl_3$): δ 7.39–7.37 (m, 2H), 7.29–7.24 (m, 2H), 7.21–7.17 (m, 1H), 5.74 (q, *J* = 7.2 Hz, 1H), 5.18 (s, 1H), 2.52 (sept, *J* = 7.2 Hz, 1H), 1.75 (d, *J* = 7.2 Hz, 3H), 1.16–1.00 (m, 24H), 0.70 (d, *J* = 7.2 Hz, 3H). **^{13}C NMR (100 MHz, $CDCl_3$):** δ 147.4, 144.4, 127.60, 126.55, 119.89, 79.6, 27.2, 21.5, 21.2, 18.1, 18.0, 13.9, 12.4. **IR (thin film):** v 3085, 2062, 3026,2959, 2942, 289, 2866, 1493, 1463 cm^{-1}. **HRMS (EI) (*m/z*):** $[M]^+$ calcd for $C_{22}H_{38}OSi$, 346.2692; found 346.2696.

(*E*)-Triethyl[(2-methyl-1,3-diphenylallyl)oxy]silane. *Major Regioisomer:*

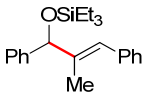


Table 2, Entry 5, Regioisomer 7: The following compound was previously reported by our group.[25]

Spectral data as previously reported.[25]

(*E*)-[(1,2-Diphenylbut-2-en-1-yl)oxy]triisopropylsilane. *Major Regioisomer:*

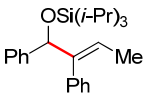


Table 4, Entry 5, Regioisomer 48: Following Procedure F, $Ni(COD)_2$ (20 mg, 0.073 mmol), SIPr·HCl salt (26 mg, 0.059 mmol), *t*-BuOK (6.7 mg, 0.059 mmol), triisopropylsilane (0.24 mL, 1.18 mmol), prop-1-yn-1-ylbenzene (71 mg, 0.61 mmol), benzaldehyde (65 mg, 0.61 mmol) gave a crude residue which was purified via flash

chromatography (100 % hexanes) to afford a mixture of regioisomers in a 80:20 isolated regioselectivity (81:19 crude regioselectivity) (233 mg, 0.61 mmol, 99% yield).

^{1}H NMR (400 MHz, $CDCl_3$): δ 7.21–7.09 (m, 8H), 6.84–6.8 (m, 2H), 6.07 (qd, *J* = 6.8 Hz, 1.2 Hz, 1H), 5.42 (s, 1H), 1.52 (dd, *J* = 7.2 Hz, 1.2 Hz, 3H), 1.18–1.10 (m, 3H), 1.05 (d, *J* = 7.2 Hz, 9H), 1.01 (d, *J* = 6.8 Hz, 9H). **^{13}C NMR (100 MHz, $CDCl_3$):** δ 145.0, 143.7, 138.3, 129.7, 127.46, 127.45, 126.6, 126.4, 121.1, 79.4, 18.1, 18.0, 14.1, 12.3. **IR (thin film):** v 3080, 3058, 3026, 2942, 2890, 2865, 1491, 1463, 1451, 1441 cm^{-1}. **HRMS (EI) (*m/z*):** $[M]^+$ calcd for $C_{25}H_{36}OSi$, 380.2535; found 380.2525.

(*E*)-{[1-(Cyclohex-1-en-1-yl)-2-methylnon-1-en-3-yl]oxy}triisopropylsilane.

Major Regioisomer:

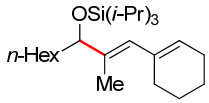


Table 4, Entry 6, Regioisomer 47: Following Procedure G, $Ni(COD)_2$ (20 mg, 0.073 mmol), IMes·HCl salt (20 mg, 0.059 mmol), *t*-BuOK (6.7 mg, 0.059 mmol), triisopropylsilane (0.24 mL, 1.18 mmol), 1-(prop-1-yn-1-yl)cyclohex-1-ene (72 mg, 0.59 mmol), 1-heptanal (68 mg, 0.59 mmol) gave a crude residue which was purified via flash chromatography (100 % hexanes) to afford a single regioisomer in a >98:2 isolated regioselectivity (97:3 crude regioselectivity) (225 mg, 0.59 mmol, 99% yield).

^{1}H NMR (400 MHz, $CDCl_3$): δ 5.65 (s, 1H), 5.54 (m, 1H), 4.05 (t, *J* = 6.4 Hz, 1H), 2.09–2.05 (m, 4H), 1.71 (s, 3H), 1.66–1.51 (m, 4H), 1.30–1.14 (m, 10H), 1.06–1.01 (m,

21H), 0.87 (t, *J* = 6.8 Hz, 3H). **^{13}C NMR (100 MHz, $CDCl_3$):** δ 137.0, 135.1, 128.4, 126.0, 79.0, 36.3, 31.9, 29.4, 29.3, 25.6, 25.4, 23.0, 22.7, 22.3, 18.14, 18.10, 14.1, 12.7, 12.4. **IR (thin film):** ν 2931, 2865, 1464 cm^{-1}. **HRMS (EI) (*m/z*):** $[M]^+$ calcd for $C_{25}H_{48}OSi$, 392.3474; found 392.3468.

(*E*)-{[3-(Cyclohex-1-en-1-yl)dec-2-en-4-yl]oxy}triisopropylsilane. *Major Regioisomer*:

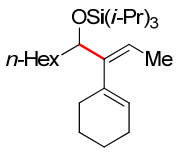


Table 4, Entry 6, Regioisomer 48: Following Procedure F, $Ni(COD)_2$ (20 mg, 0.073 mmol), SIPr·HCl salt (25 mg, 0.059 mmol), *t*-BuOK (6.7 mg, 0.059 mmol), triisopropylsilane (0.24 mL, 1.18 mmol), 1-(prop-1-yn-1-yl)cyclohex-1-ene (72 mg, 0.59 mmol), 1-heptanal (68 mg, 0.59 mmol) gave a crude residue which was purified via flash chromatography (100 % hexanes) to afford a single regioisomer in a >98:2 isolated regioselectivity (91:9 crude regioselectivity) (175 mg, 0.46 mmol, 77% yield).

^{1}H NMR (400 MHz, $CDCl_3$): δ 5.42 (qd, *J* = 6.8 Hz, 1.2 Hz, 1H), 5.33 (td, *J* = 3.6 Hz, 1.6 Hz, 1H), 4.21 (m, 1H), 2.07–1.98 (m, 4H), 1.65–1.39 (m, 7H), 1.28–1.11 (m, 10H), 1.09–0.94 (m, 21H), 0.85 (t, *J* = 6.8 Hz, 3H). **^{13}C NMR (100 MHz, $CDCl_3$):** δ 145.5, 135.5, 125.5, 119.7, 75.7, 36.0, 31.9, 29.5, 29.0, 25.4, 23.8, 23.1, 22.7, 22.4, 18.20, 18.17, 14.1, 14.0, 12.5. **IR (thin film):** ν 2928, 2865, 1464 cm^{-1}. **HRMS (EI) (*m/z*):** $[M–i\text{-}Pr]^+$ calcd for $C_{22}H_{41}OSi$, 349.2927; found 349.2928.

(*E*)-10,10-Diisopropyl-2,2,3,3,11-pentamethyl-8-phenyl-4,9-dioxa-3,10-disiladodec-6-ene. *Major Regioisomer:*

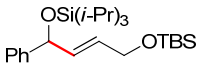


Table 4, Entry 7, Regioisomer 47: Following Procedure G, $Ni(COD)_2$ (20 mg, 0.073 mmol), IMes·HCl salt (20 mg, 0.059 mmol), *t*-BuOK (6.7 mg, 0.059 mmol), triisopropylsilane (0.24 mL, 1.18 mmol), *tert*-butyldimethyl(prop-2-yn-1-yloxy)silane (101 mg, 0.59 mmol), benzaldehyde (63 mg, 0.59 mmol) gave a crude residue which was purified via flash chromatography (100 % hexanes) to afford a single regioisomer in a >98:2 isolated regioselectivity (93:7 crude regioselectivity) (227 mg, 0.52 mmol, 88% yield).

^{1}H NMR (400 MHz, $CDCl_3$): δ 7.33–7.25 (m, 4H), 7.20–7.16 (m, 1H), 5.75–5.73 (m, 2H), 5.25 (d, *J* = 4.0 Hz, 1H), 4.13 (dd, *J* = 3.2 Hz, 0.8 Hz, 2H), 1.13–1.04 (m, 3H), 1.02 (d, *J* = 6.8 Hz, 9K), 0.98 (d, *J* = 6.8 Hz, 9H), 0.86 (s, 9H), 0.02 (d, *J* = 1.2 Hz, 6H). **^{13}C NMR (100 MHz, $CDCl_3$):** δ 144.4, 134.1, 128.3, 128.1, 126.9, 126.0, 75.2, 63.2, 25.9, 18.3, 18.05, 18.01, 12.3, -5.2. **IR (thin film):** v 3085, 3062, 3026, 2944, 2891, 2865, 1471, 1463 cm^{-1}. **HRMS Electrospray (*m/z*):** $[M+Na]^+$ calcd for $C_{25}H_{46}O_2Si_2Na$, 475.2934; found 457.2926.

9,9-Diethyl-2,2,3,3-tetramethyl-6-methylene-7-phenyl-4,8-dioxa-3,9-disilaundecane.

Major Regioisomer:

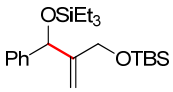


Table 4, Entry 7, Regioisomer 48: Following Procedure H, $Ni(COD)_2$ (7.7 mg, 0.036 mmol), **43c·HBF$_4$** salt (19 mg, 0.030 mmol), *n*-BuLi (2.5 M in hexanes) (12 μL, 0.030 mmol), triethylsilane (0.96 mL, 0.60 mmol), *tert*-butyldimethyl(prop-2-yn-1-yloxy)silane (61 mg, 0.36 mmol), benzaldehyde (31 mg, 0.29 mmol) gave a crude residue which was purified via flash chromatography (100 % hexanes) to afford a mixture of regioisomers in a 84:16 isolated regioselectivity (85:15 crude regioselectivity) (99 mg, 0.25 mmol, 86% yield).

^{1}H NMR (400 MHz, $CDCl_3$): δ 7.34–7.20 (m, 5H), 5.27 (s, 1H), 5.22 (s, 1H), 5.15 (d, *J* = 1.2 Hz, 1H), 4.11 (d, *J* = 14.8 Hz, 1H), 3.88 (d, *J* = 14.8 Hz, 1H), 0.90 (t, *J* = 8.0 Hz, 9H), 0.87 (s, 9H), 0.58 (q, *J* = 8.0 Hz, 6H), -0.02 (s, 3H), -0.03 (s, 3H). **^{13}C NMR (100 MHz, $CDCl_3$):** δ 151.0, 143.0, 127.9, 127.0, 126.2, 109.1, 75.6, 62.3, 25.8, 18.3, 6.8, 4.8, -5.5. **IR (thin film):** ν 3087, 3063, 3028, 2954, 2929, 2876, 2856, 1492, 1471, 1462 cm^{-1}. **HRMS Electrospray (*m/z*):** $[M+Na]^+$ calcd for $C_{22}H_{40}O_2Si_2Na$, 415.2465; found 415.2458.

(*E*)-Triisopropyl[(1-phenylnon-2-en-1-yl)oxy]silane. *Major Regioisomer:*

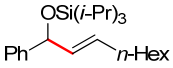


Table 4, Entry 8, Regioisomer 47: Following Procedure G, $Ni(COD)_2$ (20 mg, 0.073 mmol), IMes·HCl salt (20 mg, 0.059 mmol), *t*-BuOK (6.7 mg, 0.059 mmol), triisopropylsilane (0.24 mL, 1.18 mmol), 1-octyne (67 mg, 0.59 mmol), benzaldehyde (63 mg, 0.59 mmol) gave a crude residue which was purified via flash chromatography (100 % hexanes) to afford a single regioisomer in a >98:2 isolated regioselectivity (97:3 crude regioselectivity) (191 mg, 0.50 mmol, 82% yield).

^{1}H NMR (400 MHz, $CDCl_3$): δ 7.35–7.33 (m, 2H), 7.30–7.26 (m, 2H), 7.21–7.17 (m, 1H), 5.64 (dt, *J* = 15.2 Hz, 6.8 Hz, 1H), 5.51 (dd, *J* = 15.2 Hz, 6.4 Hz, 1H), 5.19 (d, *J* = 6.8 Hz, 1H), 1.98 (app q, *J* = 6.8 Hz, 2H), 1.36–1.20 (m, 8H), 1.14–1.06 (m, 3H), 1.03 (d, *J* = 6.8 Hz, 9H), 1.00 (d, *J* = 6.8 Hz, 9H), 0.86 (t, *J* = 6.8 Hz, 3H). **^{13}C NMR (100 MHz, $CDCl_3$):** δ 145.0, 134.2, 130.0, 128.0, 126.7, 125.9, 75.9, 32.7, 32.1, 29.2, 28.9, 22.6, 18.05, 18.04, 14.1, 12.3. **IR (thin film):** v 3085, 3062, 2956, 2940, 2926, 2865, 1491, 1463 cm^{-1}. **HRMS (EI) (*m/z*):** $[M]^+$ calcd for $C_{24}H_{42}OSi$, 374.3005; found 374.3007.

Triethyl[(2-methylene-1-phenyloctyl)oxy]silane. *Major Regioisomer:*

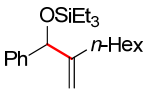


Table 4, Entry 8, Regioisomer 48: Following Procedure D, $Ni(COD)_2$ (7.7 mg, 0.036 mmol), **43c·HBF_4** salt (19 mg, 0.030 mmol), *n*-BuLi (2.5 M in hexanes) (12 μL, 0.030 mmol), triethylsilane (0.96 mL, 0.60 mmol), 1-octyne (39.6 mg, 0.30 mmol), benzaldehyde (32 mg, 0.30 mmol) gave a crude residue which was purified via flash chromatography (100 % hexanes) to afford a mixture of regioisomers in a 93:7 isolated regioselectivity (88:12 crude regioselectivity) (71 mg, 0.21 mmol, 71% yield).

^{1}H NMR (400 MHz, $CDCl_3$): δ 7.36 (m, 2H), 7.31 (m, 2H), 7.23 (m, 1H), 5.22 (s, 1H), 5.14 (s, 1H), 4.87 (s, 1H), 1.95 (dt, *J* = 16.0 Hz, 7.5 Hz, 1H), 1.76 (dt, *J* = 16.0 Hz, 7.5 Hz, 1H), 1.39–1.20 (m, 8H), 0.93 (t, *J* = 7.5 Hz, 9H), 0.86 (t, *J* = 7.0 Hz, 3H), 0.59 (q, *J* = 8.0 Hz, 6H). **^{13}C NMR (100 MHz, $CDCl_3$):** δ 152.0, 143.5, 127.8, 126.3, 109.2, 78.0, 31.7, 30.5, 29.1, 27.6, 22.5, 14.0, 6.77, 4.78. **IR (thin film):** v 3063, 3023, 2954, 2929, 2874, 2857, 1491, 1456 cm^{-1}. **HRMS (EI) (*m/z*):** $[M]^+$ calcd for $C_{21}H_{36}OSi$, 332.2535; found 332.2532.

(*E*)-Triisopropyl[(2-methylundec-3-en-5-yl)oxy]silane. *Major Regioisomer:*

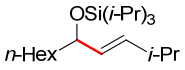


Table 4, Entry 9, Regioisomer 47: Following Procedure G, $Ni(COD)_2$ (20 mg, 0.073 mmol), IMes·HCl salt (20 mg, 0.059 mmol), *t*-BuOK (6.7 mg, 0.059 mmol), triisopropylsilane (0.24 mL, 1.18 mmol), 3-methylbut-1-yne (41 mg, 0.59 mmol), 1-heptanal (68 mg, 0.59 mmol) gave a crude residue which was purified via flash chromatography (100 % hexanes) to afford a single regioisomer in a >98:2 isolated regioselectivity (97:3 crude regioselectivity) (155 mg, 0.46 mmol, 74% yield).

^{1}H NMR (400 MHz, $CDCl_3$): δ 5.44 (dd, J = 16.0 Hz, 6.8 Hz, 1H), 5.31 (ddd, *J* = 15.6 Hz, 7.6 Hz, 1.2 Hz, 1H), 4.08 (td, *J* = 6.8 Hz, 5.6 Hz, 1H), 2.24 (dsept, *J* = 7.6 Hz, 6.8 Hz, 1H), 1.58–1.35 (m, 2H), 1.31–1.17 (m, 8H), 1.06–1.00 (m, 21H), 0.95 (dd, *J* = 7.2 Hz, 2.8 Hz, 6H), 0.86 (t, *J* = 7.2 Hz). **^{13}C NMR (100 MHz, $CDCl_3$):** δ 137.4, 130.8, 74.2, 38.8, 31.9, 30.6, 29.4, 25.0, 22.6, 22.4, 22.2, 18.16, 18.12, 14.1, 12.4. **IR (thin film):** v 2958,

2929, 2865, 1464 cm^{-1}. **HRMS (EI) (*m/z*):** $[M-i\text{-}Pr]^+$ calcd for $C_{18}H_{37}OSi$, 297.2614; found 297.2622.

Triethyl[(2-methyl-3-methylenedecan-4-yl)oxy]silane. *Major Regioisomer:*

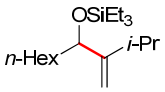
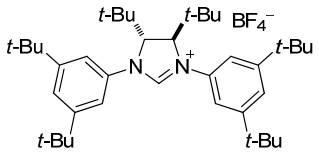


Table 4, Entry 9, Regioisomer 48: Following Procedure H, $Ni(COD)_2$ (7.7 mg, 0.036 mmol), **43c·HBF_4** salt (19 mg, 0.030 mmol), *n*-BuLi (2.5 M in hexanes) (12 μL, 0.030 mmol), triethylsilane (0.96 mL, 0.60 mmol), 3-methylbut-1-yne (26 mg, 38 mmol), 1-heptanal (34 mg, 0.30 mmol) gave a crude residue which was purified via flash chromatography (100 % hexanes) to afford a single regioisomer in a >98:2 isolated regioselectivity (95:5 crude regioselectivity) (68 mg, 0.23 mmol, 76% yield).

^{1}H NMR (400 MHz, $CDCl_3$): δ 4.94 (s, 1H), 4.78 (s, 1H), 4.01 (t, *J* = 5.6 Hz, 1H), 2.20 (sept, *J* = 6.8 Hz, 1H), 1.50–1.34 (m, 2H), 1.30–1.14 (m, 8H), 1.02 (d, *J* = 7.2 Hz, 3H), 0.99 (d, *J* = 6.8 Hz, 3H), 0.91 (t, *J* = 8.0 Hz, 9H), 0.84 (t, *J* = 6.8 Hz, 3H), 0.54 (q, *J* = 7.6 Hz, 6H). **^{13}C NMR (100 MHz, $CDCl_3$):** δ 158.6, 106.8, 75.7, 37.2, 31.8, 29.3, 29.0, 25.6, 23.8, 23.0, 22.6, 14.0, 6.9, 4.9. **IR (thin film):** ν 2957, 2923, 2875, 1459 cm^{-1}. **HRMS (EI) (*m/z*):** $[M]^+$ calcd for $C_{18}H_{38}OSi$, 298.2692; found 298.2684.

5.2.5. Chapter 4 Ligands for Nickel-Catalyzed Reductive Couplings

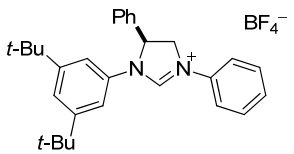
(4*R*,5*R*)-4,5-di-*tert*-butyl-1,3-bis(3,5-di-*tert*-butylphenyl)-4,5-dihydro-1*H*-imidazol-3-ium tetrafluoroborate (58):



Scheme 88, Ligand 58: Literature precedent was followed for ligand **58**, modified using 1-bromo-3,5-di-*tert*-butylbenzene.[74,76] This ligand was difficult to purify and only the diagnostic peaks have been assigned in the impure sample.

^{1}H NMR (400 MHz, $CDCl_3$): δ 9.24 (s, 1H), 7.42 (m, 2H), 7.35–7.28 (m, 2H), 6.98–6.95 (m, 2H), 4.51 (s, 2H), 1.34 (s, 36H), 0.96 (s, 18H). **^{13}C NMR (100 MHz, $CDCl_3$):** δ 135.7, 136.4, 123.0, 119.0, 72.4, 36.4, 35.2, 31.2, 26.2. **IR (thin film):** v 2963, 2870, 1673, 1587 cm^{-1}. **HRMS Electrospray (*m/z*):** $[M–BF_4]^+$ calcd for $C_{39}H_{63}N_2$, 559.4986; found 559.4994.

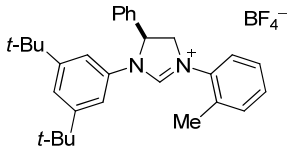
(*S*)-1-(3,5-di-*tert*-butylphenyl)-3,5-diphenyl-4,5-dihydro-1*H*-imidazol-3-ium tetrafluoroborate (64):



Scheme 88, Ligand 64: Literature precedent was followed for ligand **64**, modified using *tert*-butyl phenylcarbamate and 1-bromo-3,5-di-*tert*-butylbenzene.[77]

^{1}H NMR (400 MHz, $CDCl_3$): δ 8.94 (s, 1H), 7.46–7.25 (m, 11H), 7.09 (m, 2H), 6.07 (dd, *J* = 12.0 Hz, 8.0 Hz, 1H), 5.17 (t, *J* = 12.0 Hz, 1H), 4.30 (dd, *J* = 11.6 Hz, 8.0 Hz, 1H), 1.20 (s, 18H). **^{13}C NMR (100 MHz, $CDCl_3$):** δ 153.1, 151.4, 135.9, 133.2, 133.8, 130.2, 129.9, 129.7, 128.2, 127.4, 122.8, 119.2, 116.4, 66.2, 57.7, 35.1, 31.1. **IR (thin film):** ν 2963, 1619, 1589 cm^{-1}. **HRMS Electrospray (*m/z*):** $[M–BF_4]^+$ calcd for $C_{29}H_{35}N_2$, 411.2800; found 411.2793.

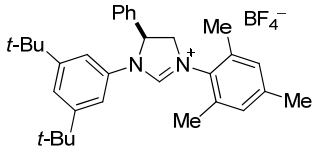
(*S*)-1-(3,5-di-*tert*-butylphenyl)-5-phenyl-3-(*o*-tolyl)-4,5-dihydro-1*H*-imidazol-3-ium tetrafluoroborate (65):



Scheme 88, Ligand 65: Literature precedent was followed for ligand **65**, modified using *tert*-butyl *o*-tolylcarbamate and 1-bromo-3,5-di-*tert*-butylbenzene.[77]

^{1}H NMR (400 MHz, $CDCl_3$): δ 8.34 (s, 1H), 7.70–7.67 (m, 1H), 7.48–7.29 (m, 9H), 7.08 (m, 2H), 6.19 (dd, *J* = 11.6 Hz, 8.0 Hz, 1H), 5.11 (t, *J* = 12.0 Hz, 1H), 4.24 (dd, 11.6 Hz, 8.0 Hz, 1H), 2.45 (s, 3H), 1.19 (18H). **^{13}C NMR (100 MHz, $CDCl_3$):** δ 154.7, 153.0, 136.4, 134.2, 133.9, 133.8, 131.8, 130.3, 129.7, 128.0, 127.7, 126.8, 122.6, 116.7, 66.5, 60.6, 35.0, 31.1, 17.9. **IR (thin film):** ν 2963, 2869, 1623, 1593 cm^{-1}. **HRMS (EI) (*m/z*):** $[M]^+$ calcd for $C_{30}H_{37}N_2$, 425.2951; found 425.2956.

(*S*)-1-(3,5-di-*tert*-butylphenyl)-3-mesityl-5-phenyl-4,5-dihydro-1*H*-imidazol-3-ium tetrafluoroborate (67):



Scheme 88, Ligand 67: Literature precedent was followed for ligand **67**, modified using *tert*-butyl mesitylcarbamate and 1-bromo-3,5-di-*tert*-butylbenzene.[77]

^{1}H NMR (400 MHz, $CDCl_3$): δ 8.66 (s, 1H), 7.49 (m, 2H), 7.39–7.24 (m, 4H), 7.14 (m, 2H), 6.62 (s, 2H), 6.43 (dd, *J* = 12.4 Hz, 7.6 Hz, 1H), 4.93 (t, *J* = 12.0 Hz, 1H), 4.04 (dd, *J* = 12.0 Hz, 7.6 Hz, 1H), 2.34 (s, 6H), 1.25 (s, 3H), 1.19 (s, 18H). **^{13}C NMR (100 MHz, $CDCl_3$):** δ 155.5, 153.1, 140.5, 136.6, 133.8, 130.3, 130.0, 129.7, 129.5, 127.1, 122.3, 115.6, 65.5, 59.6, 35.1, 31.0, 21.0. **IR (thin film):** v 2964, 2870, 1666, 1625, 1592 cm^{-1}. **HRMS Electrospray (*m/z*):** $[M–BF_4]^+$ calcd for $C_{32}H_{41}N_2$, 453.3269; found 453.3271.

5.2.6. General Procedure for Asymmetric Nickel-Catalyzed Reductive Couplings

The following general procedure was followed for NHC ligands **58** and **64**–**66**: To a solid mixture of $Ni(COD)_2$ (12 mol %, 0.057 mmol), NHC·HBF_4 salt (10 mol %, 0.047 mmol), and *t*-BuOK (10 mol %, 0.047 mmol) was added THF (0.125 M). The resulting solution was stirred for 15 min at rt until the solution turned dark brown in appearance. Then 2-hexyne (1.0 equiv, 0.47 mmol), benzaldehyde (1.0 equiv, 0.47 mmol), and di-*tert*-butylsilane (1.2 equiv) were added via syringe pump addition over 20 minutes and the reaction mixture was allowed to stir until starting materials were consumed. The reaction

mixture was filtered through silica gel eluting with 50% EtOAc/hexanes. The solvent was removed *in vacuo*, and the crude residue was purified via flash chromatography on silica gel to afford the desired products. The regiochemical ratio of products was determined by GCMS analysis and *ee* analysis was performed using an OD-H chiral HLPC column following TBAF deprotection.

Spectral data as previously reported for Table 4, Entry 3**.**

Literature Cited

(1) This chapter includes portions from the following source, reprinted with permission of the publisher: Malik, H. A.; Baxter, R. D.; Montgomery, J. Nickel-Catalyzed Reductive Couplings and Cyclizations. In Catalysis Without Precious Metals; 1st Ed. Bullock, R. M., Ed. Wiley-VCH: Weinheim, 2010; pp 181–210. No further use of this material is permitted with the written permission of the publisher of the original work.

(2) *Metal catalyzed reductive C–C bond formation - A Departure from Preformed Organometallic Reagents*; Springer: Heidelberg, 2007.

(3) Montgomery, J. Nickel-Catalyzed Cyclizations, Couplings, and Cycloadditions Involving Three Reactive Components. *Acc. Chem. Res.* **2000**, *33*, 467–473.

(4) Montgomery, J. Nickel-Catalyzed Reductive Cyclizations and Couplings. *Angew. Chem. Int. Ed.* **2004**, *43*, 3890–3908.

(5) Montgomery, J.; Sormunen, G. J. In *Metal Catalyzed Reductive C–C Bond Formation: A Departure from Preformed Organometallic Reagents*; Krische, M. J., Ed.; Springer: Berlin, 2007; Vol. 279, p 1–23.

(6) Moslin, R. M.; Miller-Moslin, K.; Jamison, T. F. Regioselectivity and Enantioselectivity in Nickel-Catalyzed Reductive Coupling Reactions of Alkynes. *Chem. Commun.* **2007**, 4441–4449.

(7) Ikeda, S. Nickel-Catalyzed Coupling of Carbonyl Compounds and Alkynes or 1,3-dienes: An Efficient Method for the Preparation of Allylic, Homoallylic, and Bishomoallylic Alcohols. *Angew. Chem. Int. Ed.* **2003**, *42*, 5120–5122.

(8) Jang, H. Y.; Krische, M. J. Catalytic C–C Bond Formation via Capture of Hydrogenation Intermediates. *Acc. Chem. Res.* **2004**, *37*, 653–661.

(9) Ngai, M. Y.; Kong, J. R.; Krische, M. J. Hydrogen-Mediated C–C Bond Formation: A Broad New Concept in Catalytic C–C Coupling. *J. Org. Chem.* **2007**, *72*, 1063–1072.

(10) Sato, F.; Urabe, H.; Okamoto, S. Synthesis of Organotitanium Complexes from Alkenes and Alkynes and their Synthetic Applications. *Chem. Rev.* **2000**, *100*, 2835–2886.

(11) Lysenko, I. L.; Kim, K.; Lee, H. G.; Cha, J. K. Low-Valent Titanium-Mediated Stereoselective Alkylation of Allylic Alcohols. *J. Am. Chem. Soc.* **2008**, *130*, 15997–16002.

(12) Ryan, J.; Micalizio, G. C. An Alkoxide-Directed Carbometalation of Internal Alkynes. *J. Am. Chem. Soc.* **2006**, *128*, 2764–2765.

(13) Crowe, W. E.; Rachita, M. J. Titanium-Catalyzed Reductive Cyclization of δ,ε-Unsaturated Ketones and Aldehydes. *J. Am. Chem. Soc.* **1995**, *117*, 6787-6788.

(14) Kablaoui, N. M.; Buchwald, S. L. Development of a Method for the Reductive Cyclization of Enones by a Titanium Catalyst. *J. Am. Chem. Soc.* **1996**, *118*, 3182–3191.

(15) Kim, I. S.; Ngai, M.-Y.; Krische, M. J. Enantioselective Iridium-Catalyzed Carbonyl Allylation from the Alcohol or Aldehyde Oxidation Level via Transfer Hydrogenative Coupling of Allyl Acetate: Departure from Chirally Modified Allyl Metal Reagents in Carbonyl Addition. *J. Am. Chem. Soc.* **2008**, *130*, 14891–14899.

(16) Skucas, E.; Ngai, M.-Y.; Komanduri, V.; Krische, M. J. Enantiomerically Enriched Allylic Alcohols and Allylic Amines via C–C Bond-Forming Hydrogenation: Asymmetric Carbonyl and Imine Vinylation. *Acc. Chem. Res.* **2007**, *40*, 1394–1401.

(17) Sato, Y.; Takimoto, M.; Hayashi, K.; Katsuhara, T.; Takagi, K.; Mori, M. Novel Stereoselective Cyclization via π-Allylnickel Complex Generated from 1,3-Diene and Hydride Nickel Complex. *J. Am. Chem. Soc.* **1994**, *116*, 9771–9772.

(18) Sawaki, R.; Sato, Y.; Mori, M. Ligand-Controlled Highly Stereoselective Syntheses of *E*- and *Z*-Allylsilanes from Dienes and Aldehydes Using Nickel Complex. *Org. Lett.* **2004**, *6*, 1131–1133.

(19) Kimura, M.; Ezoe, A.; Mori, M.; Iwata, K.; Tamaru, Y. Regio- and Stereoselective Nickel-Catalyzed Homoallylation of Aldehydes with 1,3-Dienes. *J. Am. Chem. Soc.* **2006**, *128*, 8559–8568.

(20) Oblinger, E.; Montgomery, J. A New Stereoselective Method for the Preparation of Allylic Alcohols. *J. Am. Chem. Soc.* **1997**, *119*, 9065–9066.

(21) Ni, Y.; Amarasinghe, K. K. D.; Montgomery, J. Nickel-Catalyzed Cyclizations and Couplings with Vinylzirconium Reagents. *Org. Lett.* **2002**, *4*, 1743–1745.

(22) Tang, X. Q.; Montgomery, J. Nickel-Catalyzed Preparation of Bicyclic Heterocycles: Total Synthesis of (+)-Allopumiliotoxin 267A, (+)-Allopumiliotoxin 339A, and (+)-Allopumiliotoxin 339B. *J. Am. Chem. Soc.* **2000**, *122*, 6950–6954.

(23) Tang, X.-Q.; Montgomery, J. Nickel Catalysis in the Stereoselective Preparation of Quinolizidine, Pyrrolizidine, and Indolizidine Alkaloids: Total Synthesis of (+)-Allopumiliotoxin 267A. *J. Am. Chem. Soc.* **1999**, *121*, 6098–6099.

(24) Huang, W. S.; Chan, J.; Jamison, T. F. Highly Selective Catalytic Intermolecular Reductive Coupling of Alkynes and Aldehydes. *Org. Lett.* **2000**, *2*, 4221–4223.

(25) Mahandru, G. M.; Liu, G.; Montgomery, J. Ligand-Dependent Scope and Divergent Mechanistic Behavior in Nickel-Catalyzed Reductive Couplings of Aldehydes and Alkynes. *J. Am. Chem. Soc.* **2004**, *126*, 3698–3699.

(26) Colby, E. A.; O'Brie, K. C.; Jamison, T. F. Total Syntheses of Amphidinolides T1 and T4 via Catalytic, Stereoselective, Reductive Macrocyclizations. *J. Am. Chem. Soc.* **2005**, *127*, 4297–4307.

(27) Chan, J.; Jamison, T. F. Enantioselective Synthesis of (–)-Terpestacin and Structural Revision of Siccanol Using Catalytic Stereoselective Fragment Couplings and Macrocyclizations. *J. Am. Chem. Soc.* **2004**, *126*, 10682–10691.

(28) Chrovian, C. C.; Knapp-Reed, B.; Montgomery, J. Total Synthesis of Aigialomycin D: Surprising Chemoselectivity Dependence on Alkyne Structure in Nickel-Catalyzed Cyclizations. *Org. Lett.* **2008**, *10*, 811–814.

(29) Knapp-Reed, B.; Mahandru, G. M.; Montgomery, J. Access to Macrocyclic Endocyclic and Exocyclic Allylic Alcohols by Nickel-Catalyzed Reductive Cyclization of Ynals. *J. Am. Chem. Soc.* **2005**, *127*, 13156–13157.

(30) Miller, K. M.; Luanphaisarnnont, T.; Molinaro, C.; Jamison, T. F. Alkene-Directed, Nickel-Catalyzed Alkyne Coupling Reactions. *J. Am. Chem. Soc.* **2004**, *126*, 4130–4131.

(31) Miller, K. M.; Jamison, T. F. Ligand-Switchable Directing Effects of Tethered Alkenes in Nickel-Catalyzed Additions to Alkynes. *J. Am. Chem. Soc.* **2004**, *126*, 15342–15343.

(32) Moslin, R. M.; Jamison, T. F. Mechanistic Implications of Nickel-Catalyzed Reductive Coupling of Aldehydes and Chiral 1,6-Enynes. *Org. Lett.* **2006**, *8*, 455–458.

(33) Moslin, R. M.; Miller, K. M.; Jamison, T. F. Directing Effects of Tethered Alkenes in Nickel-Catalyzed Coupling Reactions of 1,6-Enynes and Aldehydes. *Tetrahedron* **2006**, *62*, 7598–7610.

(34) Luanphaisarnnont, T.; Ndubaku, C. O.; Jamison, T. F. *anti*-1,2-Diols via Ni-Catalyzed Reductive Coupling of Alkynes and α-Oxyaldehydes. *Org. Lett.* **2005**, *7*, 2937–2940.

(35) Sa-ei, K.; Montgomery, J. Highly Diastereoselective Preparation of anti-1,2-Diols by Catalytic Addition of Alkynylsilanes to α-Silyloxyaldehydes. *Org. Lett.* **2006**, *8*, 4441–4443.

(36) Miller, K. M.; Huang, W.-S.; Jamison, T. F. Catalytic Asymmetric Reductive Coupling of Alkynes and Aldehydes: Enantioselective Synthesis of Allylic Alcohols and α-Hydroxy Ketones. *J. Am. Chem. Soc.* **2003**, *125*, 3442–3443.

(37) Chaulagain, M. R.; Sormunen, G. J.; Montgomery, J. New *N*-Heterocyclic Carbene Ligand and Its Application in Asymmetric Nickel-Catalyzed Aldehyde/Alkyne Reductive Couplings. *J. Am. Chem. Soc.* **2007**, *129*, 9568–9569.

(38) Ogoshi, S.; Arai, T.; Ohashi, M.; Kurosawa, H. Nickeladihydrofuran. Key Intermediate for Nickel-Catalyzed Reaction of Alkyne and Aldehyde. *Chem. Commun.* **2008**, 1347–1349.

(39) Baxter, R. D.; Montgomery, J. Dehydrogenative Cyclocondensation of Aldehydes, Alkynes, and Dialkylsilanes. *J. Am. Chem. Soc.* **2008**, *130*, 9662–9663.

(40) Regioselectivity of internal alkynes was consistent between Et_2SiH_2 and Et_3SiH across various ligand classes.

(41) Amarasinghe, K. K. D.; Montgomery, J. Enantioselective Total Synthesis of (+)-Testudinariol A Using a New Nickel-Catalyzed Allenyl Aldehyde Cyclization. *J. Am. Chem. Soc.* **2002**, *124*, 9366–9367.

(42) Malik, H. A.; Chaulagain, M. R.; Montgomery, J. Cooperativity of Regiochemistry Control Strategies in Reductive Couplings of Propargyl Alcohols and Aldehydes. *Org. Lett.* **2009**, *11*, 5734−5737.

(43) Wharton, P.; Bohlen, D. Communications- Hydrazine Reduction of α,β-Epoxy Ketones to Allylic Alcohols. *J. Org. Chem.* **1961**, *26*, 3615−3616.

(44) Arundale, E.; Mikeska, L. A. The Olefin-Aldehyde Condensation. The Prins Reaction. *Chem. Rev.* **1952**, *51*, 505−555.

(45) Waitkins, G. R.; Clark, C. W. Selenium Dioxide: Preparation, Properties, and Use as Oxidizing Agent. *Chem. Rev.* **1945**, *36*, 235−289.

(46) Basavaiah, D.; Rao, A. J.; Satyanarayana, T. Recent Advances in the Baylis-Hillman Reaction and Applications. *Chem. Rev.* **2003**, *103*, 811−892.

(47) Evans, D. A.; Andrews, G. C. Allylic sulfoxides. Useful intermediates in organic synthesis. *Acc. Chem. Res.* **1974**, *7*, 147−155.

(48) Molander, G. A. Application of Lanthanide Reagents in Organic Cynthesis. *Chem. Rev.* **1992**, *92*, 29−68.

(49) Furstner, A. Carbon−Carbon Bond Formations Involving Organochromium(III) Reagents. *Chem. Rev.* **1999**, *99*, 991−1046.

(50) Oppolzer, W.; Radinov, R. N. Synthesis of (*R*)-(−)-Muscone by an Asymmetrically Catalyzed Macrocyclization of an ω-Alkynal. *J. Am. Chem. Soc.* **1993**, *115*, 1593−1594.

(51) Wipf, P.; Xu, W. J. Preparation of Allylic Alcohols by Alkene Transfer from Zirconium to Zinc. *Tetrahedron Lett.* **1994**, *35*, 5197−5200.

(52) Kataoka, Y.; Miyai, J.; Oshima, K.; Takai, K.; Utimoto, K. Reactions Between Tantalum- or Niobium-Alkyne Complexes and Carbonyl Compounds. *J. Org. Chem.* **1992**, *57*, 1973−1981.

(53) Bahadoor, A. B.; Flyer, A.; Micalizio, G. C. A Pentenyl Dianion-Based Strategy for Convergent Synthesis of Ene-1,5-diols. *J. Am. Chem. Soc.* **2005**, *127*, 3694–3695.

(54) Patman, R. L.; Chaulagain, M. R.; Williams, V. M.; Krische, M. J. Direct Vinylation of Alcohols or Aldehydes Employing Alkynes as Vinyl Donors: A Ruthenium Catalyzed C–C Bond-Forming Transfer Hydrogenation. *J. Am. Chem. Soc.* **2009**, *131*, 2066–2067.

(55) Karen M. Miller, Elizabeth A. C. Katrina S. W. Timothy F. J. Asymmetric Catalytic Reductive Coupling of 1,3-Enynes and Aromatic Aldehydes. *Adv. Synth. Catal.* **2005**, *347*, 1533–1536.

(56) Saito, N.; Katayama, T.; Sato, Y. Nickel-Catalyzed Highly Regioselective Multicomponent Coupling of Ynamides, Aldehydes, and Silanes: A New Access to Functionalized Enamides. *Org. Lett.* **2008**, *10*, 3829–3832.

(57) Takacs, J. M.; Lawson, E. C.; Clement, F. On the Nature of the Catalytic Palladium-Mediated Elimination of Allylic Carbonates and Acetates To Form 1,3-Dienes. *J. Am. Chem. Soc.* **1997**, *119*, 5956–5957.

(58) Tsuji, J.; Mandai, T. Palladium-Catalyzed Hydrogenolysis of Allylic and Propargylic Compounds with Various Hydrides. *Synthesis* **1996**, *1996*, 1–24.

(59) Corey, E. J.; Achiwa, K. A Method for Deoxygenation of Allylic and Benzylic Alcohols. *J. Org. Chem.* **1969**, *34*, 3667–3668.

(60) Molander, G. A.; St. Jean, D. J.; Haas, J. Toward a General Route to the Eunicellin Diterpenes: The Asymmetric Total Synthesis of Deacetoxyalcyonin Acetate. *J. Am. Chem. Soc.* **2004**, *126*, 1642–1643.

(61) Pilli, R. A.; Victor, M. M.; de Meijere, A. First Total Synthesis of Aspinolide B, A New Pentaketide Produced by Aspergillus ochraceus. *J. Org. Chem.* **2000**, *65*, 5910–5916.

(62) Gao, F.; Hoveyda, A. H. α-Selective Ni-Catalyzed Hydroalumination of Aryl- and Alkyl-Substituted Terminal Alkynes: Practical Syntheses of Internal Vinyl Aluminums, Halides, or Boronates. *J. Am. Chem. Soc.* **2010**, *132*, 10961–10963.

(63) Reichard, H. A.; McLaughlin, M.; Chen, M. Z.; Micalizio, G. C. Regioselective Reductive Cross-Coupling Reactions of Unsymmetrical Alkynes. *Eur. J. Org. Chem.* **2010**, 391–409.

(64) Melaimi, M.; Soleilhavoup, M.; Bertrand, G. Stable Cyclic Carbenes and Related Species beyond Diaminocarbenes. *Angew. Chem. Int. Ed.* **2010**, *49*, 2–42.

(65) Kirmse, W. The Beginnings of *N*-Heterocyclic Carbenes. *Angew. Chem. Int. Ed.* **2010**, *49*, 2–6.

(66) Dorta, R.; Stevens, E. D.; Scott, N. M.; Costabile, C.; Cavallo, L.; Hoff, C. D.; Nolan, S. P. Steric and Electronic Properties of *N*-Heterocyclic Carbenes (NHC): A Detailed Study on Their Interaction with Ni(CO)4. *J. Am. Chem. Soc.* **2005**, *127*, 2485–2495.

(67) Ragone, F.; Poater, A.; Cavallo, L. Flexibility of *N*-Heterocyclic Carbene Ligands in Ruthenium Complexes Relevant to Olefin Metathesis and Their Impact in the First Coordination Sphere of the Metal. *J. Am. Chem. Soc.* **2010**, *132*, 4249–4258.

(68) Lavallo, V.; Ishida, Y.; Donnadieu, B.; Bertrand, G. Isolation of Cyclopropenylidene–Lithium Adducts: The Weiss–Yoshida Reagent. *Angew. Chem. Int. Ed.* **2006**, *45*, 6652–6655.

(69) Malik, H. A.; Sormunen, G. J.; Montgomery, J. A General Strategy for Regiocontrol in Nickel-Catalyzed Reductive Couplings of Aldehydes and Alkynes. *J. Am. Chem. Soc.* **2010**, *132*, 6304–6305.

(70) Unpublished Initial Results from Houk and Coworkers.

(71) Guo, H.; Dong, C.-G.; Kim, D.-S.; Urabe, D.; Wang, J.; Kim, J. T.; Liu, X.; Sasaki, T.; Kishi, Y. Toolbox Approach to the Search for Effective Ligands for Catalytic Asymmetric Cr-Mediated Coupling Reactions. *J. Am. Chem. Soc.* **2009**, *131*, 15387–15393.

(72) Moser, R.; Boskovic, Z. V.; Crowe, C. S.; Lipshutz, B. H. CuH-Catalyzed Enantioselective 1,2-Reductions of a-b-Unsaturated Ketones. *J. Am. Chem. Soc.* **2010**, *132*, 7852–7853.

(73) Yang, Y.; Zhu, S.-F.; Zhou, C.-Y.; Zhou, Q.-L. Nickel-Catalyzed Enantioselective Alkylative Coupling of Alkynes and Aldehydes: Synthesis of Chiral Allylic Alcohols with Tetrasubstituted Olefins. *J. Am. Chem. Soc.* **2008**, *130*, 14052–14053.

(74) Roland, S.; Mangeney, P. Addition of Grignard Reagents to Chiral 1,2-Bisimines: A Diasteroselective Preparation of Unsymmetrical 1,2-Diamines. *Eur. J. Org. Chem.* **2000**, *2000*, 611–616.

(75) Lee, Y.; Li, B.; Hoveyda, A. H. Stereogenic-at-Metal Zn- and Al-Based *N*-Heterocyclic Carbene (NHC) Complexes as Bifunctional Catalysts in Cu-Free Enantioselective Allylic Alkylations. *J. Am. Chem. Soc.* **2009**, *131*, 11625–11633.

(76) Roland, S.; Mangeney, P.; Alexakis, A. A Practical and Efficient Synthesis of Enantiomerically Pure Di-*Tert*-Butylethanediamine. *Synthesis* **1999**, 228–230.

(77) May, T. L.; Brown, M. K.; Hoveyda, A. H. Enantioselective Synthesis of All-Carbon Quaternary Stereogenic Centers by Catalytic

Asymmetric Conjugate Additions of Alkyl and Aryl Aluminum Reagents to Five-, Six-, and Seven-Membered-Ring β-Substituted Cyclic Enones. *Angew. Chem. Int. Ed.* **2008**, *47*, 7358–7362.